THESIS FOR THE DEGREE OF DOCTOR OF PHILOSOPHY

Sialic acid-targeting strategies to understand its role in inflammation and arthritis

LOISE RÅBERG

Department of Life Sciences

CHALMERS UNIVERSITY OF TECHNOLOGY

Gothenburg, Sweden 2026

Sialic acid-targeting strategies to understand its role in inflammation and arthritis

LOISE RÅBERG
ISBN 978-91-8103-437-0

Doktorsavhandlingar vid Chalmers tekniska högskola
Ny serie nr 5894
ISSN 0346-718X
https://doi.org/10.63959/chalmers.dt/5894

Department of Life Sciences
Chalmers University of Technology
SE-412 96 Gothenburg
Sweden
Telephone + 46 (0)31-772 1000

Cover:
The cover illustrates cellular communication within a pro-inflammatory microenvironment, highlighting glycans, cytokines, reactive oxygen species, damage-associated molecular patterns, soluble Siglecs, and Siglec – TLR regulation. As a therapeutic strategy, nanoparticles either target sialic acid or deliver drugs in response to the pro-inflammatory stimuli. The illustration was created with Affinity Designer.

Chalmers digitaltryck
Gothenburg, Sweden 2026

Sialic Acid-targeting Strategies to Understand its Role in Inflammation and Arthritis

LOISE RÅBERG

Department of Life Sciences, Chalmers University of Technology

ABSTRACT

Sialic acid (Sia) is a monosaccharide increasingly recognized for its pathological roles in diseases such as cancer, autoimmune disorders, and osteoarthritis (OA). Positioned at the terminal ends of glycans, Sia serves as a key interface for cellular interactions and immune regulation through engagement with Sia-binding immunoglobulin-like lectins (Siglecs). Although the role of Sia in OA remains poorly defined, altered Sia expression has been reported on chondrocytes, in synovial fluid, and on lubricin, supporting its involvement in inflammatory processes. Despite the complexity of OA, disease-modifying therapeutics remain limited. The disease is characterized by cartilage degeneration and chronic inflammation, with monocytes and macrophages playing key roles. This thesis aims to elucidate the immunoregulatory functions of Sia and evaluate its potential as a target for disease-modifying strategies using nanotechnology.

Given the emerging evidence for Sia involvement in OA, improved understanding of the spatiotemporal dynamics of Sia and associated pathways may enable targeted immunomodulation. We identified the presence of Siglec-5/14 in OA synovial fluid, suggesting a functional role in disease. First, focusing on monocytes, a previously uncharacterized immunoregulatory role of Siglec-5 in modulating pro-inflammatory toll-like receptor 4 (TLR4) signaling was identified. Second, we observed inflammation-induced alterations in Sia metabolism which did not correspond with increased cell-surface Sia. Lastly, using an enzyme-based cartilage degradation model, we showed that Sia removal led to cartilage breakdown, reinforcing its importance for cartilage integrity. Together, these findings provide mechanistic insight into the role of Sia in OA pathogenesis.

Building on these findings, Sia, pH changes, and cartilage degradation products were utilized for selective targeting and controlled drug release using polymeric nanoparticles (PNPs). Functionalization with phenylboronic acid (PBA) enabled multivalent and reversible binding to Sia, resulting in measurable immunomodulatory effects on monocyte migration in a transwell assay. Furthermore, pH-responsive drug release was demonstrated in a relevant biological model, underscoring its applicability in inflammation. Finally, glycosylation within the biomolecular corona influences nanoparticle-microenvironment interactions, with glycan structures emerging as key determinants of nanoparticle behavior and therapeutic performance.

Collectively, these findings highlight a mechanistic role for sialylation in inflammation and support glycan-targeting strategies as a foundation for Sia-directed immune modulation in OA.

Keywords: Sialic acid, osteoarthritis, nanoparticles, inflammation, Siglec, TLR4

LIST OF PUBLICATIONS

I. Sialoglycans modulate Siglec-5-TLR4 interactions in osteoarthritis
Loise Råberg, Fan Jia, Ula von Mentzer, Vignesh Venkatakrishnan, Niclas G. Karlsson, Alexandra Stubelius
iScience (2025), volume 28, issue 12, 113979, doi: 10.1016/j.isci.2025.113979

II. Dynamic release from acetalated dextran nanoparticles for precision therapy of inflammation
Gizem Erensoy, **Loise Råberg**, Ula von Mentzer, Luca Dirk Menges, Endri Bardhi, Anna-Karin Hultgård Ekwall, and Alexandra Stubelius
ACS Applied Bio Materials (2024), volume 7, issue 6, 3810–3820, doi: 10.1021/acsabm.4c00182

III. Multivalent boronolectin nanoparticles modulate monocyte migration via sialic acid shielding in osteoarthritis
Loise Råberg, Hanna Mårtensson, Gizem Erensoy, Viktoria de Carvalho, Ghadah Al-Wassiti, Martina Sundqvist, Ben J. Boyd, Anna-Karin Hultgård Ekwall, Carmen Corciulo, Alexandra Stubelius
ChemRxiv, doi: 10.26434/chemrxiv.15000907/v1

IV. Glycosylation-driven interactions of nanoparticles with the extraular matrix: Implications for inflammation and drug delivery
Ula von Mentzer, Fritjof Havemeister, **Loise Råberg**, Hemapriya Kothuru Chinnadurai, Gizem Erensoy, Elin K. Esbjörner, Alexandra Stubelius
Biomaterials Advances (2025), volume 171, 214230, doi: 10.1016/j.bioadv.2025.214230

V. Comparative tools to understand the role of sialic acid in osteoarthritis
Ratish Rajgopalan Nair, **Loise Råberg**, Yuen Yi Lam, Ben J. Boyd, Alexandra Stubelius
Manuscript

Other papers originating from PhD work not included in this thesis:

VI. Synovial fluid profile dictates nanoparticle uptake into cartilage - implications of the protein corona for novel arthritis treatments
Ula von Mentzer, Tilia Selldén, **Loise Råberg**, Gizem Erensoy, Anna-Karin Hultgård Ekwall, Alexandra Stubelius
Osteoarthritis and Cartilage (2022), volume 30, issue 10, 1356-1364, doi: 10.1016/j.joca.2022.07.002

VII. Long-term effect of ovary removal on the joints of aged mice
Sofia Wüstenhagen, Lindsay Zentveld, Francesco Longo, **Loise Råberg**, Alexandra Stubelius, Riddhi Vyas, Anders Nguyen, Julia M. Scheffler, Mattias N. D. Svensson and Carmen Corciulo
Laboratory Animal Research (2026), volume 42, doi: 10.1016/j.joca.2022.07.002

CONTRIBUTION REPORT

Below follows a description of my (LR) contributions to the papers and manuscripts included in this thesis, where the initials are derived from the list of publications:

I. LR designed all studies together with AS. LR performed and analyzed all results related to flow cytometry, cytokine quantification, and immunocytochemistry. The proteomics analysis and LC-MS was performed by co-authors. Data analysis, data interpretation, figures, and writing was performed by LR together with AS.

II. LR designed the biological parts of the study with AS. LR performed the biological evaluation of the nanoparticles *in vitro*, analyzed and interpreted the result and wrote the related text.

III. LR planned all studies related to the biological evaluation of the nanoparticles together with AS. LR performed all experiments involving flow cytometry, immunocytochemistry, immunohistochemistry, and immune cell migration. All work related to polymer synthesis and nanoparticle formulation was performed by GE. Data analysis, data interpretation, figures, and writing was performed by LR together with AS.

IV. LR designed and performed the experiments involving immunological assessment of cytokines. LR wrote the corresponding methods part and was involved in reading and commenting on the manuscript drafts.

V. LR planned all studies related to the biological assessment together with AS. LR performed and analyzed all biological data, sialic acid quantification and flow cytometric evaluation. Data related to the synthesis and characterization of the probes was performed by RN. Data analysis, data interpretation, figures, and writing was performed by LR together with RN and AS.

PREFACE

This dissertation was submitted for the partial fulfillment of the degree of Doctor of Philosophy. The original work presented in this dissertation was carried out between February 2022 and May 2026 at the Department of Life Sciences at Chalmers University of Technology, under the supervision of Associate Professor Alexandra Stubelius. The research was funded by the Swedish Research Council.

Loise Råberg
May 2026

Abbreviations

AcDex – acetalated dextran nanoparticles
ADAMTS5 - a disintegrin and metalloproteinase with thrombospondin motifs 5
Asn – asparagine
DAMPs – damage-associated molecular patterns
DDS – drug delivery system
DMOADs – disease-modifying osteoarthritis drugs
ECM – extracellular matrix
FLS – fibroblast-like synoviocytes
GAG – glycosaminoglycans
GalNAc – *N*-acetylgalactosamine
GlcNAc – *N*-acetylglucosamine
GT – glycosyltransferase
IA – intra-articular
IL-1β – interleukin-1 beta
ITIM - immunoreceptor tyrosine-based inhibition motif
LPS – lipopolysaccharide
MAL-I – *Maackia amurensis* lectin I
ManNAc – *N*-acetylmannosamine
MMP – matrix metalloproteinase
MS – mass spectrometry
NEU - neuraminidase
Neu5Ac – *N*-acetylneuraminic acid
NF-kβ – nuclear factor kappa beta
NP – nanoparticles
NSAID – nonsteroidal anti-inflammatory drug
OA – osteoarthritis
PAMAM - polyamidoamine
PEG - polyethylene glycol
PEI - polyethylenimine
PLGA – poly(lactic-co-glycolic acid)
PNA – peanut agglutinin
PNP – polymeric nanoparticle
ROS – reactive oxygen species
Ser – serine
Sia – sialic acid
Siglec – sialic acid-binding immunoglobulin-like lectin
SNA – *sambucus nigra* agglutinin
ST – sialyltransferase
Thr – threonine
TLR4 – toll-like receptor 4
TNF – tumor necrosis factor
WGA – wheat germ agglutinin

Table of Contents

1. Introduction

Glycosylation is present in all cells and tissues and plays an important role in both health and disease. Dysregulated activity of glycosyltransferases (GTs), glycosidases, and altered substrate availability can shift glycan expression patterns, thereby affecting processes such as protein folding and stability, cell adhesion, cell metabolism, and immune regulation. Multiple human diseases, including cancer, autoimmune disorders, diabetes, and osteoarthritis (OA), have been associated with aberrant glycosylation patterns.[1-4] Sialic acid (Sia) is an especially interesting monosaccharide in this regard as it is presented at the terminal ends of glycans, serving as a first point of contact in immune cell communication and recruitment.[4,5] Altered sialylation has been reported in OA, including elevated levels of Sia in synovial fluid (SF),[6] reduced sialylation of the glycoprotein lubricin,[7] and increased α2,3-linked Sia on chondrocytes.[8,9]

For decades, OA was scientifically viewed as a simple mechanical "wear and tear" process linked to aging. As of today, this view has been replaced due to experimental and clinical evidence supporting OA as a whole-joint, multifactorial, and complex disease, with low-grade chronic inflammation as a central component.[10,11] While the whole joint is affected, cartilage degeneration remains a key hallmark associated with progressed OA. To date, no pharmacological treatments exist that can halt or reverse the progression of OA.[12] This is due to the fundamental lack of understanding of the pathology driving the disease. Recent advances in experimental techniques have revealed a link between OA progression and chondrocyte senescence, inflammation of the synovial membrane, activation of fibroblast-like synoviocytes (FLS), local acidification, and recruitment and proliferation of immune cells such as monocytes and macrophages.[13,14] These findings indicate that inflammation could be an earlier and more mechanistically relevant therapeutic target. Multiple efforts have been made to develop disease-modifying therapeutics, including the development of antibody therapies and enzyme inhibitors, targeting pro-inflammatory cytokines and catabolic enzymes. Due to absence of disease-modifying effects, modest improvement in pain scores, and unsatisfactory safety profiles, no therapies have reached clinical approval.[15,16]

An understudied mechanism that may contribute to disease progression involves aberrant glycosylation of proteins and lipids, processes that are essential for maintaining cartilage tissue integrity and governing immune cell responses.[17] Sia-binding immunoglobulin-like lectins (Siglecs) are a family of surface receptors that have gained increasing attention in cancer therapy due to their role as glyco-immune checkpoints.[18] Emerging evidence linking altered sialylation to OA, together with the largely unexplored regulatory functions of Siglecs, points to a potential immunomodulatory axis for disease-modifying therapeutic intervention in OA. However, detailing Sia's role on the receptor level remain challenging with the tools we have today.

In this thesis conventional Sia-detecting techniques were employed to investigate the role of sialylation in OA and inflammation. In addition, Sia-targeting nanomaterials were developed to enhance selectivity and enable immunomodulatory effects. Targeting the joint microenvironment is inherently challenging, because the dense, avascular, and negatively charged cartilage matrix together with the rapid turnover of SF, represents significant biological

barriers that limit drug penetration and retention.[19] Advances in the nanomedicine field offer a promising avenue to overcome these limitations. Nanoparticles (NPs) demonstrate advantages as drug delivery systems (DDS) due to their tunable material composition, size, surface charge, and functionalization, enabling improved targeted delivery and controlled release.[20] However, as NP behavior in complex biological environments remains difficult to predict, improved characterization and evaluation in relevant biological models are essential for the development of clinically translatable nanotherapeutics.

This thesis aims to expand the understanding of Sia- and Siglec-mediated regulation using available commercial strategies and nanotechnology to enhance Sia detection and explore disease-modifying approaches. In **paper I**, I demonstrated that monocyte Siglec-5 regulates Toll-like receptor 4 (TLR4) signaling by binding sialoglycans, revealing a previously unrecognized regulatory mechanism in OA that may be targeted to modulate inflammation. In **paper II**, I investigated the characteristic local acidification associated with inflammation as a trigger for controlled release of an encapsulated model drug from polymeric NPs (PNPs). To induce inflammation-associated acidification, TLR4 was activated in macrophages using lipopolysaccharide (LPS). I showed that the PNPs released the encapsulated model drug in response to the inflammatory environmental cues, demonstrating that careful consideration of the pathological microenvironment is critical for developing more effective and safer DDS. As a strategy to improve Sia detection and target pathological Sia-mediated recruitment of monocytes into joints, a biocompatible Sia-shielding PNP was developed in **paper III**. I showed that this PNP provided proof-of-concept that intricate NP design can achieve precise Sia-targeting with immunomodulatory effects, highlighting Sia as a promising therapeutic target. Given the association between altered glycosylation and OA, I demonstrated in **paper IV** that size- and charge-dependent associations of cartilage-derived glycoproteins give rise to distinct immunological responses by monocyte-derived macrophages. These findings emphasize the importance of considering glycans as critical entities of DDS design. Finally, in **paper V**, I further underscore the role of Sia in OA using several commercially available Sia-detecting methods, including the thiobarbituric acid assay, enzyme-based approaches, metabolic labeling, and lectin staining. The strengths and limitations of these approaches were compared with our synthesized Sia-selective probes, highlighting potentials for improved detection, need for further method development, and future therapeutic applications of OA.

2. Osteoarthritis

OA is one of the leading causes of disability worldwide. Currently, the global burden is estimated at approximately 7-8%, with 595 million people reported suffering in 2020.[21,22] However, the true global burden is most likely underestimated due to sparse data input from certain geographic regions combined with heterogeneity in diagnostic methods. As life expectancy is increasing, the incidence of OA is expected to rise.[22,23] Although OA is often considered a disease of modern societies, it is not a novel disorder. Radiological patterns of OA have been identified in ancient human remains, including mummies, as well as dinosaur fossils dating back 70 million years.[24] Several risk factors are associated with OA, including age, female sex, genetic predisposition, joint trauma, and obesity. Clinical manifestations typically include pain, stiffness, and functional impairment. Current therapeutic strategies have focused on symptom management rather than the underlying mechanisms, which has limited the development of disease-modifying osteoarthritis drugs (DMOADs).[12]

Knee OA accounts for up to 85% of all OA cases worldwide, followed by hand and hip OA.[21,25] Given that the knee is the largest joint in the human body, the susceptibility to degenerative changes is perhaps not surprising. In the healthy knee joint, articular cartilage covers the tibia and femur, cushioning the bone to facilitate frictionless movement. Joint stability is maintained by primary stabilizers such as ligaments and secondary stabilizers such as muscles.[26] Articular cartilage is a specialized avascular, white connective tissue, composed of chondrocytes embedded within an extracellular matrix (ECM). The ECM is rich in collagen type II (COL II), proteoglycans, fibronectin, lubricin, elastin, glycosaminoglycans (GAGs), and water.[27] The high presence of GAGs in cartilage generates a negative charge, an important feature in the tissues' ability to dynamically interact and retain water for its load-bearing capacity.[28] The joint cavity contains SF, which is produced by synovial cells and lubricates the cartilage surface and facilitates joint movement through its high content of hyaluronic acid and lubricin.[26,29]

OA affects the entire joint and is characterized by cartilage degeneration and chronic inflammation. While excessive mechanical loading from joint trauma can damage cartilage, it is also linked to cellular senescence of chondrocytes, activation of FLS, synovial macrophage activation, and infiltration of monocytes that differentiate into pro-inflammatory macrophages.[30] Chondrocyte senescence is a permanent cell-cycle arrest state accompanied by altered cellular metabolism, morphology, and function, limiting their ability to produce and maintain ECM components.[31] Increasing evidence highlights inflammation as a central component of OA, although its manifestation varies considerably between individuals and disease endotypes.[32] Activation of tissue-resident macrophages, together with the recruitment of monocytes and other immune cells, contributes to the pathophysiology of OA. These changes lead to subchondral bone remodeling, formation of bone spurs, and joint narrowing (Figure 1).[23] While genome-wide profiling and omics studies have identified OA-associated genes, substantial variability between individuals and differences across disease stages significantly influence the results, limiting the translation of these findings into effective universal therapeutic targets.[33,34] In **papers I, III, IV, and V** of this thesis, I explored the role and therapeutic potential of glycans, such as Sia in monocyte-driven inflammation in the context of OA.

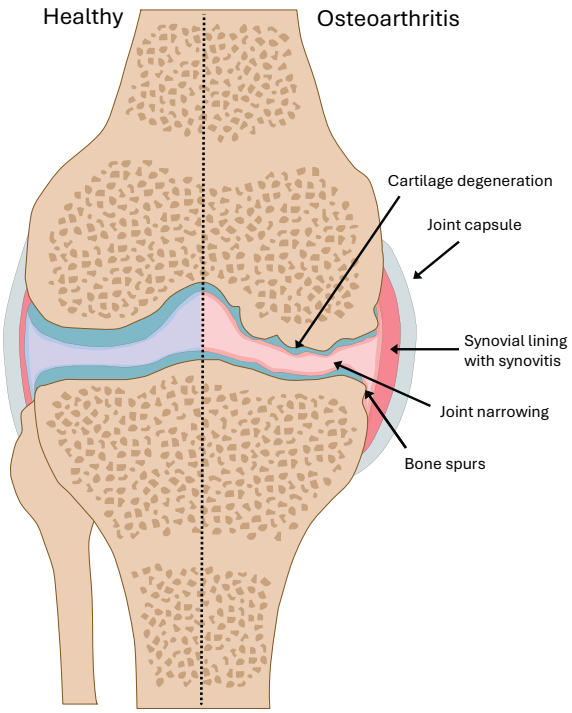

Figure 1. Illustration of a healthy and osteoarthritis knee joints. Cartilage degeneration, synovitis, formation of bone spurs, and narrowing of the joint are common characteristics of osteoarthritis. Created with affinity designer.

2.1. Inflammation

The inflammatory component of OA has been increasingly recognized as a central player in the disease. However, the limited ability to detect inflammation in the early onset of OA has hampered a clear understanding of its contribution to disease progression. Inflammation is a fundamental biological response to tissue injury or external pathogens and plays a critical role in maintaining tissue homeostasis and facilitating tissue repair. Inflammation is commonly classified as acute or chronic inflammation. As chronic inflammation represents a prolonged immune reaction, persisting for several months to years, it represents a key pathological feature of OA and has therefore emerged as an attractive target for altering disease progression. The inflammatory response is orchestrated by the innate and adaptive immune cells, and the dysregulation in immunoregulatory mechanisms contribute to chronic inflammation.[35]

2.2 Inflammation in Osteoarthritis

It was not until the 1980s and 1990s that advances in experimental techniques, along with deeper understanding of cellular mechanisms, led to the establishment of inflammation as a prominent feature of OA joints. Since then, substantial evidence has demonstrated that OA is frequently accompanied by synovial inflammation (synovitis), that chondrocyte senescence contributes to sustained secretion of pro-inflammatory cytokines such as interleukin-1 beta (IL-1β), tumor necrosis factor (TNF), and IL-6, and that recruitment of immune cells such as monocytes perpetuates disease progression.[13] Increasing evidence demonstrates that the

presence of synovitis is linked to radiographically diagnosed OA as well as pain. Synovitis is characterized by increased vascularity, hyperplasia, stromal cell activation, immune cell recruitment, and fibrosis. FLS constitute the main stromal cells of the synovium and can adopt a pro-inflammatory phenotype and interact closely with tissue-resident macrophage and recruited immune cells, including monocytes.[29] Among the immune cells present in the joint, macrophages represent the most abundant population, although monocytes, neutrophils, T cells, and mast cells are also detected.[30,36,37]

Tissue-resident macrophages represents the most abundant immune cell in OA, which contributes to pathogenesis by inducing oxidative stress, secreting proinflammatory cytokines (IL-1β, TNF, and IL-6) and matrix degrading enzymes, such as matrix metalloproteinases (MMPs) and ADAMTS-5.[37,38] Tissue-resident macrophages are constantly replenished by infiltration of circulating monocytes that differentiate into macrophages, thereby sustaining the pathological macrophage populations (Figure 2). The exact mechanism underlying monocyte infiltration remain unclear.[39] A broad range of surface markers have been detected on monocytes and macrophages in OA, underscoring the pronounced heterogeneity and functional plasticity of these cells within the synovium.[40-42] This heterogeneity is difficult to simulate *in vitro*, which has limited the ability to study their functional role. Increased macrophage presence has been linked to elevated production of reactive oxygen species (ROS) correlating with pro-inflammatory signaling.[43] Persistent secretion of cytokines and matrix-degrading enzymes disrupt chondrocyte anabolism, leading to degradation of the cartilage ECM. Cartilage degradation products are subsequently recognized as damage-associated molecular patterns (DAMPs) which activate pattern recognition receptors such as toll-like receptors (TLRs). This activation creates a vicious cycle of inflammation. The OA microenvironment is characterized by hypoxia, increased glycolysis, and lactic acid accumulation leading to mild acidosis, reaching down to pH 5, potentiating inflammation by activating immune cells.[44,45]

Given that macrophages outnumber other immune cells, together with their high plasticity, monocytes and macrophages represent attractive therapeutic targets for modulating the pro-inflammatory microenvironment. The role of Sia and TLR4 signaling was investigated in **paper I**, while therapeutic strategies utilizing the acidic pro-inflammatory microenvironment as a trigger and targeting Sia for immunomodulation of monocytes, were further explored in **paper II-III**.

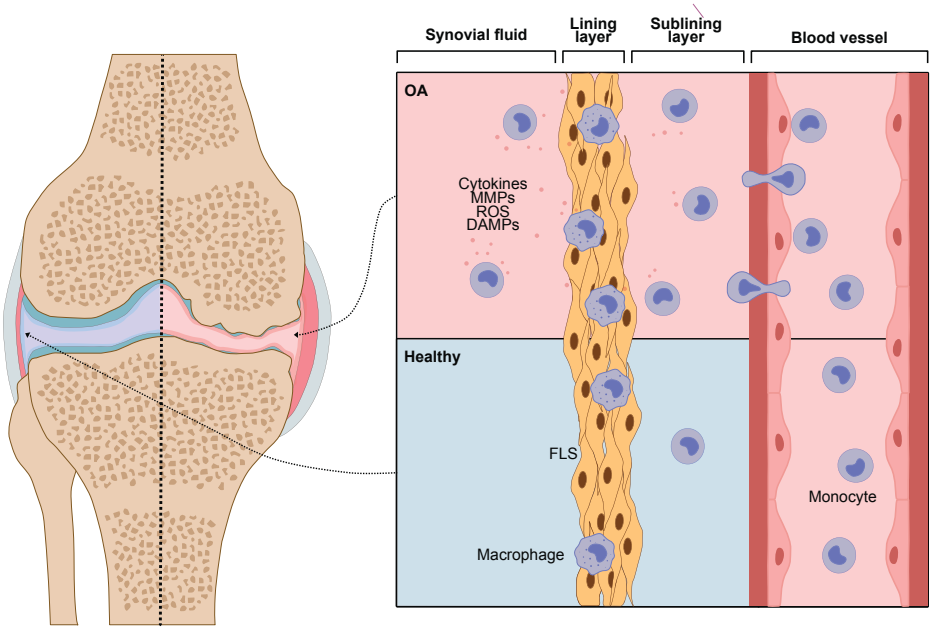

Figure 2. Synovial inflammation is characterized by activation of tissue-resident macrophages and increased infiltration of monocytes. This results in elevated secretion of cytokines, catabolic enzymes like MMPs, ROS, and DAMPs into the synovium and synovial fluid, perpetuating joint inflammation. Created with affinity designer.

2.2.1 TLR4 Signaling in Osteoarthritis

Many pro-inflammatory cytokines and catabolic mediators implicated in OA are upregulated following activation of TLRs. While primarily recognizing pathogen-associated molecular patterns, several TLRs can respond to DAMPs. One prominent example is TLR4, which in response to lipopolysaccharide (LPS) and DAMPs triggers a signaling cascade of cytokines and catabolic mediators through activation of the nuclear factor kappa β (NF-kβ). TLR4 is a glycosylated, membrane-associated receptor that is predominantly expressed on innate immune cells, including monocytes, macrophages, and dendritic cells, although chondrocytes, FLS, and osteoblasts also express TLR4.[46]

TLR4 activation is initiated by the binding of LPS to myeloid differentiation factor-2 (MD-2), resulting in the formation of an LPS/TLR4/MD-2 complex (Figure 3). Downstream signaling is transmitted either through a myeloid differentiation primary response protein 88 (MyD88)-dependent or MyD88-independent pathway. In MyD88-dependent signaling, the intracellular domain Toll/interleukin-1 receptor (TIR) domain recruits adapter protein TIRAP, which in turn recruit interleukin-1 receptor-associated kinases (IRAKs). Recruitment of IRAKs leads to NF-kβ-mediated transcription of pro-inflammatory cytokines. In contrast, MyD88-independent signaling occur via assembly of TIR domain-containing adaptor protein inducing interferon-β (TRIF) and TRIF-related adaptor molecule (TRAM), facilitating transcription of interferon regulatory factor 3 (IRF3) and production of type I interferons.[47]

TLR4 plays a pivotal role in OA pathogenesis by the upregulation of pro-inflammatory cytokines and catabolic mediators produced by macrophages, chondrocytes, and FLS. *N*-

glycosylation of TLR4 has been identified as an important regulatory feature, and enzymatic removal of terminal Sia has been shown to elicit similar pro-inflammatory responses as those induced by LPS.[48-50] Several studies have therefore investigated TLR4 as a therapeutic target for treatment of OA, often by targeting one of the adaptor proteins involved.[51] One example includes the small molecule inhibitor TAK-242 that disrupts MyD88-dependent and MyD88-independent activation by binding Cys747 in the intracellular domain of TLR4. TAK-242 has previously been investigated as an OA therapeutic and showed promising inhibitory effects on TLR4-mediated inflammatory responses.[52] In **paper I**, TAK-242 was used to inhibit TLR4 for mechanistic evaluation of the function of sialoglycans and Siglec-5.

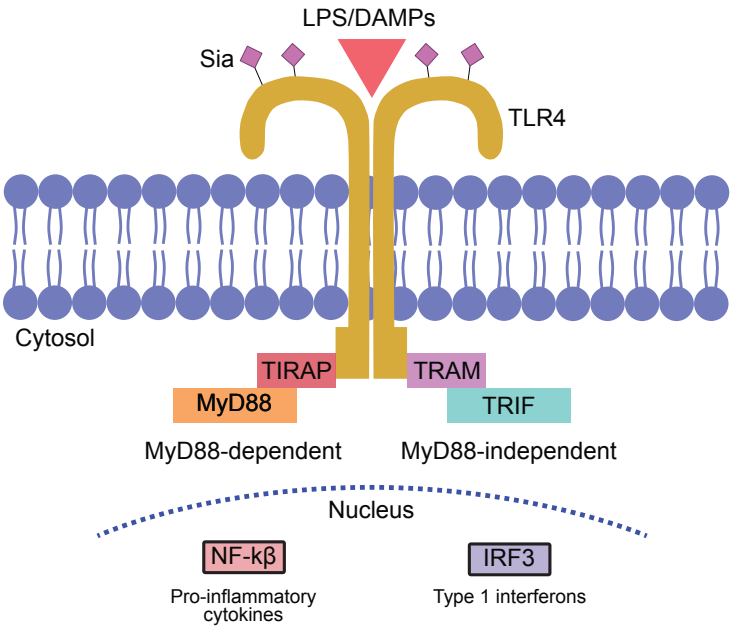

Figure 3. Activation of TLR4 by LPS or DAMPs initiates a signaling cascade by recruiting proteins in the MyD88-dependent or -independent way, leading to production of pro-inflammatory cytokines or type I interferons. Created with affinity designer.

2.3 Diagnosis and Pain Management

Diagnosis of OA is largely based on clinical presentation of symptoms along with conventional imaging techniques, including x-ray, computed tomography (CT), or magnetic resonance imaging (MRI).[30] X-ray imaging allows detection of structural alterations such as subchondral bone changes, narrowing of the joint space, and formation of bone spurs. However, early onset of OA is frequently missed using this imaging technique, as structural changes may not yet be apparent. MRI or ultrasonography enable detection of damaged soft tissues, such as synovitis, which is useful for earlier diagnosis where skeletal changes have not yet occurred.[29,53] Considerable efforts have been devoted to the identification of biomarkers in SF and serum, however, due to limited accessibility of SF, individual differences, and heterogeneity in clinical manifestations, no reliable biomarker has been identified.[30]

Current treatment strategies of OA primarily focus on alleviating pain and improving joint function to increase quality of life. Typically, patients are left with the option of using

nonsteroidal anti-inflammatory drugs (NSAIDs), analgesics, and physical therapy. In advanced stages of OA, treatments include the highly invasive joint replacement surgery.[12] Importantly, neither of these options address the underlying cellular and molecular mechanisms driving the disease, which is why, to date, no DMOADs exist. NSAIDs remain the most common treatment, however, long-term usage has been linked to gastrointestinal complications, cardiovascular disease, and renal failure.[54-57] Intra-articular injections (IA) of corticosteroids, hyaluronic acid, and platelet rich plasma are also used for pain relief, although clinical outcomes vary considerably.[15,58,59] Collectively, these limitations underscore the unmet need for disease-modifying therapeutics that can target the mechanisms driving OA, promote regeneration and stimulate tissue repair to alter the course or slow the progression of OA.

2.3.1 DMOADs

Despite the absence of approved DMOADs, substantial efforts have been made to develop DMOAD candidates and several have reached clinical trial evaluation. For example, monoclonal antibodies or receptor antagonists targeting IL-1 and TNF have reached clinical evaluation.[60-63] Enzyme inhibitors and small molecules directed against catabolic enzymes such as MMPs and ADAMTS5 have been explored as potential treatment options to reduce cartilage degradation. However, these approaches have demonstrated limited clinical efficacy with modest improvement in pain scores, insufficient cartilage regeneration and synovitis reduction.[64-66] Additionally, systemic adverse effects have hampered their translation into approved OA therapies.[15] The above-mentioned DMOAD candidates were initially developed and validated in preclinical animal models, where they demonstrated promising therapeutic effects on chondrocyte anabolic activity, inflammatory suppression, and pain alleviation. For future development of effective disease-modifying agents, nanotechnology has emerged as a promising strategy for enabling controlled drug release, thereby reducing systemic side effects.

3. Glycosylation

Glycosylation is a highly diverse and ubiquitous post-translational modification found in all life domains. Eukaryotes generally present more functionally complex glycans while prokaryotes exhibit greater structural diversity.[67] Glycosylation does not follow the central dogma of template-driven synthesis that underly the productions of DNA or proteins, this generates a vast repertoire of glycosylated structures. Cell surface glycosylation of lipids and proteins results in a dense glycocalyx, often described with the analogy of a dense forest, with glycans protruding out from the surface like branched trees, often being the first point-of contact for other cells.[68] Glycans are therefore highly involved in cell signaling, adhesion, and immune regulation. Consequently, dysregulation in glycosylation has been linked to various diseases and pathologies, glycans has thereby emerged as attractive targets for potential therapeutic intervention. A central question that remains is whether these disease-associated glycosylation changes are triggering the OA pathology or if they arise as secondary consequences of mechanical stress and chronic inflammation.

3.1 Structure and Function

Glycosylation of proteins and lipids regulates their structure and function. In proteins, glycosylation involves the covalent attachment of glycans to either the nitrogen atom of asparagine (Asn), referred to as *N*-linked glycosylation, or to the oxygen atom of serine (Ser) or threonine (Thr), referred to as *O*-linked glycosylation. *N*-linked glycosylation is often initiated in the endoplasmic reticulum (ER), where glycosyltransferases (GTs) facilitate the addition of oligosaccharides to Asn. *N*-glycans are usually branched and classified into complex, hybrid, and high mannose polysaccharides (Figure 4). Further modifications occur in the Golgi apparatus by glycosidases and GTs by the addition of *N*-acetylglucosamine (GlcNAc), mannose, galactose, fucose, and *N*-acetylneuraminic acid (Neu5Ac), also known as Sia. In contrast, *O*-linked glycosylation mainly occurs in the Golgi, and is processed by stepwise addition of individual monosaccharides. *O*-glycans are often found on mucin-type proteins, with *N*-acetylgalactosamine (GalNAc) as the initial monosaccharide. The predominant structure of *O*-glycans in mammals are derived from four core structures which may be further extended by addition of terminal Sia.[1] In addition, glycans can be covalently attached to lipids, affecting dynamic organization and mechanical properties of the lipid bilayers. [69]

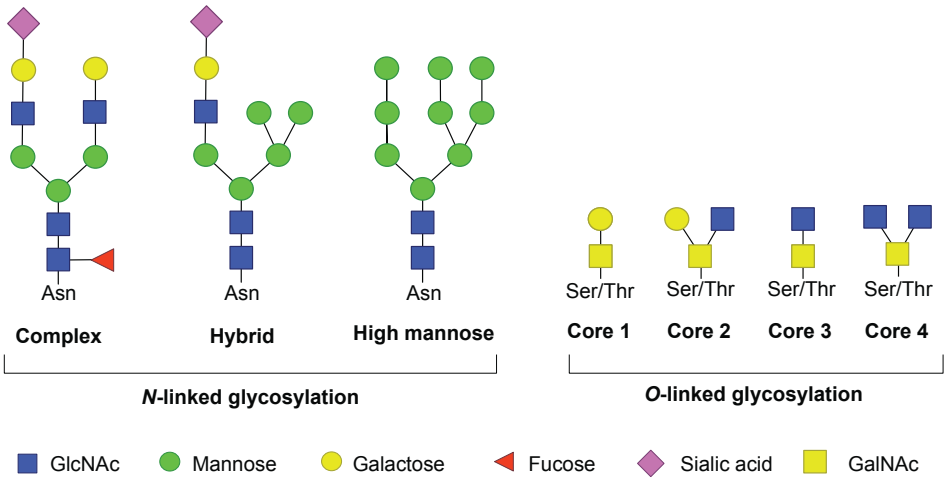

Figure 4. Illustration of *N*-linked glycosylation with complex, hybrid, and high mannose glycans, and the *O*-linked Core1-4 structures. The monosaccharide building blocks of glycans include GlcNAc, mannose, galactose, fucose, sialic acid, and GalNAc. Created with affinity designer.

3.2 Glycosylation in Health and Disease

In OA, altered glycosylation patterns have been detected in multiple joint-resident cells. In chondrocytes, senescence correlates with upregulation of enzymes involved in *O*-linked glycosylation.[70] Truncated and undersialylated lubricin have been found to activate FLS in OA joints, inducing pro-inflammatory responses.[7,71] Increased *O*-linked glycosylation has also been reported in FLS from OA and RA patients.[72] In addition, OA cartilage displays enhanced expression of complex *N*-glycosylation,[73] while increased core fucosylation has been linked to reduced expression of high-mannose *N*-linked glycosylation.[74] Although the mechanisms driving these alterations in glycosylation remain unclear, it is evident that they influence the behavior of chondrocytes, FLS, and immune cells, as well as cartilage, synovium, and synovial fluid in OA.[75]

In other disease including RA, Crohn's disease, inflammatory bowel disease (IBD), and multiple sclerosis, altered IgG glycosylation has been reported.[76,77] Dysregulated glycosylation broadly affects immune cell function, and altered *N*-linked glycosylation has been shown to influence monocyte recruitment during inflammation.[78] Truncated *O*-linked glycosylation has likewise been associated with both IBD as well as cancer.[79,80] Furthermore, changes in glycosylation of receptor proteins including notch, Wnt, and TLR4, have been linked to altered activation of downstream signaling pathways.[1,81] It is convincingly clear that specific glycan signatures on distinct molecular and cellular entities may serve as biomarkers or therapeutic targets for early detection and intervention.

3.3 Sialic Acid

The monosaccharide Sia, with a nine-carbon backbone, commonly occupies the terminal ends of glycan chains. Its position renders Sia important in cellular recognition and communication as it constitutes the first point of contact between cells. It is ubiquitously expressed in all tissues and organs of the body and plays a critical role in both health and disease. More than 50

structural derivatives of Sia have been identified, with *N*-acetylneuraminic acid (Neu5Ac) and *N*-glycolylneuraminic acid (Neu5Gc) being the most abundant forms in mammals.[5]

3.3.1 Sialic Acid Biosynthesis

The biosynthetic pathway of Sia begins in the cytosol with uridine diphosphate *N*-acetylglucosamine (UDP-GlcNAc), which is derived from the hexosamine biosynthetic pathway (Figure 5). UDP-GlcNAc is catalyzed by UDP-GlcNAc 2-epimerase into *N*-acetylmannosamine (ManNAc), which is further phosphorylated by ManNAc kinase into ManNAc-6-phosphate. Sia synthase converts ManNAc-6-phosphate into Neu5Ac-9-phosphate which is further dephosphorylated into Neu5Ac. Neu5Ac is subsequently transported into the nucleus and activated by cytidine monophosphate *N*-acetylneuraminic acid synthetase (CMAS) into CMP-Neu5Ac. The activated Sia is then transported to the Golgi apparatus where it is added to oligosaccharides by specific sialyltransferases (STs).[82] Depending on the ST involved, Sia may be added as a single unit via α2,3- or α2,6-linkage to the underlying galactose or GalNAc, or as repeating units via α2,8- and α2,9-linkages. Endogenous neuraminidases (NEUs), also referred to as sialidases, mediate the enzymatic removal of Sia in a process called desialylation. In humans, four types of sialidases have been identified: NEU1, NEU2, NEU3, and NEU4.[5]

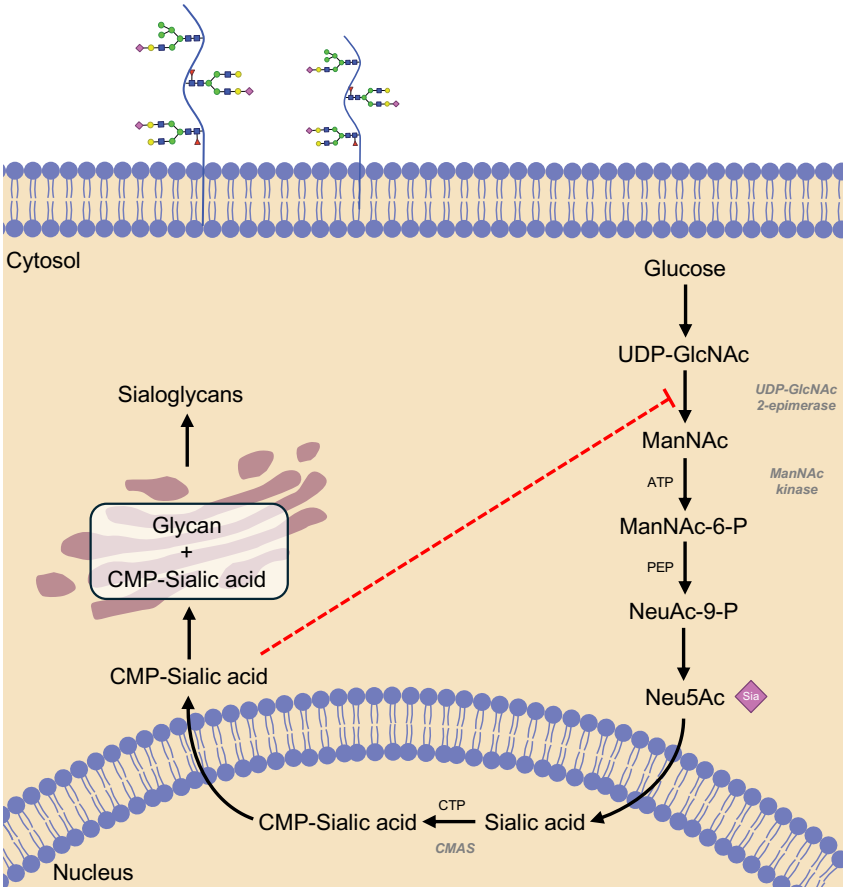

Figure 5. Sialic acid biosynthetic pathway initiated with glucose, followed by several enzymatic conversion steps into UDP-GlcNAc, ManNAc, ManNAc-6-phosphate, NeuAc-9-P, Neu5Ac, CMP-Sialic acid, and final addition to proteins and lipids. Created with affinity designer.

3.3.2 Biological Function of Sialic Acid and Siglecs

Due to the widespread expression of Sia in essentially all tissues and organs, Sia plays a pivotal role in homeostasis. Sia serves as a self-recognizing molecule and is critically involved in brain development and immune cell regulation and communication.[5,83] As it carries a carboxylic group it is negatively charged, which inhibit cell clumping. Receptors belonging to the family of Siglecs, contain an N-terminal immunoglobulin-like V-set domain capable of binding Sia via its carboxyl group. Siglecs are predominantly found on immune cell surfaces and can be of inhibitory or activating nature. The majority of human Siglecs are inhibitory and have a cytoplasmic domain called immunoreceptor tyrosine-based inhibitory motifs (ITIMs), which recruits protein tyrosine phosphatase (SHP-1 and/or -2) when phosphorylated. SHP-1 recruitment can inhibit immune reactions activated by common activating receptors such as TLR4. Human Siglecs are classified into conserved and CD33-related Siglecs.[84] CD33-related Siglecs are rapidly evolving and often differ across species, this limits the ability to understand their role in health and disease. Targeting the Siglec-Sia axis has emerged as a promising glycoimmune checkpoint approach for cancer treatment,[18,85] but represents an underexplored opportunity for targeted treatment of OA.

3.3.3 Implication of Sialic Acid in Diseases

Aberrant sialylation has been implicated in a wide range of diseases, including cancer, Alzheimer's disease, cardiovascular disorders, autoimmune diseases, and OA.[86-90] Dysregulated expression of STs and sialidases alters sialylation patterns, and because Sia is located at the outermost ends of glycans, these changes directly impact cell-cell interactions. Consequently, immune signaling mediated by Siglecs and selectins can be substantially affected. The role of sialylation is particularly documented in cancer, where hypersialyation is a common hallmark. Overexpression of Sia enables cancer cells to evade immune surveillance, facilitating metastatic spread.[87,91]

Arthritic diseases are no exception to aberrant pathological sialylation. As previously mentioned, truncated lubricin in SF exhibits reduced sialylation, which triggers pro-inflammatory responses by FLS.[7,71] In contrast, OA SF contained increased levels of Sia that correlate with radiographic severity.[6] FLS from RA patients display TNF-induced downregulation of the ST involved in adding α2,6 sialylation.[90] Likewise, primary OA chondrocytes shift their expression towards α2,3 over α2,6 sialylation.[8,9] The consequences of altered sialylation in OA likely influence Siglec engagement and immune cell recruitment via selectins, a topic explored in **paper I, III, and V**.

The involvement of Siglecs has been documented across several pathological conditions, including infections, Alzheimer's disease, AIDS, diabetes, and RA, however, their role in OA remains poorly defined. The conserved Siglec-15 contribute to RA pathology regulating osteoclast differentiation and bone resorption.[92] Sialylated TLR2 plays an indispensable role in Siglec-15-mediated osteoclast fusion, and blocking or deleting Siglec-15 in macrophage-derived osteoclasts inhibits fusion and promote bone formation.[93,94] Other Siglecs, such as Siglec-5 and Siglec-9 have been shown to broadly interact with TLRs.[95]

In addition, several Siglecs have been identified in soluble form, suggesting their ectodomains can be shed under certain conditions. Although the role of soluble Siglecs remain poorly understood, they have displayed modulatory properties on immune cells and have been proposed as potential therapeutic tools or as diagnostic biomarkers, particularly in cancer, the chronic autoimmune Sjögren's syndrome, chronic obstructive pulmonary disease, and RA.[96-101] Collectively, current evidence underscores an important role for Sia in inflammation, highlighting it as a potential target for OA therapeutic intervention.

3.3.4 Targeting Sialic Acid for Disease Modulation

Although no approved drugs currently target the Sia axis, several therapeutic approaches aim to remove, mimic, or block Sia for disease intervention, and multiple clinical trials are on-going. One randomized, controlled, multicenter phase II clinical trial is currently evaluating HLX79 (E-602, human sialidase fusion protein) in combination with the monoclonal antibody Rituximab for depletion of autoreactive B cells in an autoimmune kidney disease.[102] E-602 has further been investigated as an antibody-fusion construct for tumor cell desialylation, demonstrating anti-tumor activity, although further optimization will be required due to limited duration of the effect.[103] Another clinical trial is investigating AVD-104, a polysialic acid-coated nanoparticle (NP) targeting Siglec-7, -9, and -11 on macrophages, microglia, and monocytes of the retina in geographic atrophy, an advanced and progressive form of dry eye disease. This represents the first glycoimmune checkpoint modulating therapy to reach clinical validation for geographic atrophy.[104] Finally, a phase II clinical trial involving an anti-GD2 antibody that exerts antibody-dependent cellular toxicity upon binding disialogangliosides has demonstrated efficacy and an acceptable safety profile for treatment of neuroblastoma.[105]

Several pre-clinical studies have attempted to target Sia with promising results. An anti-6-sulfo sLex antibody inhibited lymphocyte homing in allergic rhinitis by blocking the interaction to L-selectin.[106] The inhibition of STs have been investigated as an approach to reduce tumor cell sialylation expression, which showed promising anti-tumor immunity.[107] Other strategies are focused on disrupting the Sia-Siglec axis which has been extensively explored as a glycoimmune checkpoint strategy in cancer.[108] The dynamic metabolic labeling technique has been utilized for exploiting the Sia biosynthesis pathway for functional incorporation of synthetic sugars containing targeting molecules, a strategy for targeted drug delivery and diagnostic applications.[109] Finally, nanomaterials functionalized with PBA exhibit increased affinity to Sia in acidic microenvironments characteristic of tumor cells and inflamed tissues.[110] Multiple modalities using PBA have shown sensitive, pH-dependent Sia-targeting effects suitable for anti-cancer immunity or precision drug delivery.[111,112] Given the several pre-clinical and clinical studies targeting sialylation for disease modification, this certainly represents a promising therapeutic avenue.

A limited number of studies have investigated the therapeutic potential of targeting Sia in OA. A mouse study demonstrated that *Maackia amurensis* seed lectin (MASL) reduced inflammation by partially inhibiting NF-kβ signaling in primary chondrocytes through binding α2,3-linked Sia on podoplanin (PDPN).[9] The microRNA miR-193b was investigated for modulating ST3GAL4, which demonstrated CD44 sialylation modifications that affected NF-kβ in mouse chondrocytes as a potential strategy to reduce OA progression.[113] Finally, a pilot

study investigated 3′-sialyllactose in 60 OA patients by oral administration which revealed improved pain scores, functionality, and reduced stiffness.[114] Given the substantial unmet need for DMOADs, targeting Sia-mediated pathways may represent a promising strategy to halt or reverse OA progression.

4. Nanomedicine

The field of nanomedicine integrates nanotechnology with medical science, a concept that gained formal recognition in the early 2000s. Its foundations, however, date back much earlier. In 1857, Michael Faraday synthesized nanoscale gold colloids, a significant milestone that paved the way for the field of modern nanomedicine. Meanwhile, the word "nanotechnology" did not appear in literature until the 1970s.[115] Since then, a wide range of NPs have been developed and characterized based on their size, shape, and chemical properties. The most common NPs besides polymeric nanoparticles (PNPs) include lipid-based NPs (LNPs), metal-based NPs (MNPs), and carbon-based NPs (CNPs), ranging from 1-1000 nm (Figure 6).[116] NPs offer broad flexibility to tune desirable drug delivery properties such as drug encapsulation, controlled release, modulation of immune cell communication, biosensing, bioimaging, and diagnosis.

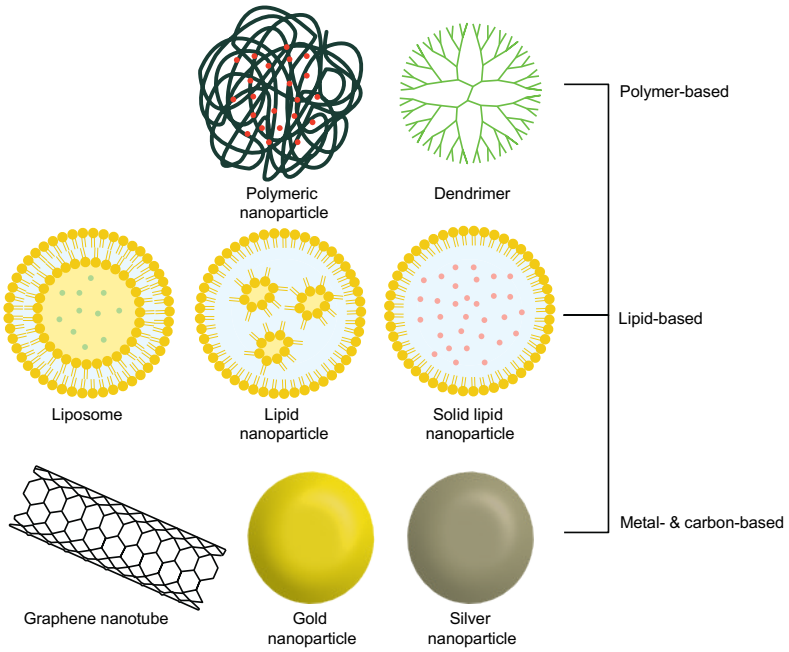

Figure 6. The most common nanoparticles used in nanomedicine, include polymeric nanoparticles and dendrimers, liposomes, lipid nanoparticles, solid lipid nanoparticles, carbon-based nanoparticles such as graphene nanotubes, and metal gold and silver nanoparticles. Created with affinity designer.

4.1 Polymeric Nanoparticles

PNPs are well-established materials for drug delivery due to their biocompatibility, enhanced drug encapsulation capacity, and tunable size. The U.S. food and drug administration (FDA) and European Medicine Agency (EMA) approved synthetic Poly(lactic-co-glycolide) (PLGA) is widely used as drug delivery vehicle due to its biocompatibility and biodegradability.[117,118] PLGA degrades into CO_2 and H_2O and is eliminated from the body through the Krebs cycle.[119] Other approved polymers include poly-(glycolic acid) (PGA) and poly-(lactic acid) (PLA), although, PLGA has emerged as the most attractive option for controlled release. Several studies have demonstrated the therapeutic potential of PLGA-based materials. For example,

PLGA was used as a vector system for delivering growth factor plasmids to the tendon-to-bone interface in a chicken model which resulted in increased healing.[119] Another study showed that loaded PLGA NPs administered to rats with spinal injury demonstrated increased locomotive function, and reduced ROS and IL-1β.[120] PLGA have also been explored as scaffolds for tissue engineering and regeneration, one study reported that 3D-printed PLGA NP scaffolds promoted osteogenesis, highlighting a promising avenue for bone tissue engineering.[121] Despite PLGA's regulatory approval, clinically used PLGA-based systems are predominantly microspheres rather than NPs. Typically, these formulations functions as drug depots for slow release and are employed for treatment of diseases such as prostate cancer, breast cancer, and endometriosis. These include Lupron Depot®, Zoladex Depot®, and Sandostatin® LAR.[122] In **paper III-IV**, PLGA was used as a core for immunomodulatory NPs.

Dextran represents another widely used natural polymer in nanomedicine due to its high density of modifiable functional groups, which enables versatile chemical customization. Derived from bacterial polysaccharides, it offers excellent biocompatibility and biodegradability. Clinically, dextran-coated iron NPs have been employed since the early 1990s for intravenous injection, providing a safer alternative to direct administration of free iron.[123] Numerous recent advances in dextran-based nanotherapeutics have further expanded its potential applications, including showing a promise in for example CAR T cell expansion.[124] In addition, dextran NPs exhibit pH-responsive behavior, where amide bonds are cleaved under acidic conditions, triggering controlled drug release, a feature particularly advantageous for cancer therapy and other inflammatory conditions such as RA.[125,126] The pH-responsive drug release of a dextran-based NP *in vitro* was investigated in **paper II**.[127]

While PLGA and dextran are linear, dendrimeric NPs, which were first reported in the 1970s, are highly branched and spherical.[128] Their structure is reminiscent of a tree, with a core, branches, and functional groups. Dendrimers have been investigated as vehicles for drug delivery, gene delivery, and as vaccines. Their small size ranging between 1-15 nm, spherical shape, and functional groups make them attractive nano-platforms. Polyamidoamine (PAMAM)-based dendrimers have been widely investigated as drug carriers and have shown promising results, however cytotoxicity has also been reported due to their cationic charge.[129] Nevertheless, several dendrimers have reached clinical approval and are used as antibacterial and antiviral agents for vaginosis, HIV, SARS-CoV-2, as transfection agents, and as MRI contrast agents.[130-132] Small cationic dendrimers have previously been investigated for OA treatment as their small size is suitable for cartilage tissue penetration.[133-135] In **paper IV**, the immunological response to dendrimers associated with catabolic glycoprotein-coronas were investigated.

4.1.1 Other Nanomaterials

Several LNPs have been developed, including liposomes, solid lipid NPs, and lipid-polymer hybrid NPs. LNPs gained significant global recognition following the development of the Covid-19 vaccines in 2020.[136] However, they may suffer from degradation, drug leakage, and accumulation in hepatocytes.[137,138] Gold and silver NPs represent the most common MNPs, and several MNP formulations have progressed to clinical trials, primarily in the context of cancer therapy, and some MNPs have been FDA approved, mainly as contrast agents for MRI.[139,140]

However, the small size of MNPs results in high surface-area-to-volume ratio, which can promote nonspecific interactions with biomolecules and lead to unintended cellular uptake, raising toxicity concerns.[141,142] CNPs exhibit unique chemical, physical, and biological characteristics that have been investigated for drug delivery, tissue engineering, and imaging. The most common constituents are graphene, fullerene, and carbon nanotubes. Functionalized CNPs have shown promising anti-cancer effects *in vitro* and *in vivo*.[143,144] To date, no CNP has reached FDA-approval.[145]

4.2 Physicochemical Properties

Physicochemical properties including size, shape, dispersity, aggregation, colloidal stability, optical properties, morphology, and surface functionalization, can be optimized to affect biodistribution, metabolic behavior, and circulation time of a nanomaterial.[20] One study found that the size of PLGA-based NPs affected biodistribution, with small ~120 nm NPs being endocytosed in the lung and bone marrow, while larger NPs, up to 440 nm were sequestered in the liver and spleen.[146] Smaller particles are generally more readily taken up by cells, as larger particles results in decreased surface-to-volume ratio and reduced contact area with cells.[147] In terms of charge, cationic NPs are better for targeting cells over anionic NPs, however, they are generally more cytotoxic due to their strong interaction with negatively charged cell membranes.[148] Colloidal stability is important for long-acting treatments of for example chronic diseases but may possess more cytotoxic effects. Short-acting carriers are usually more biocompatible, but not appropriate for long-term treatments due to their fast elimination.[20]

In order for NPs to reach their full potential, surface functionalization is usually required. Surface modification can involve covalent or non-covalent interaction of inorganic, organic, or biomolecular modifications.[149] A common functionalization is modification with PEG to increase hydrophilicity and colloidal stability.[20] For targeted drug and gene delivery, antibody functionalization represents a common strategy.[150-152] Boronic acids have emerged as lectin-mimetic functionalization units for targeted delivery to cancer cells overexpressing Sia. Boronic acid derivatives possess unique pH-dependent affinity that favors binding of Sia in acidic tumor microenvironments or inflamed sites such as in OA joints. They form reversible covalent boronate esters with the diols of Sia and have therefore been investigated for drug loading, biorthogonal chemistry, and biosensing. [110,153] Boronic acids have gained increased recognition in recent years due to the FDA-approval of several BA-containing drugs.[154,155] For diagnosis, biodistribution, or drug release by PNPs, functionalization can include the addition of fluorescent tags. This may include covalent attachment or encapsulation within the core as a model drug. Fluorescently tagged NPs can be analyzed for colocalization with target molecules.[156]

4.3 Administration and Elimination of Nanoparticles

Common administration routes for NPs include oral, intravenous, subcutaneous or intramuscular administration.[147] For oral administration, the acidic environment and presence of enzymes in the stomach and gastrointestinal tract can lead to NP degradation, especially of peptide-containing NPs. Injection of NPs overcomes the rapid degradation and clearance by first-pass metabolism. Functionalization strategies can circumvent certain biological barriers,

where opsonization for example can be prevented by PEGylation, and are then referred to as "stealth" NPs.[157] However, elimination from circulation is not straightforward and may lead to NP accumulation. The two main mechanisms for elimination involve renal elimination and hepatobiliary elimination. Renal filtration is limited to particles with a hydrodynamic diameter in the 5 nm range. Hepatobiliary elimination is underexplored and nonbiodegradable NPs may accumulate in the liver, while biodegradable NPs can be excreted with feces.[158] Another option is local injection which has been widely applied in orthopedics, and can reduce systemic side effects due to the lower drug concentration needed.[159] Drug-loaded PLGA-based microspheres have been used as drug depots of prolonged controlled release in the joint, such as the FDA approved corticosteroid triamcinolone (Zilretta).[160] The local joint environment presents multiple barriers to consider, such as the viscous SF containing lubricin, hyaluronic acid, and ECM proteins and glycoproteins that can adsorb to NPs in the form of coronas. Other barriers include phagocytosing macrophages, the highly anionic dense cartilage tissue, and the rapid turnover of SF.[19] Administration route, biological barriers, and elimination of NPs are important aspects to consider in the design and formulation process to ensure clinical translation.

4.4 Nanotherapeutic Strategies for Osteoarthritis Treatment

The application of nanotherapeutics present a promising avenue for OA treatment due to their tunable physicochemical composition. IA injection of nanotherapeutics represents the most common administration route due to localization of the drug at the disease site with reduced systemic side effects.[161] IA injection of free drugs suffers rapid clearance and off-target effects. Drug delivery by nanocarriers can overcome these limitations due to increased targeting ability and drug encapsulation. Several studies have designed NPs with promising effects in OA. pH-responsive NPs have shown promising results in terms of cartilage penetration, lubrication, and controlled release *in vivo*. The acidification of joints offers a triggering mechanism that can be utilized for controlled release.[14,162] A PLGA nanocomposite microgel showed increased retention in cartilage and synoviocytes in mice, with no adverse effects observed.[163] Another study, demonstrated how ghrelin mRNA-loaded anionic PLGA NPs showed severity-responsive delivery to cartilage lesions with high loss of GAGs. Ghrelin, a peptide hormone has demonstrated anti-inflammatory effects in cartilage, and delivery of ghrelin-mRNA led to reduced cartilage degradation, thickening of subchondral bone, and reduced pain in a mouse model.[164] Other studies have employed dendrimers due to their cationic charge and small size, favorable for cartilage penetration. A PEG-PAMAM NP acted as a sponge/scavenger and effectively removed cell-free DNA, resulting in anti-inflammatory effects and increased retention time in the joint in a rat model.[165,166] While the pre-clinical studies demonstrated optimistic results in altering OA progression, only a handful of nanoplatforms have reached clinical trial. These are primarily limited to empty or dexamethasone-loaded liposomes for pain relief rather than treatment of the underlying cause.[167,168] Zilretta, a PLGA-microsphere formulation encapsulating triamcinolone acetonide for extended IA release, has been FDA approved for the treatment of OA pain.[160] Future nanotherapeutics should consider the integration of immunomodulatory properties in nanomaterials for optimal disease-modifying effects in OA.

5. Experimental Methods

This chapter outlines common experimental approaches concerning the study of OA, glycosylation, NP characterization, and NP evaluation. Past, present, and emerging methods are discussed while detailing the strategies used in this thesis.

5.1 Models to Study Osteoarthritis

To elucidate the cellular and molecular mechanisms driving OA pathology, relevant biological models are required. In this section, a list of well-established as well as emerging experimental approaches are discussed.

5.1.1 Human Samples

OA studies based on human-derived samples show physiological and clinical relevance, however, are frequently constrained by small patient cohorts, pronounced biological heterogeneity, and diverse clinical presentation. Collectively, these factors complicate robust patient stratifications.[169] As a result of the limited availability in patient-samples, OA pathology and therapeutics are predominantly investigated using *in vitro* and *in vivo* models. In this work we acquired a limited number of OA patient-derived SFs which were included and improved the physiological relevance to **paper I** and **III.**

5.1.2 *In vitro* Assays

Traditional *in vitro* models primarily focus on chondrocytes cultured in monolayers or 3D environments. Inflammatory conditions are typically induced using cytokines such as IL-1β, TNF, or IL-6. Other cells used includes primary FLS, monocytes, or macrophages derived from established cell lines or primary sources. *In vitro* models offer many advantages but also often fail to recapitulate the complex physiological joint environment. Despite this, *in vitro* assessment of pharmacological treatments remains important for *in vivo* prediction. [170,171] Proper characterization of drugs *in vitro* can reduce the number of animals required for *in vivo* studies, aligning with the 3R principle for ethical research. Accordingly, many of the studies included in **paper I-V** were performed *in vitro* with cells cultured in monolayers at standard conditions (37°C in a humidified environment containing 5% CO_2). A range of commercialized cell lines derived from different tissues and species, as well as primary cells from human donors were used, including the cell lines from human liver (HepG2), kidney (HEK293T), monocytes (U937), chondrocytes (Tc28a2), neutrophil-like cells (HL60), and T cells (Jurkat), as well as murine macrophages (RAW264.7). Immortalized cell lines were used as they generally are robust, easy to handle, inexpensive, and reproducible. In contrast, primary cells, isolated from buffy coats derived from anonymous blood donors, were used as they reflect the *in vivo* environment more closely giving them an advantage for translational research.[172]

5.1.3 More Complex *in vitro* Models

Recent advances have led to the development of more physiologically relevant culture platforms, including organoids, co-culture systems, explant models, and organ-on-a-chip models.[173] Cartilage organoids offer a promising approach to simulate native cartilage architecture, enabling mechanistic studies and drug screening.[174] Co-culture systems that combine multiple cell types allows modeling of complex cell-cell interactions and can be

integrated into microfluidic organ-on-a-chip devices. Interactions between chondrocytes, osteoblasts, fibroblasts, and macrophages have been demonstrated using such platforms.[175,176] In **paper I** and **III**, we employed a co-culture system combining primary monocytes with OA SF to investigate immune cell activation and migration in a disease-relevant OA milieu. Native cartilage explant models are widely used to study mechanical loading, drug delivery, cartilage degradation, and can be combined with other cells.[134,177] In **paper IV-V**, porcine cartilage explants treated with catabolic enzymes were used to assess how glycosylated ECM components influence nanoparticles and how loss of Sia is associated with cartilage degeneration.

5.1.4 *In vivo* Models

As current *in vitro* models cannot fully replicate the complexity of the joint, many studies rely on preclinical animal models. Rodents, including mice and rats are commonly used due to their short generation time, low cost, genetic manipulability, and ease of handling. OA can be induced surgically, chemically, or mechanically, or allowed to develop spontaneously. These models are indispensable as they provide a functional joint for studying disease mechanisms and therapeutic responses. However, rodents differ from humans in terms of anatomy, biochemistry, and immunologically. Consequently, many therapies that show promise in animals fail in clinical translation. As a result, more predictive *in vitro* platforms, advanced engineered models, and large clinical datasets are urgently needed to better bridge the gap between preclinical research and human disease.[173,178,179] No *in vivo* studies were performed in this work, but NP staining was performed on mouse spleen sections in **paper III,** providing a physiologically relevant model for evaluation of NP-specific cell targeting.

5.2 Primary Cell Isolation

In this thesis, primary human peripheral blood mononuclear cells (PBMCs), monocytes, and T cells were isolated from buffy coats. PBMCs were obtained by density gradient centrifugation, enabling the separation of mononuclear cells (monocytes, T cells, B cells, NK cells) from granulocytes and red blood cells. The gradient medium typically has a density of 1.077 g/mL, leaving PBMCs with lower density at the upper fraction while higher density cells such as red blood cells and granulocytes end up in the pellet (Figure 7).[180] Monocytes were isolated using two different techniques: plastic-adhesion and negative selection by RosetteSep. Plastic adhesion separates monocytes from PBMCs by exploiting their ability to grow and adhere on tissue culture-treated plastic surfaces. While this procedure suffers in the yielded purity of cells, it provides an easy and cost-effective approach to isolate monocytes. In contrast, negative isolation by RosetteSep allows improved enrichment purity of both monocytes and T cells by crosslinking unwanted cell populations with red blood cells but often suffer from platelet contamination. The resulting RosetteSep-treated buffy coat is layered over a density gradient medium and centrifuged, the unwanted crosslinked cells subsequently sediment in the pellet, leaving monocytes or T cells in the upper PBMC fraction.[181] Another widely used isolation technique includes magnetic bead isolation, both for negative and positive selection. Positive selection using magnetic beads is a more expensive approach with enhanced purity yield, but has been demonstrated to alter the phenotype by binding for example CD14.[160]

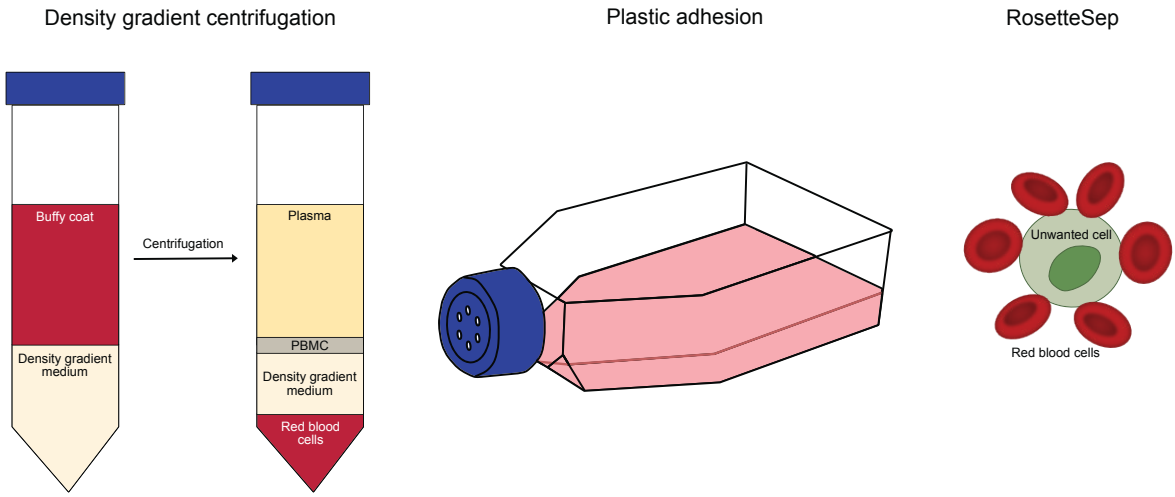

Figure 7. Primary human peripheral blood mononuclear cells were isolated using density gradient centrifugation, primary human monocytes were isolated by plastic adhesion or RosetteSep, and T cells were isolated by RosetteSep. Created with affinity designer.

5.3 Detection and Quantification of Glycans

Detection and characterization of glycans remain challenging due to their inherent structural heterogeneity. The sequential addition of a monosaccharide is dictated by the previous residues, resulting in extensive diversity and absence of a defined final structure. Historically, these features have limited the development of new techniques for comprehensive detection of glycans. In this section, the current standard approaches along with newer techniques are described.

5.3.1 Mass Spectrometry and NMR

To date, mass spectrometry (MS) remains the gold standard for analysis of glycan structures. Conventional full scan MS techniques provide a spectrum based on molecular mass that can elucidate the monosaccharide composition of glycans. However, MS is often coupled with additional separation methods as MS alone cannot distinguish glycans of similar mass. Common separation methods include liquid chromatography (LC), capillary electrophoresis (CE), high performance liquid chromatography (HPLC), and ultrahigh pressure liquid chromatography (UPLC).[182,183] In **paper I**, we used LC-MS to confirm that sialidase removed Sia from monocyte-associated glycans. Despite its widespread use for glycan analysis, MS has several limitations, including tedious sample preparation, difficulties in resolving isobaric and isomeric structures, and complicated and demanding data analysis. Problems with solving isomeric structures can be solved with coupling to existing and emerging derivatization techniques.[184] Other detection methods include nuclear magnetic resonance (NMR), which is less sensitive and has a lower throughput compared with MS, but has nevertheless been shown to be a powerful tool for structure analysis of *N*-linked glycans.[183]

5.3.2 Lectin-based Detection

Lectin-based approaches such as lectin blotting, lectin microarrays, and lectin immunohistochemistry, exploit lectins as they are natural carbohydrate-binding proteins. Although lectins cannot resolve the complete glycan structure, they enable rapid detection of distinct motifs, such as mannose, galactose, and Sia.[185] Lectin-based approaches represent one of the most common, easy, and inexpensive approaches to detect sialoglycans. *Maackia amurensis* lectin (MAL) and *Sambucus nigra* agglutinin (SNA) are widely used lectins used for Sia detection, with MAL detecting α2,3-linked Sia and SNA detecting α2,6-linked Sia. Lectins conjugated to a fluorophore allow detection through fluorescence microscopy, microplate reader, or flow cytometry (Figure 8). However, some lectins such as wheat germ agglutinin (WGA) that targets Sia and *N*-acetyl-D-glucose, can cause cell agglutination/clumping, making it difficult for analysis by flow cytometry. In **paper I**, **III**, and **V**, lectin-based approaches were used to confirm sialidase-specificity and inflammation-associated alterations in sialylation using flow cytometry and confocal microscopy. To increase specificity to certain sialylated structures, antibodies have been developed and explored for diagnostic and therapeutic purposes. Some examples include anti-GDS targeting disialogangliosides in neuroblastoma,[105] a novel monoclonal antibody (L2A5) targeting truncated sialyl-Tn,[186] and a monoclonal antibody targeting 6-sulfo sialyl lewis x (sLex).[106]

5.3.3 Metabolic Labeling

Glycan biosynthesis and turnover can be measured using metabolic labeling, a technique based on biorthogonal chemistry, a Nobel prize winning method pioneered by Prof. Carolyn Bertozzi.[187,188] Here, a synthetic monosaccharide precursor containing a biorthogonal functional group is supplied to cells. The incorporated monosaccharides can subsequently be detected using click-chemistry. Metabolic labeling is the only method that can track metabolically activate subsets of glycans in a dynamic *in vitro* or *in vivo* setting, providing an important tool for studying the dynamic regulation in physiological and pathological conditions.[189,190] This technique was employed for detection of the metabolism of Sia by Tc28a2 chondrocytes, HL60 neutrophils, and U937 monocytes in **paper III** and **V**. Here, we used a synthetic DBCO-tagged *N*-acetylmannoseamine derivative (*N*-dibenzocyclooctyne-tetra-acetylmannosamine, Ac_4ManNDBCO), a precursor to Sia. The DBCO tag can react with an azide reporter through click-chemistry, in our case we used Cy5-azide (Figure 8). As DBCO is quite bulky and hydrophobic, it can be more favorable to functionalize the sugar precursor with an azide and use DBCO with a fluorophore instead. However, the metabolic labeling still provided a simple and relatively fast approach for detection of inflammation-related changes in Sia metabolism. Incorporation of a synthetic sugar can be detected using a microplate-reader, flow cytometry, or by fluorescence imaging.

5.3.4 Thiobarbituric Acid Assay

One of the earliest Sia detection methods is the colorimetric thiobarbituric acid assay, also known as the Warren method, developed by L. Warren in 1959.[191] In this assay, Sia is oxidized to formylpyruvic acid by reaction with sodium periodate in concentrated phosphoric acid. The resulting formylpyruvic acid subsequently reacts with thiobarbituric acid, forming a distinct pink chromophore, which can be detected by measuring optical density at 549 nm or

fluorometric analysis with excitation of 555 nm and emission of 585 nm. The fluorometric procedure is approximately tenfold more sensitive than the colorimetric approach. While the method is limited to detection of free Sia, sample processing using sulfuric acid at 80°C followed by centrifugation at 14,000 rpm to remove debris, enables quantification of total Sia. Although the assay is relatively simple and rapid, it can become labor-intensive as sample numbers increase. In addition, the thiobarbituric acid may react with other carbohydrates, affecting sensitivity.[192] Nevertheless, the method remain in use and provide a cost-effective approach for detection of Sia in samples such as serum and plasma.[193] It can be used for detecting Sia in more complex tissue samples as well, however as it involves acidic processing the samples will be destroyed. In my work I used the thiobarbituric acid assay for total quantification of Sia in OA SF in **paper V**, which provided a quite rapid and inexpensive strategy.

5.3.5 Enzymatic Approaches

Enzymatic approaches are also widely employed to study Sia and Sia-mediated interactions. The use of sialidases from external sources, such as from *Clostridium perfringens*, is common, inexpensive, and provides a sensitive enzymatic strategy for selective removal of Sia, which can be combined with downstream use of established detection methods (Figure 8).[194,195] Enzymatic removal of Sia using sialidases led to the discovery of multiple glycan-binding proteins such as Factor H, selectins, Siglecs, and CD28 co-stimulation with CD80.[196-199] Inactive sialidases have shown promising use as detection tools due to their preserved affinity for Sia while lacking the ability to hydrolyze it.[192] Sialidase was used in **paper I**, **III**, and **V** to understand the functional consequence on Siglec-5-TLR4 interactions and the specificity of our developed Sia-targeting nanoparticles and probes. While it is sensitive it may however not be possible to remove all Sia.

5.3.6 Boronic Acid Lectin Mimetics

Boronic acid derivatives such as PBA, have emerged as promising, inexpensive, and stable tools to target Sia as they readily interact with 1,2 or 1,3 diols, forming reversible boronate esters (Figure 8). PBA can interact with the glycerol sidechain between carbon 7 and 9 on Sia, although the interaction is stronger to free Sia.[200] PBA functionalized NPs have been investigated and demonstrated promising therapeutic effects by targeting hypersialylated cancer cells and potential use as diagnostic agents.[110,112,201] In **paper III** we investigated the Sia-targeting ability of a PLGA-based NP functionalized with multiple PBA units for increased avidity, and in **paper V**, PBA was conjugated to the fluorescent dye with FRET-based sensor capability for direct monitoring of Sia binding.

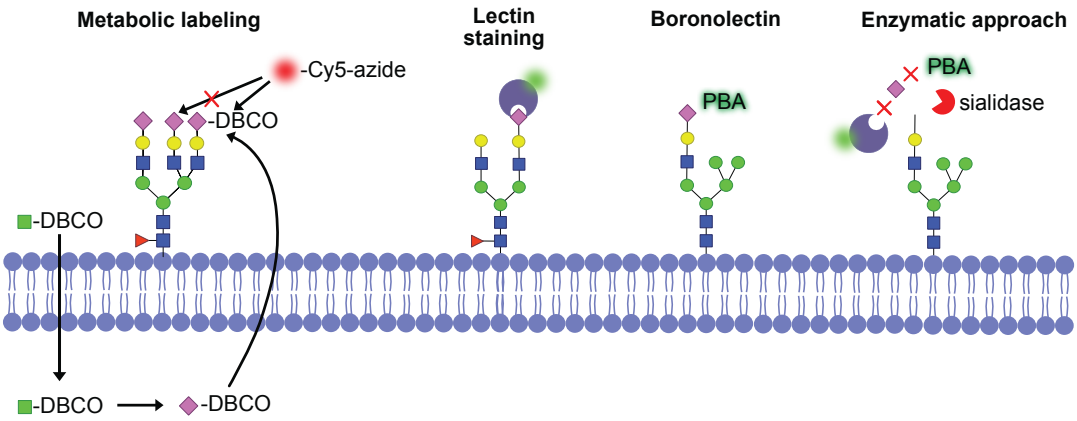

Figure 8. Methods used for detecting Sia in this thesis including metabolic labeling, lectin staining, boronolectin strategies, and enzymatic approaches. Created with affinity designer.

5.4 Nanoparticle Characterization

To ensure efficacy, stability, and safety of NPs, thorough physicochemical characterization is required along with comprehensive biological evaluation. Although physicochemical characterization is not the primary focus of this thesis, the most common approaches will be briefly introduced. The following section then discusses gold-standard *in vitro* methodologies for biological evaluation.

5.4.1 Chemical Characterization

Typical formulation strategies for PNPs include emulsification, nanoprecipitation, solvent evaporation, dialysis, microfluidics, or electrospray techniques.[137] In **paper II-III**, nanoprecipitation was used for NP formulation. Although PNPs have shown promising potential as DDS for treatment of multiple diseases, challenges remain due to toxicity of residual solvents, burst release, poor drug loading, and scalability issues. [137,202] For future clinical translation, these challenges need to be addressed for optimal PNP development. To achieve optimal development, proper characterization is paramount. The size, stability, and polydispersity of NPs are commonly evaluated using dynamic light scattering (DLS) and X-ray Diffraction. All NPs included in this thesis have been characterized through DLS to ensure uniform size but also for evaluation of stability over time. Several microscopic techniques such as scanning electron microscopy (SEM), transmission electron microscopy (TEM), and atomic force microscopy (AFM) are commonly used for assessing size, shape, and morphology. The shape and size of the NPs in **paper II-IV** were evaluated using SEM. AFM was used for evaluating distinct glycoprotein patterns associated with NPs in **paper IV**. Chemical composition can be evaluated using Fourier transform infrared spectroscopy (FTIR) and nuclear magnetic resonance (NMR).[202] NMR was used in **paper III** and **V**, and FTIR was used in **paper V**.

5.4.2 Biological Characterization

Following chemical characterization, biological evaluation is performed to ensure biocompatibility, specificity, and proper drug release. NP toxicity screening is usually performed on commercial cell lines using colorimetric assays such as Alamar blue, MTT, and

LDH assays. According to the international standard ISO 10993-5, all medical devices are required to be tested, and cytotoxicity is considered when viability goes below 70%.[118] Despite efforts to standardize cytotoxicity testing, considerable variations in results have been observed between different laboratories.[203] In this thesis, the resazurin viability assay, commercially known as Alamar Blue, was employed for evaluation of nanomaterial biocompatibility across various cell lines. Resazurin is a non-toxic blue dye, that upon uptake, is reduced to the highly fluorescent compound resorufin by NADPH or NADH in the mitochondria. Resorufin is excited between 530-570 nm and emits light between 580-610 nm. The measured fluorescence intensity is directly proportional to relative cell viability.[204] Resazurin viability assay and LDH offer advantages over MTT as they are non-destructive, simple, and not as time consuming. In contrast, the resazurin assay and MTT showed greater signal-to-noise ratio compared to LDH.[205]

In recent years, extensive efforts have been made to develop alternative ways to investigate NP specificity and behavior *in vitro* by setting up vessel-on-a-chip and organ-on-a-chip models, enabling assessment in dynamic flow and influence of shear stress.[206] In **paper III**, we used a simple version of the vessel-on-a-chip model for investigating whether our PNPs could bind cells in a dynamic environment mimicking blood circulation. Additionally, we have evaluated NP specificity by integrating enzymatic methods and evaluated NP binding with flow cytometry and confocal microscopy. While significant improvements in chemical and biological characterization of nanomaterials have been made, challenges remain due to instability, low reproducibility, and failure to replicate complex biological environments.

As a pH-sensitive PNP was developed in **paper II** to enable drug release in response to acidic environments, a ROS-detecting probe was used as a model drug. The 2,7-dichlorofluorescein diacetate (DCFH-DA) was chosen as model drug cargo as it is a cell-permeable fluorogenic probe reacting to ROS. When stimulating cells with agents such as LPS to induces pro-inflammatory responses, the metabolic activity is expected to rise which generally lowers the pH. When DCFH-DA enters the cytoplasm of a cell, local esterases cleave off acetyl groups, yielding DCFH, which is further oxidized by ROS into 2'-7'dichlorofluorescein (DCF). DCF is highly fluorescent and emits green fluorescence at excitation wavelength 485 nm and emission wavelength of 530 nm. This probe provides a cost-effective approach for ROS detection, which can be quantified using a microplate reader, flow cytometry, or fluorescence microscopy.[207]

5.5 Readout and Imaging Techniques

Flow cytometry, cytokine quantification assays, and confocal imaging are three techniques used for analytical and immunological assessment throughout this work. These techniques are described in the following section.

5.5.1 Flow Cytometry

Flow cytometry is a well-established single cell laser technology, used to study cells or particles, usually containing fluorescent conjugates (Figure 9). Flow cytometry is divided into three different components: fluidics, optics, and electronics. In the fluidics system, a process called "hydrodynamic focusing" is carried out. Here, cells or particles in suspension are

pressurized to the interrogation point by sheath fluid (PBS or water). At the interrogation point the sample is excited by one or more laser beams of different wavelengths, generating scattering of light and fluorescence emission signals. Light scatter is detected based on light along the laser, called forward scatter (FSC), and light scatter at a 90° angle is called side scatter (SSC). Together these allow discrimination of cells based on size and internal complexity/granularity. This optical output is directed and amplified by specific detectors, such as optical filters and dichroic mirrors, allowing detection of multiple fluorophores. Due to high dynamic range and low intensity levels of photons emitted by cells, the signals are amplified in the electronics system. Many flow cytometers use photomultiplier tube detectors, but avalanche photodiodes (APD) are common too. Essentially what they do is to convert photons into photoelectrons, then dynodes multiply the signal, and as photoelectrons move towards the amplifier, a voltage pulse is generated and finally converted to a digital signal. [208]

Flow cytometry was employed for several different applications in **paper I, III-V**, such as evaluating cell viability using live dead stains, detecting surface markers and receptors such as TLR4 and Siglec-5, exploring binding affinities of fluorescence-conjugated NPs, establishing sialylation patterns using lectins, and to evaluate the loading efficiency of FITC in PLGA NPs.

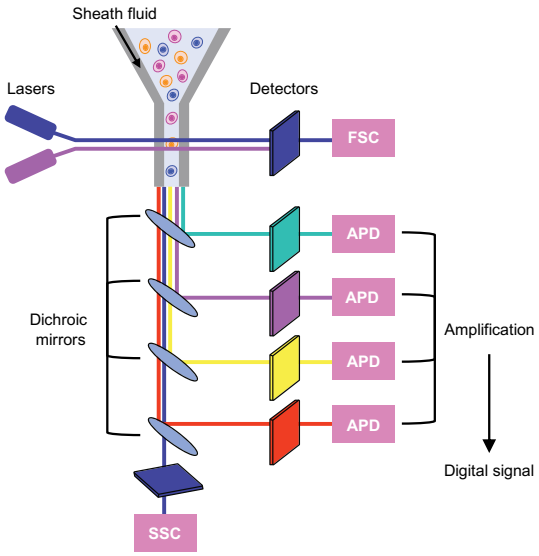

Figure 9. Illustration of how cells are focused to the interrogation point by sheath fluid, subjected to laser beams, and how scattered and emitted light is directed to different detectors and filters and finally converted to a digital signal. Created with affinity designer.

5.5.2 Cytokine Quantification

Quantification of cytokines released in cell supernatants or biological fluids provides information about immune responses and inflammation. Immunoassays such as enzyme-linked immunosorbent assay (ELISA) and multiplex immunoassays (Luminex and LEGENDplex) were used to assess cytokine concentrations.

Detection of single analytes such as IL-6 were performed through the classical sandwich ELISA in **paper I** and **III**. Briefly, a 96 well plate is coated with a capture antibody against the analyte

of interest. A detection antibody forms a sandwich complex if the analyte has bound allowing colorimetric quantification. The classical sandwich ELISA is relatively cheap and simple and only requires a plate reader. However, it often requires 100 µL of the sample.

The LEGENDplex assay is based on the same principle but allows quantification of up to 14 analytes simultaneously. The kit comes with two bead populations of different sizes and APC fluorescence, as well as pre-coated antibodies for the individual targets. Once the sample has bound, a cocktail of biotinylated antibodies is added. Subsequently, PE-streptavidin is added. The data is collected by flow cytometry where the two bead populations are separated by FSC against SSC, and the analytes by APC expression. PE-streptavidin allows determination of cytokine concentrations. The LEGENDplex assay was employed to analyze monocyte cytokine production in **paper III** and **IV**. It provided a relatively user-friendly manual, software support, sensitivity, and only requires 25 µL of the sample. However, it is an expensive detection method.

The Luminex® Bio-plex utilize the Luminex xMAP technology, allowing detection of up to 100 analytes. We used a Luminex assay in **paper I**, enabling robust screening of 27 analytes simultaneously. The assay principle resembles the sandwich ELISA, with bead-coupled capture antibodies and biotinylated detection antibodies, both targeting the antigens in a sandwich complex. PE-streptavidin generates a fluorescent signal to allow quantification of the analytes which is detected using a Bio-plex system.[209] While it is a sensitive, relatively easy and a rapid approach, it requires 50 µL of the sample, it is expensive, and require its own Bio-plex system for the readout.

5.5.3 Confocal Microscopy

Confocal imaging is a fluorescence imaging technique widely used for biological imaging and 3D tissue analysis. In a confocal microscope, the laser light passes through dichroic mirrors that reflects it onto the sample specimen by the objective. Emitted light is passed back through the objective into the pinhole, which directs in-focus light into the detector by obstructing out-of-focus light. This technology generates high resolution imaging compared to simple light microscopy, where the detector captures light also outside of the focal plane. The ability by confocal microscopy to restrict the illumination to the in-focus area only, allows this technology to perform optical sectioning, providing information about spatial structure and reconstruction of 3D architecture. The two main confocal microscopes include the laser scanning confocal microscope (LSCM) and the spinning disc confocal microscope. The spinning disc is often favored for live-cell imaging as its multiple pinholes can capture images faster compared to LSCM.[210] In my work I have used LSCM as I have only imaged fixed cells (**paper I**, **III**, and **V**) or tissues (**paper III**).

6. Original Work

This chapter summarizes the main findings of the thesis (**papers I-V**). First, the sialoglycan-dependent Siglec-5 regulation of TLR4 signaling in OA is discussed (**paper I**). By exploiting the inflammatory and acidic conditions of inflammation, the performance of a developed PNP capable of releasing cargo is evaluated in a macrophage model (**paper II**). This is followed by the investigation of our developed Sia-targeting PNPs, assessing their biocompatibility and application for modulating monocyte migration as a treatment strategy for OA (**paper III**). The NP interaction with glycosylated ECM degradation products and their influence on macrophage immune responses are investigated, emphasizing the importance to consider biological barriers for optimal NP design (**paper IV**). Finally, several techniques used for Sia identification and detection are explored and compared to our in-house developed fluorescent probes (**paper V**).

6.1 Siglec-5 Regulates TLR4 in Osteoarthritis

Deciphering how aberrant sialylation contributes to shaping the inflammatory landscape of diseases like OA, may provide new insights into the mechanisms driving the pathology. The role of Siglecs has been increasingly studied in various diseases, particularly in cancer, whereas their role in OA has gained limited attention. Targeting the Siglec-Sia axis has emerged as a glycoimmune-checkpoint modulation capable of reprogramming immune cells, a therapeutic strategy primarily directed to promote anticancer immunity. The previous detection of soluble Siglec-5/14 in OA SF by our group prompted us to investigate its role in TLR4-mediated monocyte signaling.[134] To complicate the story, Siglec-5 and Siglec-14 are polymorphic and share sequence homology but elicit opposite immune effects. Siglec-5 functions as an inhibitory receptor and Siglec-14 as an activating receptor. Many commonly used approaches for studying Siglecs, including antibody-based staining and proteomics analysis, are often unable to reliably distinguish between these two receptors, posing a significant challenge for their study. Consequently, we could not determine whether the soluble Siglec in SF corresponded to Siglec-5 or Siglec-14. The study initially employed the Siglec-5-binding antibody clone 1A5, which also stains Siglec-14. Subsequently, more specific antibodies were used to delineate which Siglec was involved in TLR4 regulation.

Siglec-5 is expressed on several immune cells including monocytes, macrophages, neutrophils, and T cells.[211] The abundant expression of monocytes and macrophages in OA joints, lead us to hypothesize that they might play a significant role in Siglec-5/14 signaling and contribute to the generation of soluble Siglec-5/14 in SF. Additionally, sialylated TLR4 is highly involved in OA pathology and therefore represents a potential ligand for Siglec-5/14-mediated regulation. To model the complex OA environment, primary human monocytes were cultured in presence of 25% SF from 7 OA patients (SF1-7). Quantification of surface TLR4 and Siglec-5/14 revealed distinct patterns of expression depending on OA SF, which correlated inversely (Figure 10A-C). These findings suggests that Siglec-5/14 is instrumental in TLR4 regulation, providing new mechanistic insights into OA that may be valuable for the development of future therapeutic strategies.

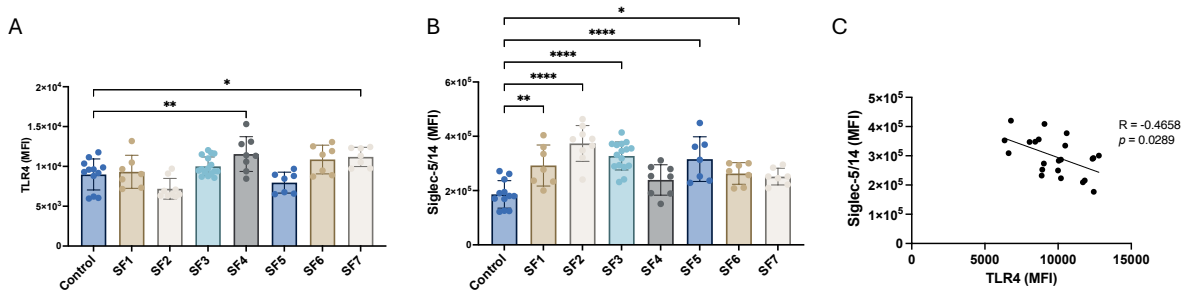

Figure 10. (**A-B**) Median fluorescence intensity (MFI) of TLR4 and Siglec-5/14 on the cell membrane of primary human blood monocytes (n=3) at 24 hours of culturing in presence of 25% synovial fluid from n=7 OA patients. (**C**) Correlation between Siglec-5/14 and TLR4 MFI on monocytes exposed to n=7 OA SFs on monocytes (n=3). Data represents mean ± SD; statistical analysis was performed using one-way ANOVA with Dunnett's multiple comparisons test (A–B). Correlation analysis was performed using Spearman's correlation test (C) (∗p < 0.05; ∗∗p < 0.01; ∗∗∗p < 0.001; ∗∗∗∗p < 0.0001).

Due to the limited availability of OA SF, a standardized experimental platform was established to mimic Siglec-5/14 – TLR4 regulation in monocytes. We employed M-CSF to induce survival and differentiation, while LPS was used to induce TLR4-mediated inflammation (Figure 11A-B). Under these conditions, we identified that low TLR4 expression induced by LPS was accompanied with high Siglec-5/14 expression, supporting its regulation of TLR4 signaling and use as model condition. TLR4 remained stable on monocytes stimulated with M-CSF, likely due to TLR4 being inactive. By including an antibody specific to Siglec-14, we sought to understand the specific staining patterns of Siglec-5 vs Siglec-14. Staining of Siglec-14 did not produce the same expression pattern as with Siglec-5/14-targeting antibody (Figure 11C).We therefore hypothesized that the inverse expression between TLR4 and Siglec-5/14 most likely was attributed to inhibitory Siglec-5 rather than the activating Siglec-14. Furthermore, we employed the SHP-1 inhibitor TPI-1 to inhibit the potential Siglec-5-mediated TLR4 regulation in LPS-stimulated monocytes. Inhibition of SHP-1 resulted in elevated production of cytokines such as MCP-1, IL-6, and IL-8, thereby strengthening the hypothesis that Siglec-5 exerts inhibitory effects on TLR4-driven inflammation in OA.

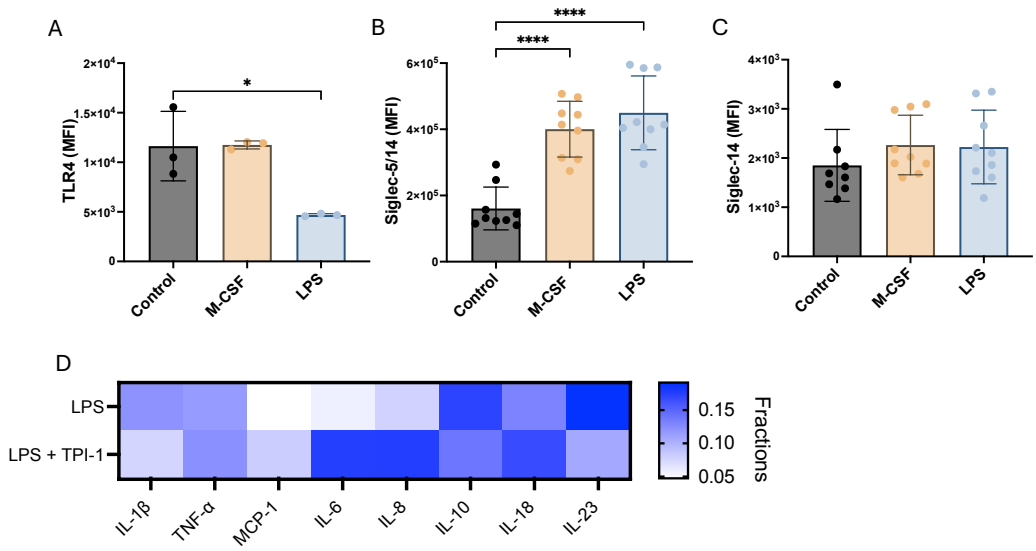

Figure 11. (**A-C**) MFI of membrane-associated TLR4, Siglec-5/14, and Siglec-14 on primary human blood monocytes stimulated with M-CSF or LPS for 24 hours and compared to the unstimulated control. Data represents mean ± SD (n=1 for TLR4, and n=3 for Siglec-5/14 and Siglec-14). (**D**) A panel of 13 cytokines were analyzed using the LEGENDplex Human Inflammation Panel 1 (13-plex) in the supernatants of monocytes stimulated with LPS with and without the SHP-1 inhibitor TPI-1 (100 ng/mL) (n=3). Statistical analysis was performed using one-way ANOVA with Dunnett's multiple comparisons test (A-C) (****$p < 0.0001$).

To uncover further evidence of Siglec-5 – TLR4 interactions, we assessed spatial expression patterns for potential colocalization. Colocalization analysis was performed using the JACoP plugin in ImageJ, where Mander's colocalization coefficients M1 and M2 were quantified in monocytes stained with antibodies specific against TLR4 and Siglec-5 (Figure 12A). M1 represents the fraction of TLR4 overlapping with Siglec-5, whereas M2 represents the fraction Siglec-5 overlapping with TLR4. At baseline (0 hours), a strong TLR4 overlap with Siglec-5 was revealed, in contrast to a weak Siglec-5 overlap with TLR4 (Figure 12B-C). This pattern suggests that sialylated TLR4 is tightly regulated by Siglec-5, while Siglec-5 is likely engaged to other sialylated ligands. After 24 hours, M1 colocalization was reduced across all conditions, whereas M2 was only reduced for LPS. The reduction of colocalization across all conditions may pertain to sialylation changes that disrupts the interaction, an effect that may be stronger under more pronounced inflammatory conditions. However, the variable expression of TLR4 and Siglec-5 observed in Figure 11, may indicate spatial and temporal expression changes, such as Siglec-5 interacting with other sialylated structures.

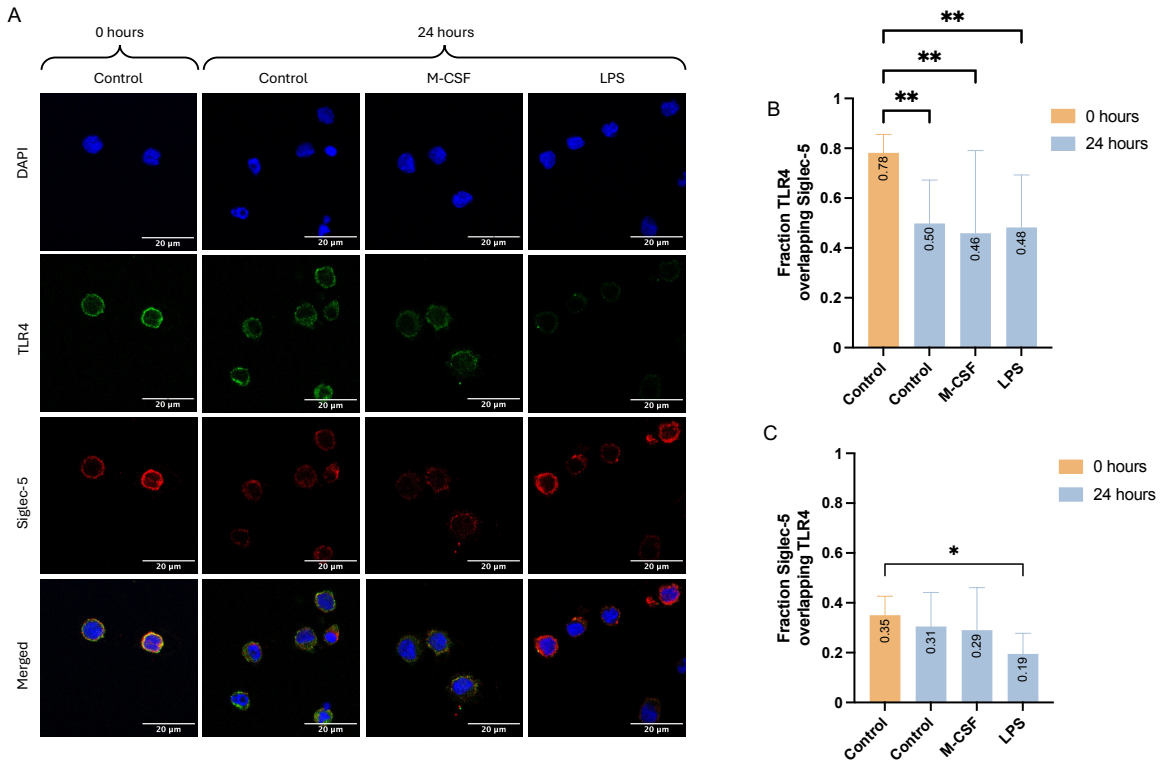

Figure 12. (**A**) Representative immunofluorescence images of primary human blood monocytes at baseline (0 hours), and control, M-CSF, and LPS at 24 hours. The DAPI stains the nucleus, and the green and red color represents TLR4 and Siglec-5, respectively. Scale bars represent 20 µm. Brightness and contrast were altered the same to remove background and better depict the relative expression. (**B-C**) Mander's colocalization coefficient (MCC), with M1 representing fraction TLR4 overlapping Siglec-5, and M2 representing Siglec-5 overlapping TLR4. Data represents mean ± SD generated from 4 to 7 unprocessed images per condition (n=2). Statistical analysis was performed using one-way ANOVA with Dunnett's multiple comparisons test ($*p < 0.05$, $**p < 0.01$).

The small molecule inhibitor TAK-242 was employed to selectively block TLR4 signaling in monocytes to confirm its impact on inflammation. Analysis of a panel of cytokines and chemokines provided evidence of high inflammation in LPS stimulated monocytes compared to M-CSF stimulation, as expected (Figure 13A). The efficiency of TAK-242 as a TLR4 inhibitor was confirmed, as cytokines produced in response to LPS were markedly reduced. Furthermore, TAK-242 resulted in reduced surface expression of Siglec-5/14, while no corresponding effect was observed on monocytes stained with the Siglec-14 specific antibody (Figure 13B-C). Collectively, this adds another layer of evidence that Siglec-5 is the primary mediator of TLR4 regulation, rather than Siglec-14.

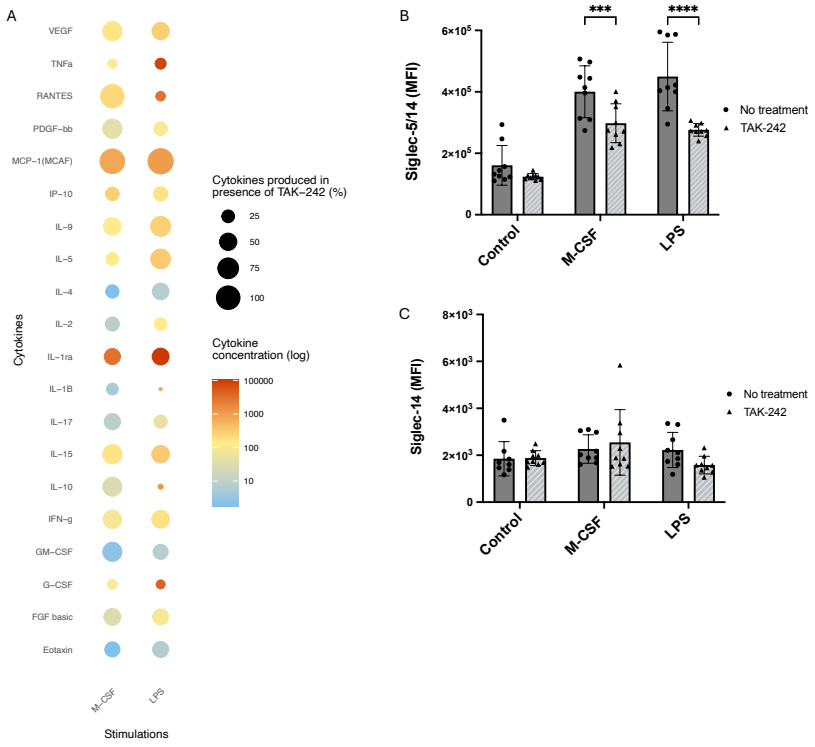

Figure 13. (**A**) The Bio-Plex Pro Human Cytokine Grp I Panel 27-Plex was used to screen a panel of cytokines and chemokines in the supernatants of primary human blood monocytes after 24 hours of stimulation with M-CSF or LPS, in presence or absence of the TLR4 inhibitor TAK-242 (n=3). Cytokine levels from monocytes stimulated in the absence of TAK-242 are indicated by "Cytokine concentration (log)," and the "Cytokines produced in presence of TAK-242 (%)" indicates how effective TAK-242 was at limiting cytokine secretion compared to without TAK-242. (**B-C**) The MFI of membrane-associated Siglec-5/14 and Sigec-14 on primary human blood monocytes stimulated with M-CSF or LPS at 24 hours was assessed in presence or absence of TAK-242. Data represents mean ± SD (n=3). Statistical analysis was performed using two-way ANOVA with Sidak's multiple comparisons test (****$p < 0.0001$).

Previous studies have reported that LPS-mediated activation of TLR4 is linked to host upregulation of sialidases. An exogenous sialidase was thereby employed to remove Sia to explore the resulting impact on Siglec-5 – TLR4 interactions. Monocytes were stained with antibodies specific for TLR4 and Siglec-5 to examine how Sia-removal influences receptor colocalization (Figure 14A). Using the same analytical approach as in Figure 13, MCC M1 and M2 were compared. At 24 hours, the fraction of TLR4 overlapping with Siglec-5 remained similar to the control, whereas the fraction of Siglec-5 overlapping with TLR4 was significantly reduced. When considered together with the reduced M2 observed under LPS stimulation (Figure 13C), these findings underscore the importance of Sia expression on TLR4 for Siglec-5-mediated regulation. In parallel, analysis of a panel of cytokines and chemokines in supernatant from sialidase-treated monocytes, in presence and absence of TAK-242 was performed. This demonstrated that Sia-removal activates the TLR4 pathway, as TAK-242 achieved a marked reduction of all measured analytes (Figure 14D).

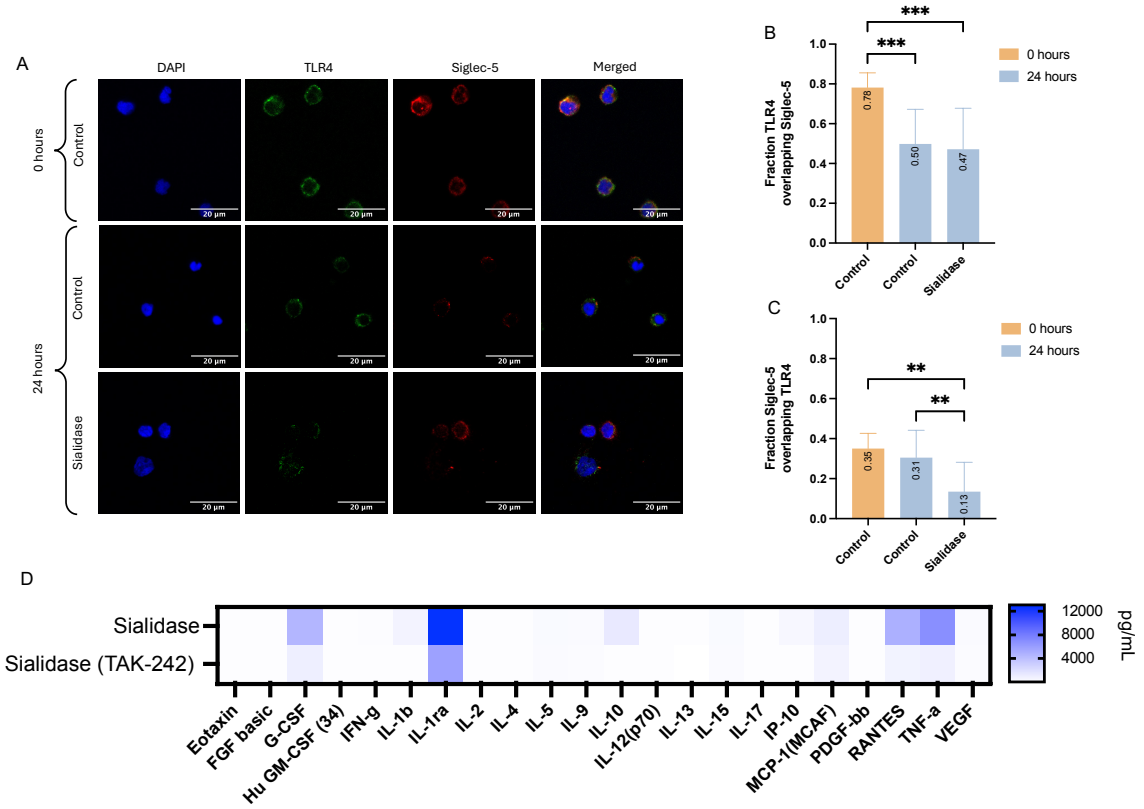

Figure 14. (**A**) Colocalization of TLR4 and Siglec-5 was investigated in primary human blood monocytes treated with sialidase for 24 hours compared to the control at 0 and 24 hours. Brightness and contrast were altered the same to remove background and illustrate the relative expression of TLR4 and Siglec-5. (**B-C**) MCC representing "Fraction TLR4 overlapping with Siglec-5" and "Fraction Siglec-5 overlapping with TLR4", respectively. The controls used are the same as in Figures 3B and 3C. Values were acquired from 4 to 7 unprocessed images per slide (n=2).

Finally, patient-derived data were integrated with the individual stimulation conditions to better characterize the inflammatory profile of OA monocytes. Therefore, the secreted IL-6 in the supernatants were quantified and compared between monocytes stimulated with SF1-7 and M-CSF, LPS, or sialidase (Figure 15A). Monocytes stimulated with SF1-7 generally produced markedly lower IL-6 levels compared with the individual stimulations. Given that cytokines and DAMPs in SF typically induce low-grade joint inflammation, IL-6 secretion was anticipated to be lower compared with the individual stimulations. Interestingly, stimulation with SF5 lead to noticeable higher IL-6 levels, highlighting interpatient variability.

To further investigate the relationship between IL-6 profiles and monocyte phenotypes, clustering analysis was performed on flow cytometry data based on the expression of CD14, CD16, TLR4, Siglec-5/14, and Siglec-9. This generated 6 distinct populations, which were visualized using uniform manifold approximation and projection (UMAP) (Figure 15B-D). The UMAP analysis revealed that individual stimulations induced more homogenous phenotypes, while SF1-7 resulted in greater heterogenous phenotypes. Moreover, SF1-7 stimulation showed greater overlap with the M-CSF condition, consistent with a more low-grade inflammatory

profile. In contrast, monocytes stimulated with SF5 exhibited phenotypes overlapping better with high inflammation which was in line with the higher IL-6 produces.

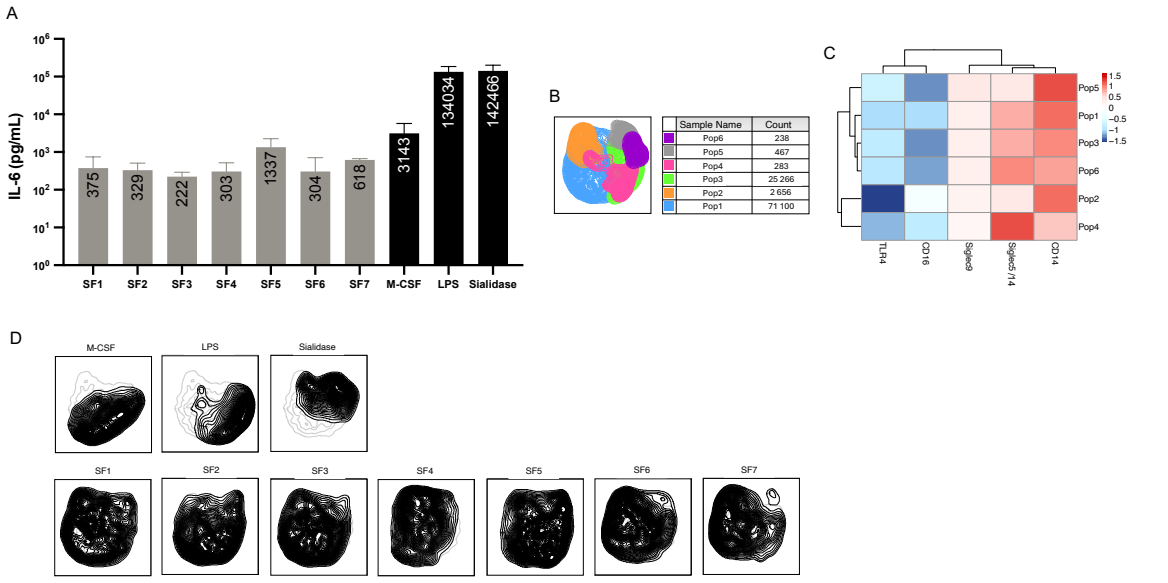

Figure 15. (**A**) The concentration of IL-6 (pg/mL) produced by stimulated primary human blood monocytes was quantified using a sandwich ELISA; gray bars represent stimulation with SFs, and black bars represent the pathway-specific stimulations (M-CSF, LPS, and sialidase). Data represents mean ± SD, n=3 biological replicates. (**B**) Concatenated monocytes stimulated with M-CSF, LPS, sialidase, and SF1-7, were downsampled to 100,000 cells before performing clustering analysis using the FlowSOM plugin. This generated six monocyte subpopulations; the table displays each population and its count, respectively. (**C**) Heatmap analysis demonstrates the six populations and their relative expression of TLR4, CD16, Siglec-9, Siglec-5/14, and CD14. (**D**) Each UMAP contour density plot represents one condition, i.e., M-CSF, LPS, sialidase, and SF1-7.

In summary, the main findings of **paper I** identify Siglec-5 as an inhibitory regulator of TLR4 signaling in monocytes exposed to OA SF. This inhibitory function relies on the presence of sialoglycans on TLR4, as high inflammation or exogenous sialidase treatment reduced sialylation and correlated with decreased Siglec-5 – TLR4 colocalization. However, Siglec-5-mediated TLR4 regulation was present even in pro-inflammatory LPS conditions, as inhibition of SHP-1 resulted in enhanced cytokine secretion. While these findings establish foundational evidence for Siglec-5-mediated TLR4 regulation, they also indicate complex and dynamic temporal and spatial receptor expression patterns influenced by sialylation and likely modifications of additional glycans. Collectively, this work provides mechanistic insights into a largely understudied regulatory pathway in OA that, to our knowledge has only been sparsely investigated, with existing studies mainly offering suggestive support for Siglec-5-mediated TLR4 regulation.[95,212] My findings highlight a potential immunomodulatory pathway for therapeutic or diagnostic intervention in OA. Additionally, interpatient-variability possibly associated with distinct OA endotypes, characterized by heightened inflammation and dysregulated TLR4 activation, may provide an especially relevant patient subgroup in which targeting Siglec-5-mediated TLR4 regulation could prove beneficial.

6.2 pH-dependent Release from Acetalated Dextran Nanoparticles

Local acidification is a common feature in inflammatory environments, observed in diseases such as RA and OA. In **paper II**, the environmental cues were exploited in the development of an acetalated dextran NP (AcDex) for precision medicine. This platform was designed to dynamically release cargo in an ON-OFF-ON manner, thereby mimicking pathophysiological flare-ups characteristic of RA, while also being relevant for OA with high inflammatory profiles. Although biochemical triggers have previously been utilized in the design of NP platforms, the AcDex system presented here offers an enhanced dynamic response with the ability to turn off release upon return to neutral pH (Figure 16).

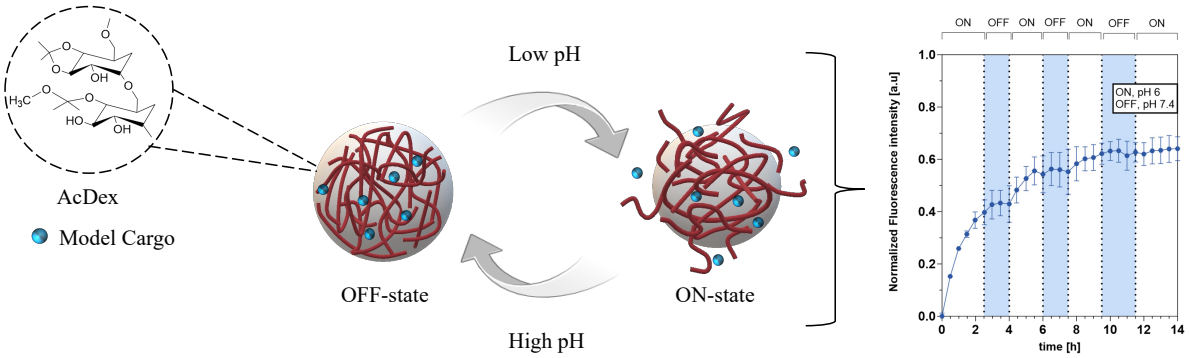

Figure 16. A schematic illustration of polymer-based acetalated dextran (AcDex) with encapsulated cargo being released in a ON/OFF/ON/OFF kinetics dependent on the pH.

To investigate whether this dynamic ON-OFF-ON release pattern could be reproduced *in vitro*, the ROS-sensitive DCFH-DA probe was encapsulated within two NP formulations: AcDex 70% and Mixed NPs (AcDex 35% and 70%). LPS stimulated murine macrophages (RAW264.7 cell line) was used as a model for ROS production under conditions associated with reduced pH. As expected, free DCFH-DA was readily converted into the fluorescent product DCF by LPS-stimulated cells (Figure 17A and D). In contrast, no statistical difference in DCF signal was observed for AcDex 70% (Figure 17B and E). For mixed NPs, LPS-stimulated macrophages triggered release of DCFH-DA, as indicated by a statistically significant conversion to DCF (Figure 17C and F). These findings demonstrate that NP design requires careful chemical and biological characterization to achieve controlled and responsive cargo release by NPs.

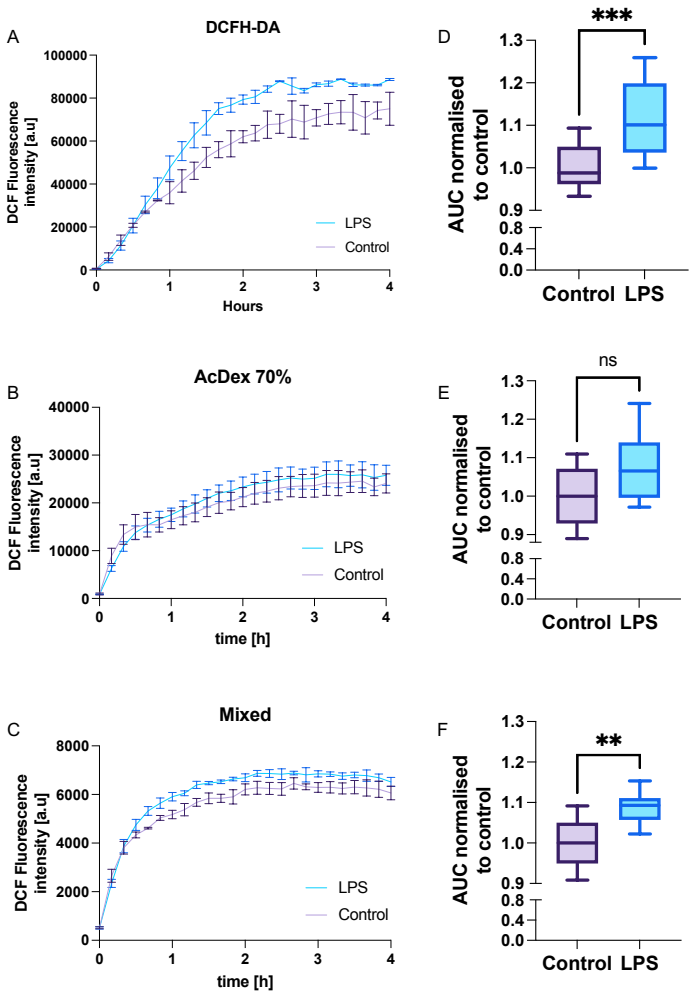

Figure 17. Metabolic conversion of DCFH-DA to DCF by RAW264.7 macrophages was recorded for 4 hours. Kinetic measurement of (**A**) free DCFH-DA, (**B**) AcDex 70% and (**C**) mixed NPs. AUC from LPS-stimulated cells was normalized to the control cells (**D**) DCFH-DA (**E**) AcDex 70% and (**F**) mixed NPs. Data represents mean ± SD for AcDex 70% and mixed NPs, (n = 8), and DCFH-DA (n = 12). Statistical analysis was performed using an unpaired t-test (**p < 0.01, ***p < 0.001).

In conclusion, my contribution to this work helped bridge the NP behavior in buffer systems to their biological relevance in inflammation. As a proof of concept, this work demonstrated that inflammation-associated environmental triggers can promote cargo release from the mixed NPs. While this platform was focusing on flareup-like pH-alterations in context of RA, it may provide a meaningful application for other chronic inflammatory diseases like OA.

6.3 Sialic Acid-Shielding Nanoparticles Modulate Monocyte Migration

The development of nanomaterial platforms for precise targeting of sialylated structures has gained increased attention as therapeutic strategies, especially in the cancer field were hypersialylation represents a common disease hallmark. Such approaches typically involve selective tumor targeting for precise drug delivery or disruption of the Siglec-Sia axis for immunomodulation. In the context of OA, persistent immune cell recruitment into joints and activation plays a central role in driving disease progression. As immune cell recruitment starts by endothelial rolling and transmigration, in part relying on Sia-selectin interactions, we postulated that selective targeting of Sia on monocytes could represent a strategy to reduce their migration. In **paper III**, a multivalent polymeric NP functionalized with PBA conjugated to a cationic polymer polyethyleneimine (PEI) was developed to target monocyte migration via Sia shielding. PBA forms reversible boronate esters with Sia, a reaction that is enhanced at lower pH. The resulting PBA-PEI@PLGA was compared to a control NP lacking PBA (PEI@PLGA). The size was determined to be ~240 nm, which we hypothesized to be an appropriate size for targeting surface Sia to achieve a shielding effect but at the same time limit immediate cell uptake. The ratio of PBA-PEI protruding out from the core shell was carefully designed for optimal multivalent binding of Sia (Figure 18A). The goal of this work was to confirm the biocompatibility and translational potential of this nanomaterial for OA treatment.

The biocompatibility of our NPs was evaluated using the resazurin cell viability assay in three different well-established cell lines (HepG2, HEK293T, and RAW264.7). Cells treated with PBA-PEI@PLGA were all viable under all concentration for up to 24 hours, whereas an increased metabolic activity was observed in HepG2 and RAW264.7 cells treated with PEI@PLGA (Figure 18B). NP biocompatibility was also characterized in a more physiologically relevant model cell using primary human blood donor-derived monocytes. In this condition, it was revealed that PBA functionalized NPs were biocompatible, while PEI@PLGA lead to cytotoxicity and high IL-6 production (Figure 18C-D). Cationic materials, including PEI, have previously been shown to induce cytotoxicity, therefore the unsatisfactory safety profile of PEI@PLGA came to no surprise. However, the improved biocompatibility of PBA-PEI@PLGA highlights how functionalization of NPs can enhance the properties of nanomaterials.

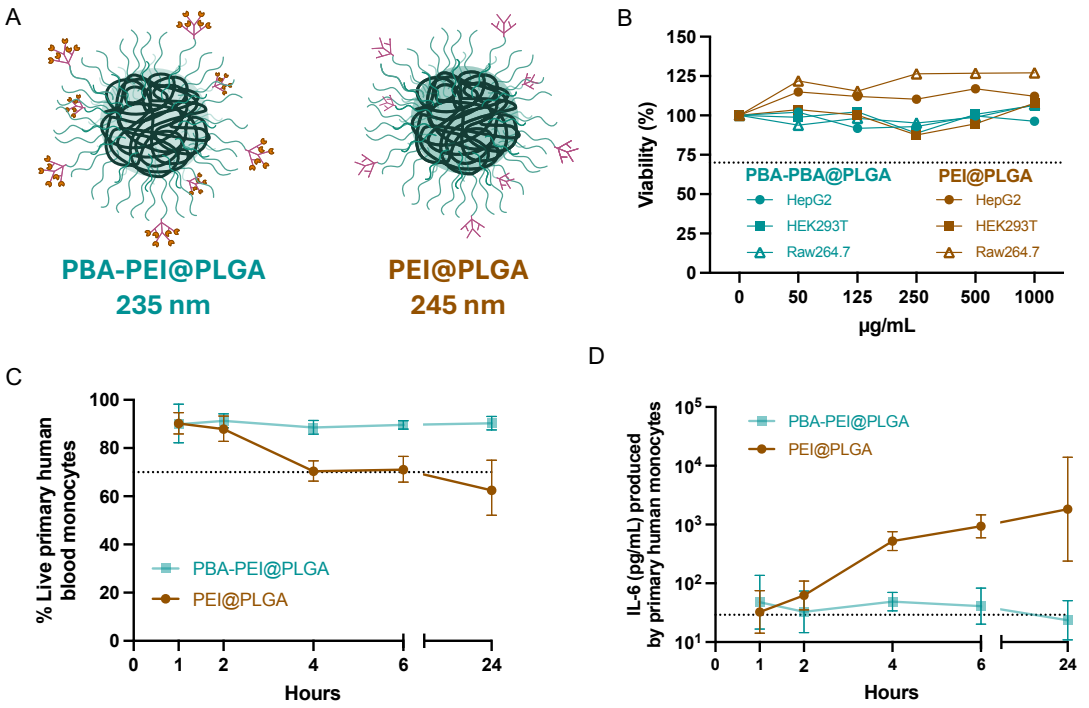

Figure 18. (**A**) The illustrations represent polymeric PLGA-based NPs termed PBA-PEI@PLGA and PEI@PLGA and their sizes of 235 and 245 nm, respectively. (**B**) Viability of human liver (HepG2), human kidney (HEK293T), and murine macrophages (RAW264.7) treated with NPs of varying concentrations assessed after 24 hours using the resazurin viability assay, with cytotoxicity considered below 70% viability of the control (dashed line). Data represent mean ± SD from n=1 for HepG2 and HEK293T, and n=2 for RAW264.7. (**C**) Live (%) primary human blood monocytes analyzed using flow cytometry after treatment with 250 µg/mL NPs for 24 hours. Data represent mean ± SD (n=2). (**D**) IL-6 (pg/mL) was measured in the supernatants of primary human blood monocytes after 24 hours of treatment with NPs using ELISA. Data represent mean ± SD (n=2).

Recruitment of immune cells to inflammatory sites, including OA joints, is facilitated by the binding of several receptors on endothelial cells of the vasculature, with multiple interactions relying on sialylation on the immune cell. The Sia-selective ability of PBA-PEI@PLGA was therefore paramount for targeting monocyte migration and confirmed by showing its reduced binding to monocytes treated with sialidase compared to control (Figure 19A). In contrast, the control PEI@PLGA bound monocytes independently of Sia (Figure 19B), thus displaying both cytotoxicity and lack of desired Sia-selectivity. PEI@PLGA was therefore not included in further characterization. Confocal imaging of PBA-PEI@PLGA on macrophages demonstrated predominantly surface-binding of NPs at 2 hours, supporting a shielding effect (Figure 19C). To further elucidate the shielding capacity of the NP, CD62L was used as a model protein due to its sialylation profile. Primary CD4 and CD8 T cells were exposed to three different concentrations of NPs overnight, followed by staining with an antibody against CD62L. This revealed a concentration-dependent decreased detection of CD62L on T cells, indicative of that the NPs shielded the binding of the antibody targeting CD62L (Figure 19D).

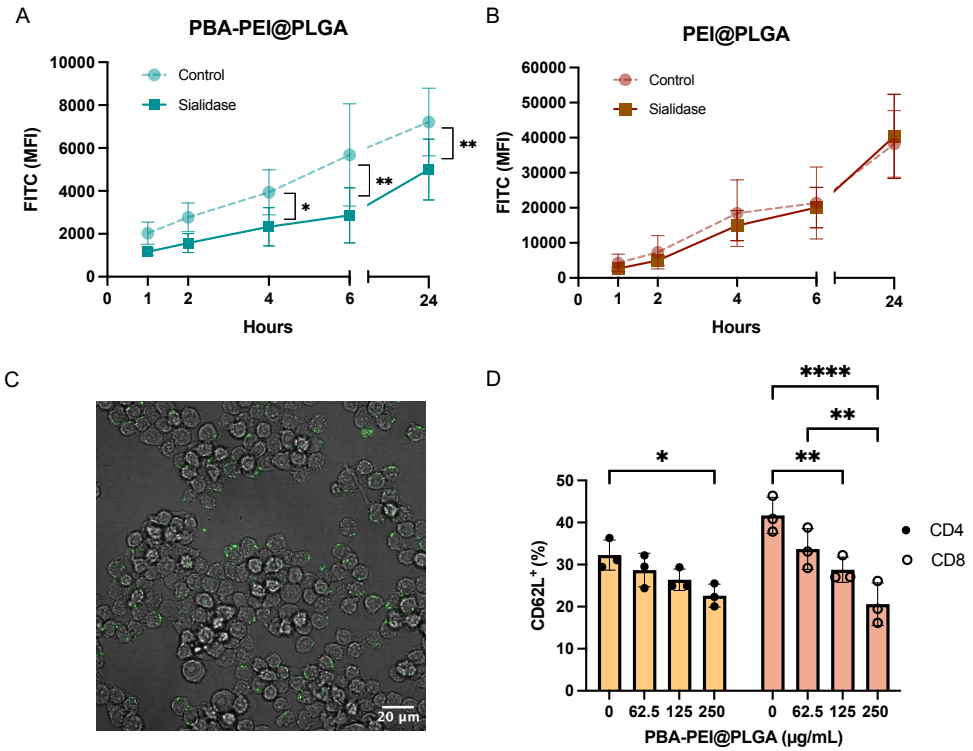

Figure 19. (**A-B**) Primary human blood monocytes were pre-stimulated with M-CSF (50 ng/mL) for two hours before either media or sialidase (100 mU/mL) was added, as well as 250 µg/mL FITC conjugated PBA-PEI@PLGA or PEI@PLGA. The binding, represented as MFI, was measured using flow cytometry after 1, 2, 4, 6, and 24 hours. Data represent mean ± SD (n=3). Statistical analysis was performed using a mixed-effects analysis followed by Sidak's multiple comparisons test (*p<0.05; **p<0.01). (**C**) RAW264.7 macrophages were incubated with PBA-PEI@PLGA (250 µg/mL) for 2 hours and imaged using confocal imaging. (**D**) PBMCs were treated with 62.5, 125, and 250 µg/mL PBA-PEI@PLGA overnight and then stained with CD4, CD8, and CD62L antibodies and analyzed using flow cytometry. Data represent mean ± SD (n=1). Statistical analysis was performed using two-way ANOVA with Sidak's multiple comparisons test (*p<0.05; **p<0.01; ****p<0.0001).

Nanomaterials offer unique opportunities for precision medicine, such as targeting specific cell populations. Our goal was to specifically modulate monocytes via membrane-linked Sia. We therefore quantified the NP binding and confirmed enhanced targeting of monocytes compared to lymphocytes (Figure 20A). Monocytes circulate in blood prior to migrating into inflammatory sites, therefore it is crucial that the targeting ability of PBA-PEI@PLGA is not compromised in a dynamic environment such as in circulation. To test this, we used a fluidic setup with comparable shear stress to capillaries and were able to conclude that the NP interaction was robust and not perturbed by circulating conditions (Figure 20B-C). The enhanced association of NPs to monocytes was further explored in fixed mouse spleen sections to determine their potential in cell specific targeting. The spleen is an organ with defined zones, including the "red zone", "white zone", and "marginal zone". The red zone contains mainly macrophages and dendritic cells, while the white zone contains lymphocytes. To explore the cell-specific targetability, spleen sections were stained with antibodies against the macrophage-specific F4/80 protein and PBA-PEI@PLGA. Visually this revealed an overlap between F4/80 and the NPs (Figure 20D), which was further reinforced by a statistically significant correlation

between the MFI of F4/80 and the NP MFI of mice (n=6) (Figure 20E). Together, these findings support a sialylation-dependent favorable binding of the NPs to monocytes, macrophages, and dendritic cells compared to lymphocytes, which could prove especially useful in immune cell-specific targeting for modulating inflammation in OA.

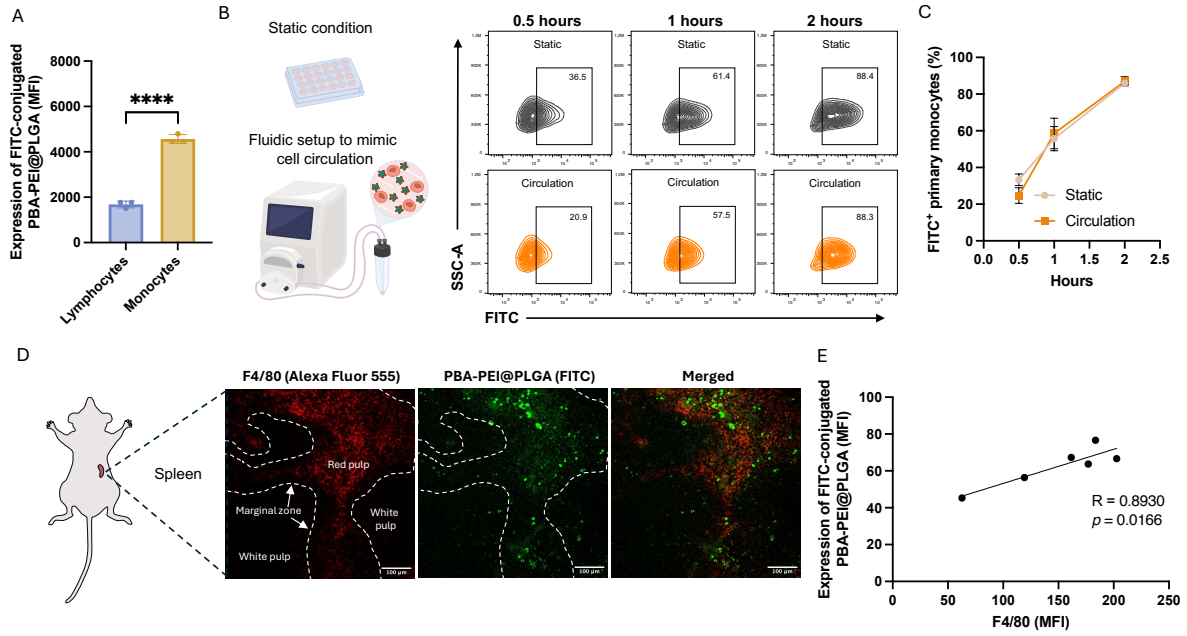

Figure 20. (**A**) Human PBMCs, were stained on ice for 30 min with 250 µg/mL of FITC conjugated PBA-PEI@PLGA and FITC MFI was analyzed using flow cytometry. Data represent mean ± SD (n=3). Statistical analysis was performed using an unpaired t-test (****p<0.0001). (**B**) Representative flow cytometric plots from human primary blood monocytes treated with PBA-PEI@PLGA (250 µg/mL) under static and circulating conditions after 0.5, 1, and 2 hours. (**C**) Binding of PBA-PEI@PLGA to static and circulating monocytes were gated as "FITC$^+$". Data represent mean ± SD (n=2-3). (**D**) Mouse spleen sections (10 µm thickness) from 3 healthy and 3 OA mice were stained with F4/80-Alexa Fluor 555 antibody (red) and PBA-PEI@PLGA (500 µg/mL) (green) and imaged using confocal microscopy with a 20× objective, scale bars represent 100 µm. (**E**) MFI of F4/80 and PBA-PEI@PLGA was analyzed on the original images and quantified. Correlation analysis was performed on pooled samples (n=6 biological replicates) using Pearson's correlation coefficients as the data passed normality test (*p<0.05).

Finally, to test inflammation-linked alterations in Sia biosynthesis, metabolic labeling was performed in U937 monocytes. Notably, elevated incorporation of Sia pertaining to inflammation was revealed (Figure 21A). As we had already determined a shielding effect by the NPs, we investigated whether this would reduce phagocytic effects by feeding primary monocytes pHrodo Red Zymosan BioParticles. While no statistically significant difference was observed, a slight increase of the negative population, i.e. monocytes that did not phagocytose zymosan pHrodo red, was observed by the highest concentration of PBA-PEI@PLGA (Figure 19B). This potential shielding of phagocytosis represents a property that could be beneficial for modulating chronic inflammation.

Furthermore, the ability for PBA-PEI@PLGA to inhibit monocyte migration via Sia was evaluated. We employed the Boyden chamber transwell assay with a 5 µm membrane and added

either MCP-1 or OA SF in the bottom chamber to trigger chemotaxis. The increased migration of monocytes migrating towards MCP-1 first proved that the model worked (Figure 21C). We thereafter showed concentration-dependent inhibition of migration towards MCP-1 when monocytes were treated with the NPs. This inhibitory effect was also evident on monocyte migration towards OA SF (Figure 21D). Due to the inherently lower ability for OA SF to act as a potent chemoattractant compared to 100 ng/mL MCP-1, our results demonstrate that the NPs have potential to reduce migration even in low-grade inflammatory conditions such as OA.

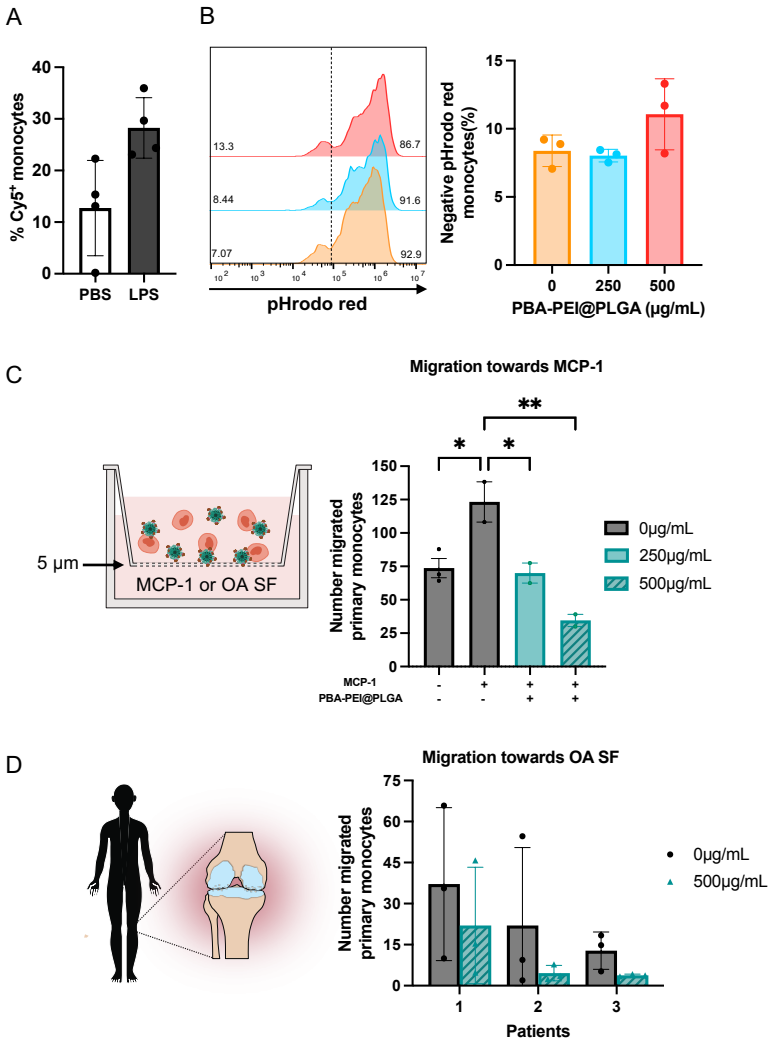

Figure 21. (**A**) Metabolic labeling of the synthetic sugar Ac4ManNDBCO (75µM) after 48 hours, detected in the monocytic cell line U937, in presence and absence of LPS. Cy5-azide (1 µg/mL) detected incorporated Sia. Data represent mean ± SD (n=1). (**B**) Histograms display a negative and positive pHrodo red population, with the negative population being quantified for primary human blood monocytes treated with 0, 250, or 500 µg/mL NPs. Data represent mean ± SD (n=1). (**C**) Primary human blood monocyte migration towards MCP-1 (100 ng/mL) was evaluated using a Boyden chamber with 5 µm membrane pores (schematic insert). Control groups included monocytes with and without MCP-1, and monocytes with MCP-1 and PBA-PEI@PLGA (250 µg/mL and 500 µg/mL) for 4 hours. The number of migrated monocytes was counted based on DAPI staining using confocal microscopy with a 20× objective. Data represent mean ± SD (n=2). Statistical analysis was performed using one-way ANOVA with Tukey's multiple comparisons test (*p<0.05; **p<0.01). (**D**) Migration of monocytes also evaluated towards 20% OA synovial fluid with or without 500 µg/mL PBA-PEI@PLGA for 4 hours. Data represent mean ± SD (n=1). The experiment was performed using OA synovial fluid from three patients (n=3).

To summarize the main findings of **paper III**, we first demonstrated how the NP design critically dictates the therapeutic potential of the material. While PEI@PLGA induced immune activation and cytotoxicity, functionalization with PBA resulted in improved biocompatibility. We then showed that the multivalent PBA units selectively target Sia on monocytes, supported by reduced binding to sialidase-treated monocytes, surface-binding to RAW264.7 macrophages, and a shielding effect of CD62L. To investigate the translational potential of this system as an injectable, a fluidic circulation setup was assembled to simulate physiological shear stress. Compared to static cultures, no difference in the level of bound NP was observed. This finding indicate that the targeting ability remained intact even under dynamic conditions, a factor that is often overlooked in *in vitro* drug screening and instead evaluated *in vivo*. Furthermore, NP shielding slightly reduced monocyte phagocytosis, suggesting immunomodulatory effects that could be beneficial in OA where DAMPs can perpetuate chronic inflammation. Finally, the concentration-dependent reduction in monocyte migration highlights an immunomodulatory effect. Collectively, these findings identify Sia on monocytes as a promising disease-modifying target for the treatment of OA.

6.4 Macrophage Response to Nanoparticle-Glycoprotein Aggregates

The catabolic degradation products in OA can limit the therapeutic potential of nanomaterials by aggregating to form NP coronas. The influence of glycoproteins on NP behavior and immunological responses represents an understudied avenue in the field. To address this, an ex vivo porcine cartilage model was set up in **paper IV** using three catabolic enzymes, including collagenase (COL), hyaluronidase (HYA), and ADAMTS5 (ADA). Four NPs with different physicochemical characteristics were included in the study: small, high charge PAMAM-based NPs ($PAMAM_H$), small, lower charge PAMAM-based NPs ($PAMAM_L$), large, high charge PLGA-based NPs ($PLGA\text{-}PEI_H$), and large, low charge PLGA-based NPs ($PLGA\text{-}PEI_L$). My contribution to this study was the evaluation of the immunological responses by primary human monocyte-derived macrophages to catabolic supernatants from the cartilage model (Figure 22).

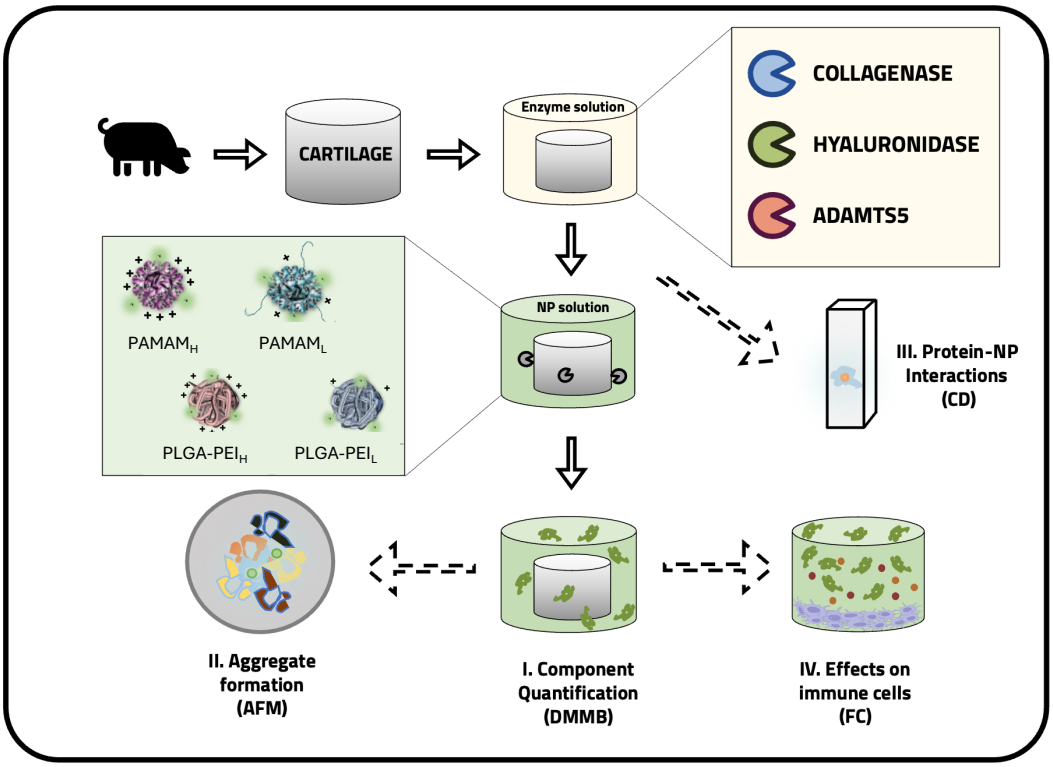

Figure 22. Schematic illustration of the ex vivo porcine cartilage model, investigating the effect of enzymatic enzymes in combination with a panel of polymeric NPs.

Immunological responses induced by NP-glycoprotein aggregates derived from the cartilage model were evaluated in monocyte-derived macrophages using a multiplex cytokine detection approach. The quantified cytokines were normalized to the no-particle control (Figure 23A-D). The ADA condition induced the highest inflammatory response, while COL induced the lowest. Compared to the unstimulated control, several cytokines were reduced in the enzyme conditions, such as IL12p70 for $PAMAM_H$ and $PAMAM_L$. By contrast, the cytokine IL-1β increased in the HYA and ADA condition for both PAMAMs, whereas TNF increased in COL for $PAMAM_L$. It was evident that $PAMAM_H$ induced the highest activation profile, which sometimes were enhanced or reduced depending on the enzymatic condition. The lower

immune activation observed by PLGA-PEI$_H$ and PLGA-PEI$_L$ verified that small cationic NPs can have cytotoxic properties and induce immune activation. The modest increase in IL-1β by PLGA-PEI$_H$ reinforced that the cationic charge is more likely to contribute immune activation than size.

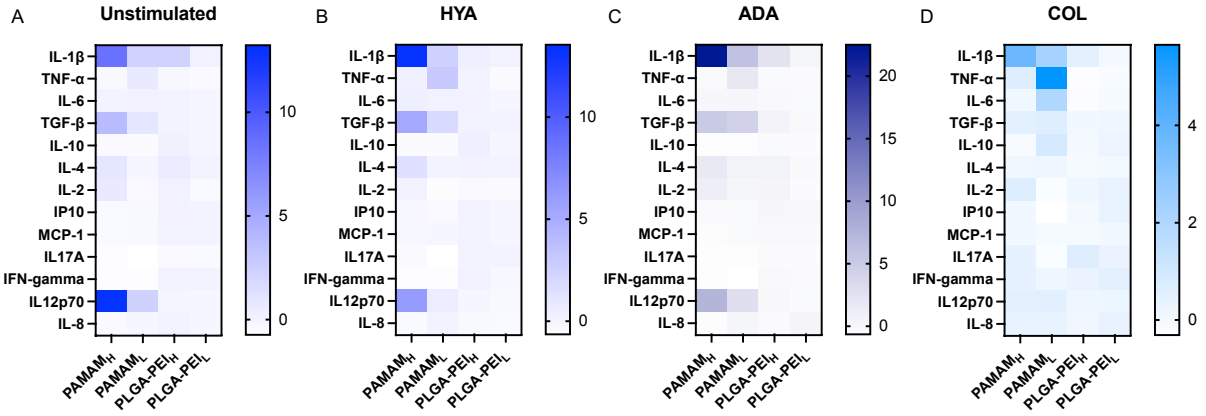

Figure 23. NP-aggregate effects on macrophage cytokine production. Cytokine production from macrophages was compared after stimulation either with explants treated with media control (**A**), hyaluronidase (HYA; **B**), ADAMTS (ADA; **C**), and collagenase (COL; **D**) and subsequent treatment of PAMAM$_H$, PAMAM$_L$, PLGA-PEI$_H$ or PLGA-PEI$_L$. Cytokine expression is presented as fold-change relative to no particle controls.

To conclude, my contribution to **paper IV** enhanced the immunological relevance of the study. The native cartilage tissue model provided a more physiologically relevant and a controlled environmental platform, which when integrated with primary macrophages, improved clinical translatability of the results. We demonstrated that NP size and charge matter for biocompatibility and that physicochemical properties influence glycoprotein interaction and downstream immune responses. These findings underscore the importance of considering interaction between cartilage-derived catabolic products and NPs to achieve optimal drug-delivery design while minimizing immune activation.

6.5 Sialic Acid Detecting Approaches

Building upon previous evidence for the role of Sia in monocytes and their therapeutic potential for monocyte immunomodulation, **paper V** aimed to expand this knowledge using both conventional methodologies and newly developed Sia-detecting probes. As outlined in the schematic overview (Figure 24), (1) the thiobarbituric acid assay was used for quantification of total Sia in OA SF. This was followed by (2) the establishment of a sialidase-treated porcine cartilage model to investigate cartilage degradation using the DMMB assay. Furthermore, (3) metabolic labeling, (4) lectin staining, and (5) the developed Sia detecting probes were employed to investigate Sia patterns in a selection of joint-relevant cells.

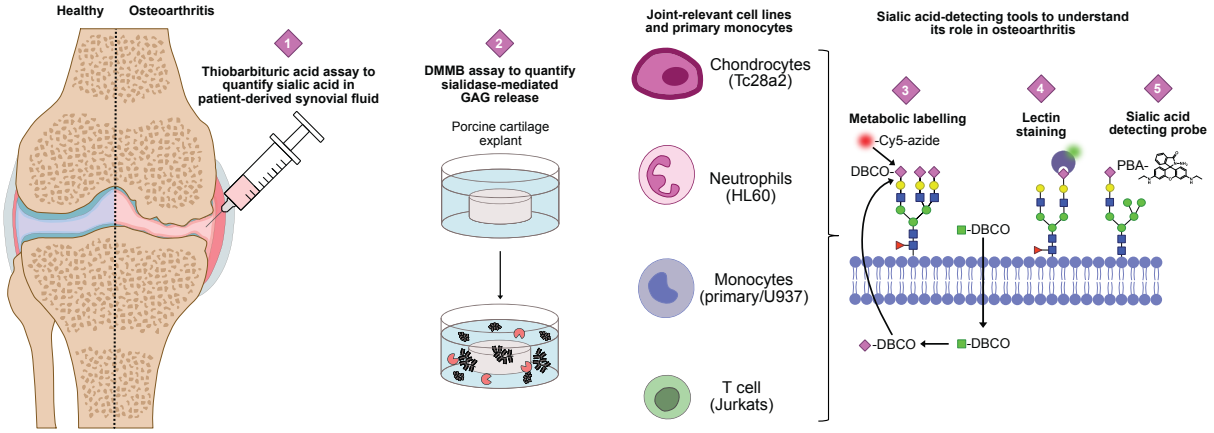

Figure 24. Schematic overview outlining the biological materials analyzed in this study as well as the techniques used for detection of Sia.

Quantification of total Sia in OA SFs using the thiobartbituric acid assay revealed inter-patient variability, suggesting the presence of distinct phenotypic disease profiles (Figure 25A). Due to lack of healthy control, only patient S297 was identified as having elevated Sia levels relative to the other patients. We therefore instead aimed to isolate the role of sialylation for cartilage structural integrity by establishing a sialidase-treated porcine cartilage explant model. Following 24 hours of sialidase treatment, the concentration of GAGs was quantified in the supernatant, revealing a sialidase concentration-dependent increase in GAG release. This indicates that altered sialylation can influence the structural integrity of cartilage (Figure 25B). To assess inflammation-associated alteration in Sia metabolism, metabolic labeling was performed on Tc28a2, HL60, and U937 cell lines using the synthetic sugar Ac_4ManNDBCO. Cy5-azide-mediated click-chemistry enabled detection of sugar incorporation, revealing a significantly increased Sia metabolism in Tc28a2 stimulated with IL-1β/TNF and HL60 stimulated with IL-1β/TNF or LPS after 24 hours (Figure 25C-D). Similarly, U937 exhibited a significant increased Sia metabolism under both inflammatory stimulations, albeit with a delayed response observed at 48 hours (Figure 25E). In a separate experiment, the relative expression of α2,3 and α2,6 Sia on primary monocytes was assessed using lectins after 24 hours of stimulation. In contrast to the metabolic labeling results, a significant reduction in sialylation was observed in LPS-stimulated monocytes (Figure 25F). As increased Sia metabolism in U937

did not correspond to increased Sia surface expression on monocytes may reflect dysregulated activity in STs and sialidases.

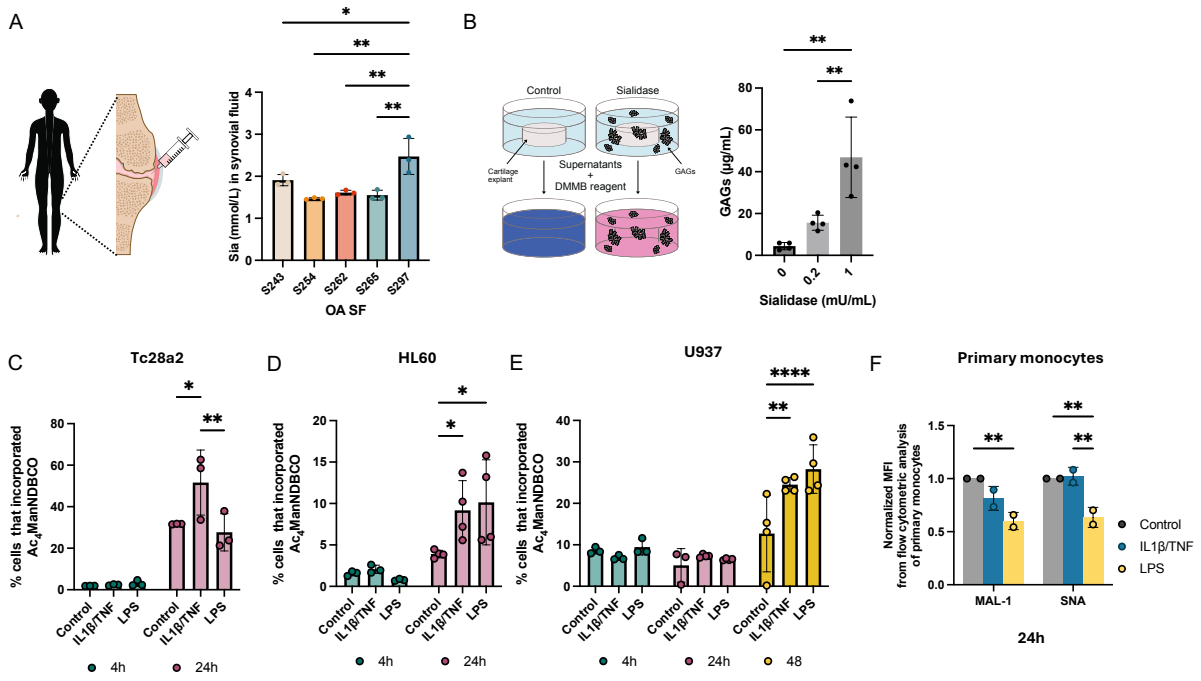

Figure 25. (**A**) Total Sia in OA SF from n=5 patients were quantified using the thiobarbituric acid assay. (**B**) A porcine cartilage explant model was sialidase-treated for 24 hours followed by GAG quantification by the DMMB assay (n=4). (**C-E**) Sia metabolism was assessed in Tc28a2, HL60, and U937 stimulated with IL-1β/TNF (10 ng/mL) or LPS (100 ng/mL) and incubated for 4, 24, U937 for an additional 48 hours. All cells were fed 75µM of the synthetic sugar Ac_4ManNDBCO. The clickable Cy5-azide (1µg/mL) was added 2 hours before flow cytometric analysis to detect incorporation of the synthetic sugar. (**F**) MFI of lectin staining with MAL-I (5 µg/mL) and SNA (1.25 µg/mL) was performed on primary monocytes after 24 hours of stimulation with IL-1β/TNF or LPS (n=2). Data represent mean ± SD. Statistical analysis for figure A and B was performed using one-way ANOVA with Tukey's multiple comparisons test while figure C-E was performed using two-way ANOVA with Sidak's multiple comparisons test. Statistical analysis for figure F was performed using a mixed-effects analysis followed by Tukey's multiple comparisons test (*p<0.05; **p<0.01; ***p<0.001; ****p<0.0001).

Lectin-based approaches represent one of the most used methods for detection of Sia. In my work Jurkat T cells were stained with several different lectins including WGA, PNA, MAL-I, and SNA, followed by analysis using flow cytometry. Live/dead staining with DAPI revealed extensive cell death associated with WGA and SNA/MAL-I, which appeared to be caused by agglutination of cells (Figure 26A). Despite this limitation with some lectins, it is a relatively sensitive approach for Sia detection, as evidenced by the reduced WGA staining observed in sialidase-treated Jurkat cells (Figure 26B).

As an effort to contribute with improved detection strategies to the field of glycobiology, two Sia-selective fluorescence-activatable probes were synthesized in our lab. In the first-generation design, 3- and 4-formylphenylboronic acid derivatives were incorporated onto a rhodamine 6G,

respectively, and denoted R6GH3FPBA and R6GH4FPBA. Upon binding of PBA to Sia, changes in the electronic environment promote a ring-opening mechanism in the rhodamine moiety, resulting in reversible fluorescence activation. This design theoretically enables the potential for real-time detection of Sia.

However, a key limitation of these first-generation probes is the exposed rhodamine core, as its hydrophobic and previously reported cytotoxicity, may influence live cells negatively. Notably, we found concentration-dependent reduction in viability of Jurkat cells, HL60, HepG2, and HEK293T cells treated with the probes for 24 hours, although R6GH3FPBA performed slightly better relative to R6GH4FPBA (Figure 26C). Instead, flow cytometric analysis was performed following shorter staining, which did not induce any cell death or aggregation (Figure 26D). Preliminary functional analysis revealed a statistically significant reduced binding of R6GH3FPBA to sialidase-treated cells (Figure 26E), and non-significant reduced binding by R6GH4FPBA (Figure 26F).

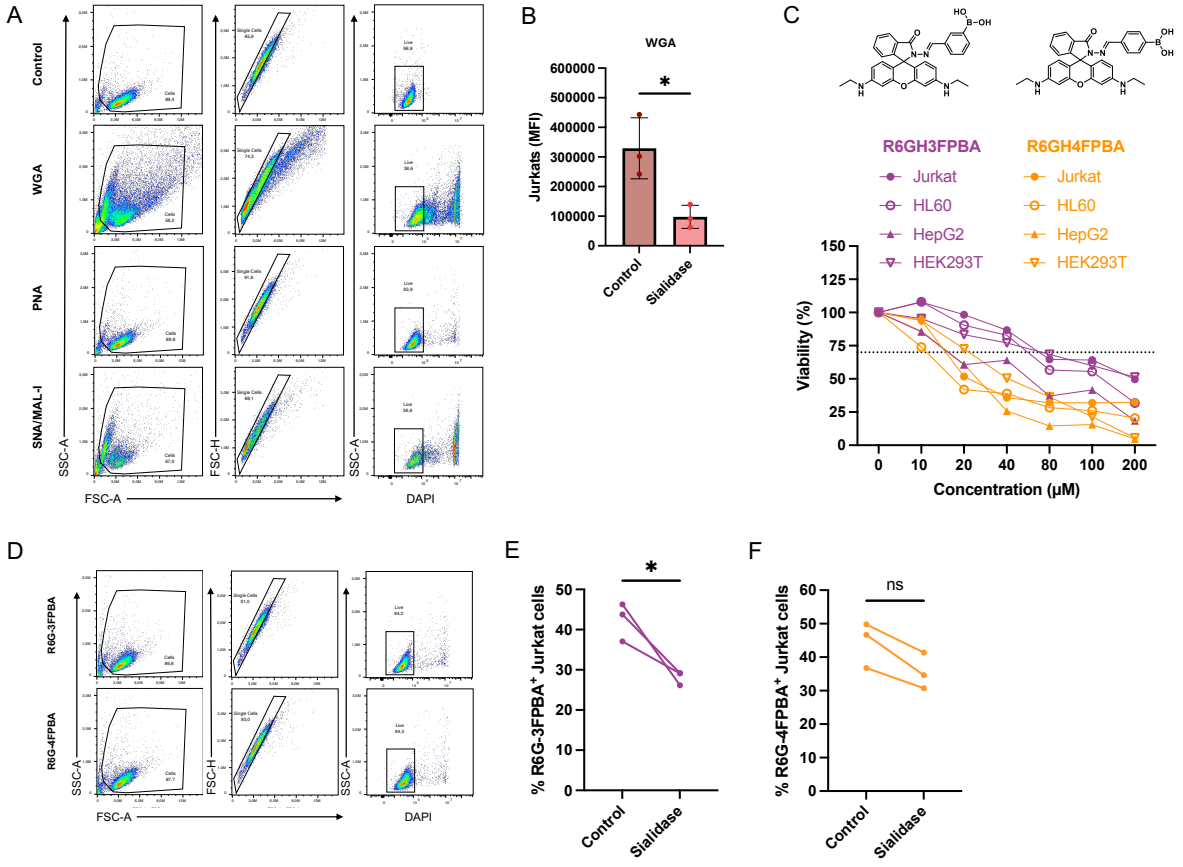

Figure 26. (**A**) Representative flow cytometric dot plots of unstained control, WGA, PNA, and SNA/MAL-I stained Jurkat cells for 30 min. (**B**) Flow cytometric evaluation of WGA (MFI) staining in 30 min sialidase treated Jurkat cells. (**C**) Viability (%) of Jurkat cells, HL60, HepG2, and HEK293T assessed after treatment with 0, 10, 20, 40, 80, 100, and 200 µM R6GH3FPBA and R6GH4FPBA for 24 hours using the resazurin assay. Cytotoxicity was considered when viability was below 70% (dashed line). (**D**) Representative flow cytometric dot plots of Jurkat cells stained with 40 µM of the probes for 30 min. (**E-F**) Sialidase-treated Jurkat cells stained with 40 µM of the probes for 30 min. MFI was analyzed by flow cytometry. Data represents mean ± SD (n=3). Statistical analysis was performed using an unpaired t-test (*p<0.05).

To summarize the findings of **paper V**, evidence of elevated Sia levels was found in SF of one out of five OA patients, which may be linked with a catabolic joint microenvironment characterized by upregulated endogenous sialidase activity. Conventional Sia-detecting thiobarbituric acid assay and enzymatic approaches were able to capture these patterns. Furthermore, analysis of Sia metabolism strongly indicates that there is an increased biosynthesis of Sia in several different cell types under inflammatory conditions. Interestingly, this enhanced metabolic activity was not reflected in corresponding increases in cell surface sialylation on primary monocytes, suggesting a potential imbalance in the glycan machinery during inflammation. However, this observation requires further validation as metabolic labeling and lectin staining was not performed on the same cell populations. In addition, two first-generation Sia-selective fluorescent probes were developed. Due to unsatisfactory safety profiles under extended live-cell conditions, these probes were instead used for shorter staining procedures followed by flow cytometric analysis. Under these conditions, the probes demonstrated more promising biocompatibility and Sia-selectivity. Current ongoing work is underway for developing the next-generation probes with enhanced hydrophilicity and biocompatibility.

7. Concluding Remarks and Future Outlooks

OA is a complex and multifaceted disease involving multiple cellular and molecular compartments within the joint. Experimental research has traditionally focused on cartilage degeneration and release of cytokines and catabolic enzymes as drivers of disease progression. While these efforts have substantially advanced our understanding of inflammatory processes in OA, they have not yet resulted in the development of effective disease-modifying treatments. In this thesis, glycobiology was integrated to add another layer for deepening the understanding of OA pathophysiology. Glycans play an important role in maintaining homeostasis, and altered glycosylation has been implicated in multiple diseases, although their exact mechanisms are often poorly defined. This thesis puts a special emphasis on the monosaccharide Sia, as its terminal location, charge, and role in immune regulation make it an attractive target for elucidating disease mechanisms and developing Sia-targeting therapies. This work is especially important as it addresses a largely understudied mechanism, thereby advancing our understanding of OA pathophysiology. As the interdisciplinary area of nanomedicine is redefining the future of healthcare, this work also explored new perspectives for disease-modifying strategies by leveraging nanotechnology.

The previous identification of soluble Siglec-5 in OA SF prompted us to investigate its potential regulatory role in monocytes, focusing on TLR4 regulation in **paper I**. While Siglec-mediated regulation of TLRs has been demonstrated before, few studies have explored Siglec-5-TLR4 interactions, and the role of Siglecs in OA remains underexplored. I demonstrate that increased Siglec-5 expression on monocytes inversely correlates with TLR4 expression. This indicates that Siglec-5 may suppress TLR4 signaling, which was further supported by increased cytokine release in SHP-I inhibited monocytes. The sequence homology between Siglec-5 and Siglec-14 may partly explain why the inhibitory Siglec-5 has received limited attention. These findings thus contribute to clarifying the functional relevance of Siglec-5 in monocyte regulation, which could be interesting in other cell types and diseases. Furthermore, spatial reorganization of Siglec interactions in response to different inflammatory stimuli was observed. To my knowledge, this aspect has not been previously investigated. This approach could be beneficial for detailing spatial expression patterns between other Siglecs and sialylated structures, to enhance our understanding of their mechanistic roles and potential ligands.

Clustering analysis of OA SF-stimulated monocytes revealed substantial phenotypic heterogeneity. Using this approach, it was possible to couple the SFs to certain inflammatory profiles, where especially increased Siglec-5 expression correlated with higher inflammation. While this appear contradictory given the inhibitory nature of Siglec-5, one could speculate that this is an attempt by the cell to suppress inflammation with a delayed response. Nevertheless, this clustering approach may be useful for understanding different endotypes of OA. In **paper V**, interpatient variability in Sia levels in SFs was revealed, with increased Sia levels potentially correlating with higher inflammation and elevated Siglec-5 on monocytes.

Based on the findings of interpatient variations, we hypothesized that they may reflect different levels of inflammation, a drug delivery system (DDS) for controlled release in response to inflammatory signals such as local acidification may in this case be a useful treatment option.

In **paper II** I evaluated the performance of our developed AcDex NPs as vehicles for controlled release. This work provided evidence of inflammation-mediated triggered release of a model drug from the AcDex NP, demonstrating that careful design of drug carriers can yield effective stimulus-responsive controlled release behavior. This DDS could in the future be loaded with corticosteroids, NSAIDs, or TAK-242, to allow pH-responsive dosing at the exact site and time it is needed. Given that approved controlled release-formulations are mainly limited to microsphere-based depot systems, this proof of concept NP platform supports a potential future for smart nanoscale materials for more dynamic responsive release profiles.

In **paper III**, direct cell targeting through Sia was investigated as a therapeutic strategy. In OA, recruitment of monocytes is a known factor, but the underlying mechanism governing this process is not fully understood. A PLGA-based NP was developed by exploiting the affinity by PBA to Sia, this NP platform was designed as a multivalent lectin-mimetic for selective targeting of Sia. This design offered direct and electrostatic interactions. Through well-established and more novel approaches, I demonstrated how this NP formulation was biocompatible, Sia-selective, and achieved reduced monocyte migration. While these findings represent a proof of concept, they provide foundational evidence for the therapeutic potential of interfering with Sia-mediated interactions as a strategy for immunomodulation. While this NP approach showed promising immunomodulatory effects, encapsulation of for example TAK-242 or another drug candidate may prove meaningful for more specific anti-inflammatory effects. As Sia is present on other cells and tissues, a more realistic approach would perhaps be to add a second targeting unit for enhanced targeting to monocytes. Furthermore, these NPs could potentially modulate the Siglec-Sia axis, which could be valuable in other disease such as cancer.

Paper IV aimed to investigate interactions between NPs of different size and charge with specific cartilage enzymatic glycoprotein products and their role in shaping immune responses. In this work I showed that size and charge matters, as smaller, positively charged NPs activated macrophages as opposed to larger more neutral NPs. However, certain glycoprotein interactions were linked to increased or decreased immune activation, suggesting that specific disease profiles might need to be considered for optimal NP design. As the specific disease microenvironment is often overlooked, this work underscores the need for physiologically relevant experimental platforms to assess specific glycoprotein-NP interactions and their biological consequences. In **paper V** I compared different commercially available methods to expand our understanding of the role of Sia in OA. In this work I demonstrated the challenges and opportunities with these methods and compared to our developed fluorescence-activatable probes. This work highlighted the complexity of Sia expression patterns linked with inflammation, demonstrating how combining several complimentary techniques can enhance our understanding of the role of Sia in OA pathophysiology.

8. Acknowledgements

First, I would like to thank my supervisor **Alexandra** for all the years I spent in your group. You have been a great leader and friend throughout this time. Thank you for the continuous support, guidance, and encouragement, and for believing in me when I doubted myself. Your curiosity and passion for science are truly admirable and contagious, and I have learnt more than I could ever have imagined.

I would also like to thank my co-supervisor **Carmen** for being supportive and encouraging. I appreciate all our scientific discussion, help with trouble-shootings, and collaborations throughout these years.

To my examiner **Elin**, thank you for your guidance and support, I greatly appreciate the helpful insights and feedback you have provided.

A special thanks to all **co-authors** involved in the articles and manuscripts of this thesis. Your expertise, insights, and valuable feedback have greatly contributed to this work.

To all Stubelius group members, thank you for your interest in my research, the many valuable scientific discussions, and, just as importantly, all the good memories we shared. A special thank you to **Ratish** for all the help with my chemistry-related questions, and **Hanna**, I am truly grateful for your endless positive energy, curiosity, and passion for science. There is never a dull day in the office with you. You are not only a colleague, but also one of my dearest friends.

I would especially want to thank former group members **Gizem** and **Ula**. You were there from the very beginning. I greatly appreciate the scientific input and expertise you have provided, your endless support, but most importantly, I appreciate all our fun memories we share.

To all previous Stubelius group members, thank you for all the memories, discussions, and help.

Thanks to all current and former **colleagues** and **friends** at the division. A special thank you to **Vesa**, I am grateful for all the years as office mates, sharing cell lab duties and CO_2 gas tube responsibilities, but most importantly having you as my friend. **Eve**, thank you for all the memories we have made over the years, and for always being so sweet, uplifting, and kind. **Viktoria** and **Elin**, thanks for being such supportive friends, thanks for all the laughter, you two truly rock. **Fritjof**, you have been part of this journey since the start, thanks being such a great friend, always helpful, and open for discussions. You always have a chair in our office. **Marziyeh**, thank you for being a great friend, being so cheerful, and for being my biggest supporter.

Finally, I would like to express my sincere gratitude for my **friends** and **family** for supporting and believing in me throughout this journey. A special thank you to **mamma**, **pappa**, **Mona**, and **Crille**, I would not be where I am today without you. **Jacob**, thank you for your endless love and support, and for always pushing me to believe in myself. I am beyond grateful to have you by my side.

9. References

1. He, M., Zhou, X. & Wang, X. Glycosylation: mechanisms, biological functions and clinical implications. *Signal Transduction and Targeted Therapy* **9**(2024).
2. Li, Q.*, et al.* Hyperglycemia-induced accumulation of advanced glycosylation end products in fibroblast-like synoviocytes promotes knee osteoarthritis. *Experimental & Molecular Medicine* **53**, 1735-1747 (2021).
3. Yu, H.*, et al.* Characterization of aberrant glycosylation associated with osteoarthritis based on integrated glycomics methods. *Arthritis Research & Therapy* **25**(2023).
4. Jia, Y., Liu, Y., Wang, Y., Li, J. & Li, G. Sialylation-induced stabilization of dynamic glycoprotein conformations unveiled by time-aligned parallel unfolding and glycan release mass spectrometry. *Chemical Science* **15**, 14431-14439 (2024).
5. Zhu, W., Zhou, Y., Guo, L. & Feng, S. Biological function of sialic acid and sialylation in human health and disease. *Cell Death Discovery* **10**(2024).
6. Cui, Z.*, et al.* Correlation between sialic acid levels in the synovial fluid and the radiographic severity of knee osteoarthritis. *Experimental and Therapeutic Medicine* **8**, 255-259 (2014).
7. Huang, S.*, et al.* Truncated lubricin glycans in osteoarthritis stimulate the synoviocyte secretion of VEGFA, IL-8, and MIP-1α: Interplay between O-linked glycosylation and inflammatory cytokines. *Frontiers in Molecular Biosciences* **9**(2022).
8. Pabst, M.*, et al.* IL-1beta and TNF-alpha alter the glycophenotype of primary human chondrocytes in vitro. *Carbohydrate Research* **345**, 1389-1393 (2010).
9. Carpintero-Fernandez, P.*, et al.* New therapeutic strategies for osteoarthritis by targeting sialic acid receptors. *Biomolecules* **10**, 637 (2020).
10. Dell'Isola, A., Recenti, F., Giardulli, B., Lawford, B.J. & Kiadaliri, A. Osteoarthritis year in review 2025: Epidemiology and therapy. *Osteoarthritis and Cartilage* **33**, 1300-1306 (2025).
11. Tang, S.*, et al.* Osteoarthritis. *Nat Rev Dis Primers* **11**, 10 (2025).
12. Lou, Z. & Bu, F. Recent advances in osteoarthritis research: A review of treatment strategies, mechanistic insights, and acupuncture. *Medicine (Baltimore)* **104**, e41335 (2025).
13. Van Den Bosch, M.H.J., Blom, A.B. & Van Der Kraan, P.M. Inflammation in osteoarthritis: Our view on its presence and involvement in disease development over the years. *Osteoarthritis and Cartilage* **32**, 355-364 (2024).
14. Li, X.*, et al.* Enhanced osteoarthritis treatment using an injectable pH-responsive and cartilage-targeted liposome-anchored kartogenin-incorporated methacrylated gelatin hydrogel microspheres. *International Journal of Biological Macromolecules* **313**, 144198 (2025).
15. Rodriguez-Merchan, E.C. The current role of disease-modifying osteoarthritis drugs. *The Archive of Bone and Joint Surgery* **11**, 11-22 (2023).
16. Brandt, M.D., Malone, J.B. & Kean, T.J. Advances and challenges in the pursuit of disease-modifying osteoarthritis drugs: a review of 2010–2024 clinical crials. *Biomedicines* **13**, 355 (2025).
17. Reily, C., Stewart, T.J., Renfrow, M.B. & Novak, J. Glycosylation in health and disease. *Nat Rev Nephrol* **15**, 346-366 (2019).
18. Saini, P., Adeniji, O.S. & Abdel-Mohsen, M. Inhibitory Siglec-sialic acid interactions in balancing immunological activation and tolerance during viral infections. *EBioMedicine* **86**, 104354 (2022).
19. Cao, Y., Ma, Y., Tao, Y., Lin, W. & Wang, P. Intra-Articular Drug Delivery for Osteoarthritis Treatment. *Pharmaceutics* **13**(2021).
20. Di, J.*, et al.* Size, shape, charge and "stealthy" surface: Carrier properties affect the drug circulation time in vivo. *Asian Journal of Pharmaceutical Sciences* **16**, 444-458 (2021).
21. Osteoarthritis. (World Health Organization, 2023).
22. Steinmetz, J.D.*, et al.* Global, regional, and national burden of osteoarthritis, 1990–2020 and projections to 2050: a systematic analysis for the Global Burden of Disease Study 2021. *The Lancet Rheumatology* **5**, e508-e522 (2023).
23. Kloppenburg, M., Namane, M. & Cicuttini, F. Osteoarthritis. *The Lancet* **405**, 71-85 (2025).

24. Buchanan, W.W., Kean, C.A., Kean, W.F. & Rainsford, K.D. Osteoarthritis. *Inflammopharmacology* **32**, 13-22 (2024).
25. Long, H.*, et al.* Prevalence Trends of Site-Specific Osteoarthritis From 1990 to 2019: Findings From the Global Burden of Disease Study 2019. *Arthritis and Rheumatology* **74**, 1172-1183 (2022).
26. Abulhasan, J. & Grey, M. Anatomy and Physiology of Knee Stability. *Journal of Functional Morphology and Kinesiology* **2**, 34 (2017).
27. Alcaide-Ruggiero, L., Cugat, R. & Domínguez, J.M. Proteoglycans in Articular Cartilage and Their Contribution to Chondral Injury and Repair Mechanisms. *International Journal of Molecular Sciences* **24**, 10824 (2023).
28. Horkay, F. & Basser, P.J. Composite Hydrogel Model of Cartilage Predicts Its Load-Bearing Ability. *Scientific Reports* **10**(2020).
29. Sanchez-Lopez, E., Coras, R., Torres, A., Lane, N.E. & Guma, M. Synovial inflammation in osteoarthritis progression. *Nature Reviews Rheumatology* **18**, 258-275 (2022).
30. Haubruck, P., Pinto, M.M., Moradi, B., Little, C.B. & Gentek, R. Monocytes, Macrophages, and Their Potential Niches in Synovial Joints – Therapeutic Targets in Post-Traumatic Osteoarthritis? *Frontiers in Immunology* **12**(2021).
31. Ji, M.-L.*, et al.* Sirt6 attenuates chondrocyte senescence and osteoarthritis progression. *Nature Communications* **13**(2022).
32. Angelini, F.*, et al.* Osteoarthritis endotype discovery via clustering of biochemical marker data. *Annals of the Rheumatic Diseases* **81**, 666-675 (2022).
33. Boer, C.G. Osteoarthritis year in review 2024: Genetics, genomics, and epigenetics. *Osteoarthritis and Cartilage* **33**, 50-57 (2025).
34. Zhai, G. & Huang, J. Genetics of osteoarthritis. *Best Practice & Research Clinical Rheumatology* **38**, 101972 (2024).
35. Bender, E.C., Tareq, H.S. & Suggs, L.J. Inflammation: a matter of immune cell life and death. *npj Biomedical Innovations* **2**(2025).
36. Chou, C.-H.*, et al.* Synovial cell cross-talk with cartilage plays a major role in the pathogenesis of osteoarthritis. *Scientific Reports* **10**(2020).
37. Zhang, K.*, et al.* Mechanisms of synovial macrophage polarization in osteoarthritis pathogenesis and their therapeutic implications. *Frontiers in Immunology* **16**(2025).
38. Zhang, H., Cai, D. & Bai, X. Macrophages regulate the progression of osteoarthritis. *Osteoarthritis Cartilage* **28**, 555-561 (2020).
39. Zhao, X.*, et al.* CCL3/CCR1 mediates CD14+CD16− circulating monocyte recruitment in knee osteoarthritis progression. *Osteoarthritis and Cartilage* **28**, 613-625 (2020).
40. Athanasou, N.A. & Quinn, J. Immunocytochemical analysis of human synovial lining cells: phenotypic relation to other marrow derived cells. *Annals of the Rheumatic Diseases* **50**, 311-315 (1991).
41. Haywood, L.*, et al.* Inflammation and angiogenesis in osteoarthritis. *Arthritis & Rheumatology* **48**, 2173-2177 (2003).
42. Manferdini, C.*, et al.* From osteoarthritic synovium to synovial-derived cells characterization: synovial macrophages are key effector cells. *Arthritis Research & Therapy* **18**(2016).
43. Sun, H.*, et al.* Blocking TRPV4 Ameliorates Osteoarthritis by Inhibiting M1 Macrophage Polarization via the ROS/NLRP3 Signaling Pathway. *Antioxidants* **11**, 2315 (2022).
44. Qian, X.*, et al.* Acidosis induces synovial fibroblasts to release vascular endothelial growth factor via acid-sensitive ion channel 1a. *Laboratory Investigation* **101**, 280-291 (2021).
45. Qian, X.*, et al.* Acidosis regulates immune progression in rheumatoid arthritis by promoting the expression of cytokines and co-stimulatory molecules in synovial fibroblasts. *Molecular Medicine* **31**(2025).
46. Gómez, R., Villalvilla, A., Largo, R., Gualillo, O. & Herrero-Beaumont, G. TLR4 signalling in osteoarthritis—finding targets for candidate DMOADs. *Nature Reviews Rheumatology* **11**, 159-170 (2015).
47. Kim, H.-J., Kim, H., Lee, J.-H. & Hwangbo, C. Toll-like receptor 4 (TLR4): new insight immune and aging. *Immunity & Ageing* **20**(2023).

48. Allendorf, D.H., Franssen, E.H. & Brown, G.C. Lipopolysaccharide activates microglia via neuraminidase 1 desialylation of Toll-like Receptor 4. *J Neurochem* **155**, 403-416 (2020).
49. Karmakar, J., Roy, S. & Mandal, C. Modulation of TLR4 Sialylation Mediated by a Sialidase Neu1 and Impairment of Its Signaling in Leishmania donovani Infected Macrophages. *Frontiers in Immunology* **10**, 2360 (2019).
50. Sundararaj, K., Rodgers, J., Angel, P., Wolf, B. & Nowling, T.K. The role of neuraminidase in TLR4-MAPK signalling and the release of cytokines by lupus serum-stimulated mesangial cells. *Immunology* **162**, 418-433 (2021).
51. Bartels, Y.L.*, et al.* Inhibition of TLR4 signalling to dampen joint inflammation in osteoarthritis. *Rheumatology (Oxford)* **63**, 608-618 (2024).
52. Khomeijani-Farahani, M.*, et al.* TAK-242 (Resatorvid) inhibits proinflammatory cytokine production through the inhibition of NF-κB signaling pathway in fibroblast-like synoviocytes in osteoarthritis patients. *Advances in Rheumatology* **64**(2024).
53. Thoenen, J., MacKay, J.W., Sandford, H.J.C., Gold, G.E. & Kogan, F. Imaging of Synovial Inflammation in Osteoarthritis, From the AJR Special Series on Inflammation. *AJR Am J Roentgenol* **218**, 405-417 (2022).
54. Whelton, A.*, et al.* Cyclooxygenase-2--specific inhibitors and cardiorenal function: a randomized, controlled trial of celecoxib and rofecoxib in older hypertensive osteoarthritis patients. *American Journal of Therapeutics* **8**, 85-95 (2001).
55. Silverstein, F.E.*, et al.* Gastrointestinal toxicity with celecoxib vs nonsteroidal anti-inflammatory drugs for osteoarthritis and rheumatoid arthritis: the CLASS study: A randomized controlled trial. Celecoxib Long-term Arthritis Safety Study. *JAMA* **284**, 1247-1255 (2000).
56. Bleumink, G.L.S., Feenstra, J., Sturkenboom, M.C.J.M. & Stricker, B.H.C. Nonsteroidal Anti-Inflammatory Drugs and Heart Failure. *Drugs* **63**, 525-534 (2003).
57. Salis, Z. & Sainsbury, A. Association of long-term use of non-steroidal anti-inflammatory drugs with knee osteoarthritis: a prospective multi-cohort study over 4-to-5 years. *Scientific Reports* **14**, 6593 (2024).
58. Migliore, A. & Procopio, S. Effectiveness and utility of hyaluronic acid in osteoarthritis. *Clinical Cases in Mineral and Bone Metabolism* **12**, 31-33 (2015).
59. Ayhan, E., Kesmezacar, H. & Akgun, I. Intraarticular injections (corticosteroid, hyaluronic acid, platelet rich plasma) for the knee osteoarthritis. *World Journal of Orthopedics* **5**, 351-361 (2014).
60. Cohen, S.B.*, et al.* A randomized, double-blind study of AMG 108 (a fully human monoclonal antibody to IL-1R1) in patients with osteoarthritis of the knee. *Arthritis Research & Therapy* **13**, R125 (2011).
61. Wang, J. Efficacy and safety of adalimumab by intra-articular injection for moderate to severe knee osteoarthritis: An open-label randomized controlled trial. *Journal of International Medicine Research* **46**, 326-334 (2018).
62. Fleischmann, R.M.*, et al.* A Phase II Trial of Lutikizumab, an Anti-Interleukin-1alpha/beta Dual Variable Domain Immunoglobulin, in Knee Osteoarthritis Patients With Synovitis. *Arthritis Rheumatology* **71**, 1056-1069 (2019).
63. Chevalier, X.*, et al.* Intraarticular injection of anakinra in osteoarthritis of the knee: A multicenter, randomized, double-blind, placebo-controlled study. *Arthritis Care & Research* **61**, 344-352 (2009).
64. Schnitzer, T.*, et al.* Evaluation of S201086/GLPG1972, an ADAMTS-5 inhibitor, for the treatment of knee osteoarthritis in ROCCELLA: a phase 2 randomized clinical trial. *Osteoarthritis Cartilage* **31**, 985-994 (2023).
65. Krzeski, P.*, et al.* Development of musculoskeletal toxicity without clear benefit after administration of PG-116800, a matrix metalloproteinase inhibitor, to patients with knee osteoarthritis: a randomized, 12-month, double-blind, placebo-controlled study. *Arthritis Research & Therapy* **9**, R109 (2007).
66. Snijders, G.F., Van Den Ende, C.H., Van Riel, P.L., Van Den Hoogen, F.H. & Den Broeder, A.A. The effects of doxycycline on reducing symptoms in knee osteoarthritis: results from a triple-blinded randomised controlled trial. *Annals of the Rheumatic Diseases* **70**, 1191-1196 (2011).

67. Dell, A., Galadari, A., Sastre, F. & Hitchen, P. Similarities and differences in the glycosylation mechanisms in prokaryotes and eukaryotes. *International Journal of Microbiology* **2010**, 148178 (2010).
68. Critcher, M., Hassan, A.A. & Huang, M.L. Seeing the forest through the trees: characterizing the glycoproteome. *Trends in Biochemical Sciences* **47**, 492-505 (2022).
69. Winkler, P.M., Campelo, F., Giannotti, M.I. & Garcia-Parajo, M.F. Impact of Glycans on Lipid Membrane Dynamics at the Nanoscale Unveiled by Planar Plasmonic Nanogap Antennas and Atomic Force Spectroscopy. *The Journal of Physical Chemistry Letters* **12**, 1175-1181 (2021).
70. Yoshimoto, M.*, et al.* Bioinformatic analysis reveals potential relationship between chondrocyte senescence and protein glycosylation in osteoarthritis pathogenesis. *Frontiers in Endocrinology* **14**(2023).
71. Afshari, A.R.*, et al.* Glycoproteoforms of Osteoarthritis-associated Lubricin in Plasma and Synovial Fluid. *Molecular & Cellular Proteomics* **24**, 100923 (2025).
72. Tran, L.S.*, et al.* ER O-glycosylation in synovial fibroblasts drives cartilage degradation. *Nature Communications* **16**(2025).
73. Lee, Y.R.*, et al.* Complex-Type N-Glycans Are Associated with Cartilage Degeneration within Different Loading Sites of the Tibial Plateau for Knee Osteoarthritis Patients. *Journal of Proteome Research* **22**, 2694-2702 (2023).
74. Homan, K.*, et al.* Articular cartilage corefucosylation regulates tissue resilience in osteoarthritis. *Elife* **12**(2024).
75. Liu, H.Z., Song, X.Q. & Zhang, H. Sugar-coated bullets: Unveiling the enigmatic mystery 'sweet arsenal' in osteoarthritis. *Heliyon* **10**, e27624 (2024).
76. Krištić, J. & Lauc, G. The importance of IgG glycosylation—What did we learn after analyzing over 100,000 individuals. *Immunological Reviews* **328**, 143-170 (2024).
77. Gaifem, J.*, et al.* A unique serum IgG glycosylation signature predicts development of Crohn's disease and is associated with pathogenic antibodies to mannose glycan. *Nature Immunology* **25**, 1692-1703 (2024).
78. Radovani, B. & Gudelj, I. N-Glycosylation and Inflammation; the Not-So-Sweet Relation. *Frontiers in Immunology* **13**(2022).
79. Festari, M.F., Jara, E., Costa, M., Iriarte, A. & Freire, T. Truncated O-glycosylation in metastatic triple-negative breast cancer reveals a gene expression signature associated with extracellular matrix and proteolysis. *Scientific Reports* **14**(2024).
80. Kudelka, M.R., Stowell, S.R., Cummings, R.D. & Neish, A.S. Intestinal epithelial glycosylation in homeostasis and gut microbiota interactions in IBD. *Nature Reviews Gastroenterology & Hepatology* **17**, 597-617 (2020).
81. Leifer, C.A. & Medvedev, A.E. Molecular mechanisms of regulation of Toll-like receptor signaling. *Journal of Leukocyte Biology* **100**, 927-941 (2016).
82. Gorenflos López, J.L.*, et al.* Real-time monitoring of the sialic acid biosynthesis pathway by NMR. *Chemical Science* **14**, 3482-3492 (2023).
83. Rawal, P. & Zhao, L. Sialometabolism in Brain Health and Alzheimer's Disease. *Frontiers in Neuroscience* **15**(2021).
84. Angata, T. & Varki, A. Discovery, classification, evolution and diversity of Siglecs. *Molecular Aspects of Medicine* **90**, 101117 (2023).
85. Wang, Y.*, et al.* Siglec-15/sialic acid axis as a central glyco-immune checkpoint in breast cancer bone metastasis. *Proceedings of the National Academy of Sciences* **121**(2024).
86. Wattchow, N.E.*, et al.* The emerging role of glycans and the importance of sialylation in cardiovascular disease. *Atherosclerosis* **403**, 119172 (2025).
87. Van Vliet, S.J. & Van Kooyk, Y. Sialic acids in cancer biology and immunity—recent advancements. *Journal of Biological Chemistry* **301**, 110641 (2025).
88. Pinho, S.S., Macauley, M.S. & Läubli, H. Tumor glyco-immunology, glyco-immune checkpoints and immunotherapy. *Journal for ImmunoTherapy of Cancer* **13**, e012391 (2025).
89. Memarian, E.*, et al.* Plasma protein *N*-glycosylation is associated with cardiovascular disease, nephropathy, and retinopathy in type 2 diabetes. *BMJ Open Diabetes Research & Care* **9**, e002345 (2021).

90. Wang, Y.*, et al.* Loss of α2-6 sialylation promotes the transformation of synovial fibroblasts into a pro-inflammatory phenotype in arthritis. *Nature Communications* **12**(2021).
91. Boelaars, K. & Van Kooyk, Y. Targeting myeloid cells for cancer immunotherapy: Siglec-7/9/10/15 and their ligands. *Trends in Cancer* **10**, 230-241 (2024).
92. Korn, M.A.*, et al.* Siglec-15 on Osteoclasts Is Crucial for Bone Erosion in Serum-Transfer Arthritis. *The Journal of Immunology* **205**, 2595-2605 (2020).
93. Dou, C.*, et al.* Sialylation of TLR2 initiates osteoclast fusion. *Bone Research* **10**, 24 (2022).
94. Zhang, W.*, et al.* $RANK^{+}TLR2^{+}$ myeloid subpopulation converts autoimmune to joint destruction in rheumatoid arthritis. *Elife* **12**(2023).
95. Chen, G.Y.*, et al.* Broad and direct interaction between TLR and Siglec families of pattern recognition receptors and its regulation by Neu1. *Elife* **3**, e04066 (2014).
96. Van Houtum, E.J.H., Büll, C., Cornelissen, L.A.M. & Adema, G.J. Siglec Signaling in the Tumor Microenvironment. *Frontiers in Immunology* **12**(2021).
97. Kang, E.A.*, et al.* Soluble Siglec-9 alleviates intestinal inflammation through inhibition of the NF-kappaB pathway. *International Immunopharmacology* **86**, 106695 (2020).
98. Vuchkovska, A.*, et al.* Siglec-5 is an inhibitory immune checkpoint molecule for human T cells. *Immunology* **166**, 238-248 (2022).
99. Lee, J.*, et al.* Soluble siglec-5 is a novel salivary biomarker for primary Sjogren's syndrome. *Journal of Autoimmunity* **100**, 114-119 (2019).
100. Huang, P.J., Low, P.Y., Wang, I., Hsu, S.D. & Angata, T. Soluble Siglec-14 glycan-recognition protein is generated by alternative splicing and suppresses myeloid inflammatory responses. *Journal of Biolological Chemistry* **293**, 19645-19658 (2018).
101. Wang, X.*, et al.* Siglec-9 is upregulated in rheumatoid arthritis and suppresses collagen-induced arthritis through reciprocal regulation of Th17-/Treg-cell differentiation. *Scandinavian Journal of Immunology* **85**, 433-440 (2017).
102. Shanghai Henlius Biotech (Responsible Party) (NCT07038382). A Study to Evaluate the Efficacy, Safety, and Tolerability of Human Sialidase Fusion Protein (HLX79) in Combination With Rituximab Injection Versus Placebo in Patients With Active Glomerulonephritis. (ClinicalTrials.gov, 2025).
103. Sharma, M.R.*, et al.* 758 GLIMMER-01: phase 1/2 trial of a first-in-class bi-sialidase (E-602) in combination with cemiplimab in patients with PD-(L)1-resistant solid tumors. A862-A862 (BMJ Publishing Group Ltd).
104. Aviceda Therapeutics, I.R.P.N. A Multiple Dose Study of AVD-104 for Geographic Atrophy (GA) Secondary to Age-Related Macular Degeneration (AMD) (SIGLEC). (2023).
105. Mora, J.*, et al.* The anti-GD2 monoclonal antibody naxitamab plus GM-CSF for relapsed or refractory high-risk neuroblastoma: a phase 2 clinical trial. *Nature Communications* **16**(2025).
106. Liu, W., Xiong, W., Liu, W., Hirakawa, J. & Kawashima, H. A novel monoclonal antibody against 6-sulfo sialyl Lewis x glycans attenuates murine allergic rhinitis by suppressing Th2 immune responses. *Scientific Reports* **13**(2023).
107. Büll, C.*, et al.* Sialic Acid Blockade Suppresses Tumor Growth by Enhancing T-cell–Mediated Tumor Immunity. *Cancer Research* **78**, 3574-3588 (2018).
108. Gray, M.A.*, et al.* Targeted glycan degradation potentiates the anticancer immune response in vivo. *Nature Chemical Biology* **16**, 1376-1384 (2020).
109. Lam, Y.Y., Tan, A., Nowell, C.J., Kempe, K. & Boyd, B.J. Systematic Investigation of Metabolic Oligosaccharide Engineering Efficiency in Intestinal Cells Using a Dibenzocyclooctyne-Monosaccharide Conjugate. *ChemBioChem* **24**(2023).
110. Zhou, S., Dai, L., Pan, L., Shen, G. & Qian, Z. Phenylboronic acid-modified nanoparticles for cancer treatment. *Chemical Communications* **61**, 4595-4605 (2025).
111. Jangid, A.K., Kim, S., Park, H.W., Kim, H.J. & Kim, K. Ex Vivo Surface Decoration of Phenylboronic Acid onto Natural Killer Cells for Sialic Acid-Mediated Versatile Cancer Cell Targeting. *Biomacromolecules* **25**, 222-237 (2024).
112. Song, D.*, et al.* Self-assembled phenylboronic acid nanomedicine targets sialic acid to synergistically activate ferroptosis via RRM1 suppression and GPX4 Inhibition for precision colon cancer therapy. *Journal of Nanobiotechnology* **23**(2025).

113. Wang, T.*, et al.* MiR-193b modulates osteoarthritis progression through targeting ST3GAL4 via sialylation of CD44 and NF-small ka, CyrillicB pathway. *Cell Signal* **76**, 109814 (2020).
114. Park, E.-J., Kim, L.-L., Go, H. & Kim, S.-H. Effects of 3′-Sialyllactose on Symptom Improvement in Patients with Knee Osteoarthritis: A Randomized Pilot Study. *Nutrients* **16**, 3410 (2024).
115. Kurul, F., Turkmen, H., Cetin, A- E., Nur Topkaya, S.,. Nanomedicine: How nanomaterials are transforming drug delivery, bio-imaging, and diagnosis. *Next nanotechnology* **Volume 7**(2025).
116. Altammar, K.A. A review on nanoparticles: characteristics, synthesis, applications, and challenges. *Frontiers in Microbiology* **14**, 1155622 (2023).
117. Mubashar Saeed, M., Tollemeto, M., Thamdrup, L. H. E., Boisen, A., Carthy, E., Dunne, N., Kinahan, D.,. Controlled Synthesis and Drug Encapsulation of Poly(lactic-co-glycolic acid) Nanoparticles Using a Continuous Flow-Focusing Microfluidic Platform. *ACS Applied Nano Materials* (2026).
118. Zielinska, A.*, et al.* Polymeric Nanoparticles: Production, Characterization, Toxicology and Ecotoxicology. *Molecules* **25**(2020).
119. Zhou, J., Zhai, Y., Xu, J., Zhou, T. & Cen, L. Microfluidic preparation of PLGA composite microspheres with mesoporous silica nanoparticles for finely manipulated drug release. *International Journal of Pharmaceutics* **593**, 120173 (2021).
120. Stapenhorst Franca, F.*, et al.* Galantamine-loaded PLGA nanoparticles reduce oxidative stress and inflammation in a rat model of spinal cord injury. *Scientific Reports* **16**(2025).
121. Babilotte, J.*, et al.* Development and characterization of a PLGA-HA composite material to fabricate 3D-printed scaffolds for bone tissue engineering. *Materials Science and Engineering: C* **118**, 111334 (2021).
122. Alsaab, H.O.*, et al.* PLGA-Based Nanomedicine: History of Advancement and Development in Clinical Applications of Multiple Diseases. *Pharmaceutics* **14**, 2728 (2022).
123. Futterer, S., Andrusenko, I., Kolb, U., Hofmeister, W. & Langguth, P. Structural characterization of iron oxide/hydroxide nanoparticles in nine different parenteral drugs for the treatment of iron deficiency anaemia by electron diffraction (ED) and X-ray powder diffraction (XRPD). *Journal of Pharmaceutical and Biomedical Analysis* **86**, 151-160 (2013).
124. Zheng, T.*, et al.* Dextran-based T-cell expansion nanoparticles for manufacturing CAR T cells with augmented efficacy. *Nature Communications* **17**, 1103 (2026).
125. Maingret, V., Courregelongue, C., Schmitt, V. & Heroguez, V. Dextran-Based Nanoparticles to Formulate pH-Responsive Pickering Emulsions: A Fully Degradable Vector at a Day Scale. *Biomacromolecules* **21**, 5358-5368 (2020).
126. Bhatnagar, P.*, et al.* pH responsive dextran nanoparticles loaded with doxorubicin and RITA against cancer cells: synergistic inhibitory effects. *Journal of Nanoparticle Research* **26**(2024).
127. Erensoy, G.*, et al.* Dynamic Release from Acetalated Dextran Nanoparticles for Precision Therapy of Inflammation. *ACS Applied Bio Materials* **7**, 3810-3820 (2024).
128. Lee, C.C., MacKay, J.A., Frechet, J.M. & Szoka, F.C. Designing dendrimers for biological applications. *Nat Biotechnol* **23**, 1517-1526 (2005).
129. Alamos-Musre, S.*, et al.* From Structure to Function: The Promise of PAMAM Dendrimers in Biomedical Applications. *Pharmaceutics* **17**(2025).
130. Paull, J.R.A.*, et al.* Astodrimer sodium nasal spray forms a barrier to SARS-CoV-2 in vitro and preserves normal mucociliary function in human nasal epithelium. *Scientific Reports* **14**, 21259 (2024).
131. Rupp, R., Rosenthal, S.L. & Stanberry, L.R. VivaGel (SPL7013 Gel): a candidate dendrimer--microbicide for the prevention of HIV and HSV infection. *International Journal of Nanomedicine* **2**, 561-566 (2007).
132. Fadaei, M.R.*, et al.* Overview of dendrimers as promising drug delivery systems with insight into anticancer and anti-microbial applications. *International Journal of Pharmaceutics: X* **10**, 100390 (2025).
133. Geiger, B.C., Wang, S., Padera, R.F., Jr., Grodzinsky, A.J. & Hammond, P.T. Cartilage-penetrating nanocarriers improve delivery and efficacy of growth factor treatment of osteoarthritis. *Sci Transl Med* **10**(2018).

134. Von Mentzer, U.*, et al.* Synovial fluid profile dictates nanoparticle uptake into cartilage - implications of the protein corona for novel arthritis treatments. *Osteoarthritis and Cartilage* **30**, 1356-1364 (2022).
135. von Mentzer, U.*, et al.* Glycosylation-driven interactions of nanoparticles with the extracellular matrix: Implications for inflammation and drug delivery. *Biomaterials Advances* **171**, 214230 (2025).
136. Chaudhary, N., Weissman, D. & Whitehead, K.A. mRNA vaccines for infectious diseases: principles, delivery and clinical translation. *Nature Reviews Drug Discovery* **20**, 817-838 (2021).
137. Jacob, S.*, et al.* Advances in Lipid-Polymer Hybrid Nanoparticles: Design Strategies, Functionalization, Oncological and Non-Oncological Clinical Prospects. *Pharmaceuticals (Basel)* **18**(2025).
138. Hosseini-Kharat, M., Bremmell, K.E. & Prestidge, C.A. Why do lipid nanoparticles target the liver? Understanding of biodistribution and liver-specific tropism. *Molecular Therapy Methods & Clinical Development* **33**, 101436 (2025).
139. Pechyen, C., Tangnorawich, B., Toommee, S., Marks, R., Parcharoen, Y., . Green synthesis of metal nanoparticles, characterization, and biosensing applications. *Sensors International* **Volume 5**(2025).
140. Zhu, L., Zhou, Z., Mao, H. & Yang, L. Magnetic nanoparticles for precision oncology: theranostic magnetic iron oxide nanoparticles for image-guided and targeted cancer therapy. *Nanomedicine (Lond)* **12**, 73-87 (2017).
141. Hheidari, A.*, et al.* Metal-based nanoparticle in cancer treatment: lessons learned and challenges. *Frontiers in Bioengineering and Biotechnology* **12**, 1436297 (2024).
142. Kumar, S.*, et al.* Advantages and Disadvantages of Metal Nanoparticles. 209-235 (Springer Nature Singapore, 2023).
143. Kaur, A.*, et al.* Assessment of aqueous graphene as a cancer therapeutics delivery system. *Scientific Reports* **15**(2025).
144. Asadi, M., Ghorbani, S.H., Mahdavian, L. & Aghamohammadi, M. Graphene-based hybrid composites for cancer diagnostic and therapy. *Journal of Translational Medicine* **22**(2024).
145. Soltani, R., Guo, S., Bianco, A. & Ménard-Moyon, C. Carbon Nanomaterials Applied for the Treatment of Inflammatory Diseases: Preclinical Evidence. *Advanced Therapeutics* **3**, 2000051 (2020).
146. Mandl, H.K.*, et al.* Optimizing biodegradable nanoparticle size for tissue-specific delivery. *J Control Release* **314**, 92-101 (2019).
147. Ozturk, K., Kaplan, M. & Calis, S. Effects of nanoparticle size, shape, and zeta potential on drug delivery. *International Journal of Pharmaceutics* **666**, 124799 (2024).
148. Wei, X.*, et al.* Cationic nanocarriers induce cell necrosis through impairment of Na+/K+-ATPase and cause subsequent inflammatory response. *Cell Research* **25**, 237-253 (2015).
149. Rizvi, M., Gerengi, H., Gupta, P. & Functionalization of Nanomaterials: Synthesis and Characterization. Vol. 1418 (ACS Symposium Series, 2022).
150. Nabih, N.W.*, et al.* Antibody-functionalized lipid nanocarriers for RNA-based cancer gene therapy: advances and challenges in targeted delivery. *Nanoscale Advances* **7**, 5905-5931 (2025).
151. Chen, M.Z.*, et al.* A versatile antibody capture system drives specific in vivo delivery of mRNA-loaded lipid nanoparticles. *Nature Nanotechnology* **20**, 1273-1284 (2025).
152. Carvalho, A.M.*, et al.* Development of CD33-Targeted Dual Drug-Loaded Nanoparticles for the Treatment of Pediatric Acute Myeloid Leukemia. *Biomacromolecules* **25**, 6503-6514 (2024).
153. Basab, K.D., Jianmin, G. & Anupam, B. Functional boronic acid materials for cell surface interaction: Emerging applications in imaging and cellular transportation. *Coordination Chemistry Reviews* **544**(2025).
154. Shirley, M. Ixazomib: First Global Approval. *Drugs* **76**, 405-411 (2016).
155. Groll, M., Berkers, C.R., Ploegh, H.L. & Ovaa, H. Crystal structure of the boronic acid-based proteasome inhibitor bortezomib in complex with the yeast 20S proteasome. *Structure* **14**, 451-456 (2006).

156. Zhukova, V.*, et al.* Fluorescently Labeled PLGA Nanoparticles for Visualization In Vitro and In Vivo: The Importance of Dye Properties. *Pharmaceutics* **13**(2021).
157. Haripriyaa, M. & Suthindhiran, K. Pharmacokinetics of nanoparticles: current knowledge, future directions and its implications in drug delivery. *Future Journal of Pharmaceutical Sciences* **9**, 113 (2023).
158. Poon, W.*, et al.* Elimination Pathways of Nanoparticles. *ACS Nano* **13**, 5785-5798 (2019).
159. Knight, B., Walker, J. & Nair, L.S. Perineural local anesthetic treatments for osteoarthritic pain. *Regenerative Engineering and Translational Medicine* **7**, 262-282 (2021).
160. Bodick, N.*, et al.* FX006 prolongs the residency of triamcinolone acetonide in the synovial tissues of patients with knee osteoarthritis. *Osteoarthritis and Cartilage* **21**, S144-S145 (2013).
161. Deng, W.*, et al.* A review of nanomaterials in osteoarthritis treatment and immune modulation. *Regenerative Biomaterials* **12**, rbaf048 (2025).
162. Ding, S.*, et al.* Supramolecular Polyzwitterionic Nanoparticles with Engineered pH-Responsiveness and Cartilage-Penetration for Osteoarthritis Therapy. *Advanced Functional Materials* **35**(2025).
163. Mancipe Castro, L.M., Sequeira, A., Garcia, A.J. & Guldberg, R.E. Articular Cartilage- and Synoviocyte-Binding Poly(ethylene glycol) Nanocomposite Microgels as Intra-Articular Drug Delivery Vehicles for the Treatment of Osteoarthritis. *ACS Biomaterials Science & Engineering* **6**, 5084-5095 (2020).
164. Dewani, M.*, et al.* A disease-severity-responsive nanoparticle enables potent ghrelin messenger RNA therapy in osteoarthritis. *Nature Nanotechnology* **21**, 455-466 (2026).
165. Hei, Y.*, et al.* Therapeutic Effects of PEG-Modified Polyamide Amine Dendrimer for Cell Free DNA Adsorption in Temporomandibular Joint Osteoarthritis. *ACS Applied Materials & Interfaces* **16**, 39153-39164 (2024).
166. Johnston, B.M., Douglas-Green, S.A., Park, J.H., Grodzinsky, A.J. & Hammond, P.T. PEG chains modulate electrostatic interactions between PAMAM and articular cartilage. *Biomaterials* **331**, 124132 (2026).
167. Hunter, D.J.*, et al.* TLC599 in patients with osteoarthritis of the knee: a phase IIa, randomized, placebo-controlled, dose-finding study. *Arthritis Research & Therapy* **24**, 52 (2022).
168. Schnitzer, T.J.*, et al.* Intra-articular MM-II for the treatment of knee osteoarthritis pain: Efficacy and safety results from a 26-week, phase 2b, placebo-controlled, double-blind, randomized dose-ranging trial. *Osteoarthritis Cartilage* **33**, 897-906 (2025).
169. Pattappa, G.*, et al.* Towards stratification in osteoarthritis: a review of the scientific terminology used in published basic research. *BMC Rheumatology* **9**(2025).
170. Johnson, C.I., Argyle, D.J. & Clements, D.N. In vitro models for the study of osteoarthritis. *Vet J* **209**, 40-49 (2016).
171. Salgado, C., Jordan, O. & Allémann, E. Osteoarthritis In Vitro Models: Applications and Implications in Development of Intra-Articular Drug Delivery Systems. *Pharmaceutics* **13**, 60 (2021).
172. Weiskirchen, S., Schröder, S.K., Buhl, E.M. & Weiskirchen, R. A Beginner's Guide to Cell Culture: Practical Advice for Preventing Needless Problems. *Cells* **12**, 682 (2023).
173. Dou, H.*, et al.* Osteoarthritis models: From animals to tissue engineering. *J Tissue Eng* **14**, 20417314231172584 (2023).
174. Gao, B.*, et al.* Cartilage organoids: an emerging platform for novel osteoarthritis therapies. *Frontiers in Cell and Developmental Biology* **13**(2025).
175. Mirazi, H. & Wood, S.T. Microfluidic chip-based co-culture system for modeling human joint inflammation in osteoarthritis research. *Frontiers in Pharmacology* **16**(2025).
176. Banh, L., Cheung, K.K., Chan, M.W.Y., Young, E.W.K. & Viswanathan, S. Advances in organ-on-a-chip systems for modelling joint tissue and osteoarthritic diseases. *Osteoarthritis and Cartilage* **30**, 1050-1061 (2022).
177. Wen, L., Grad, S., Creemers, L.B. & Stoddart, M.J. Establishment of an ex vivo cartilage damage model by combined collagenase treatment and mechanical loading. *Arthritis Research & Therapy* **27**(2025).
178. Clarkson, J.M., Martin, J.E. & McKeegan, D.E.F. A review of methods used to kill laboratory rodents: issues and opportunities. *Laboratory Animals* **56**, 419-436 (2022).

179. Akhtar, A. The flaws and human harms of animal experimentation. *Cambridge Quarterly of Healthcare Ethics* **24**, 407-419 (2015).
180. Kleiveland, C.R. Peripheral Blood Mononuclear Cells. 161-167 (Springer International Publishing, 2015).
181. Nielsen, M.C., Andersen, M.N. & Møller, H.J. Monocyte isolation techniques significantly impact the phenotype of both isolated monocytes and derived macrophages *in vitro*. *Immunology* **159**, 63-74 (2020).
182. Loponte, H.F.*, et al.* GlycoGenius: a streamlined high-throughput glycan composition identification tool. *Nature Communications* **16**(2025).
183. Ruhaak, L.R., Xu, G., Li, Q., Goonatilleke, E. & Lebrilla, C.B. Mass Spectrometry Approaches to Glycomic and Glycoproteomic Analyses. *Chemical Reviews* **118**, 7886-7930 (2018).
184. de Haan, N., Yang, S., Cipollo, J. & Wuhrer, M. Glycomics studies using sialic acid derivatization and mass spectrometry. *Nature Reviews Chemistry* **4**, 229-242 (2020).
185. Ideo, H., Tsuchida, A. & Takada, Y. Lectin-Based Approaches to Analyze the Role of Glycans and Their Clinical Application in Disease. *International Journal of Molecular Sciences* **25**, 10231 (2024).
186. Loureiro, L.R.*, et al.* Novel monoclonal antibody L2A5 specifically targeting sialyl-Tn and short glycans terminated by alpha-2–6 sialic acids. *Scientific Reports* **8**(2018).
187. Laughlin, S.T.*, et al.* Metabolic labeling of glycans with azido sugars for visualization and glycoproteomics. *Methods in Enzymology* **415**, 230-250 (2006).
188. Laughlin, S.T. & Bertozzi, C.R. Metabolic labeling of glycans with azido sugars and subsequent glycan-profiling and visualization via Staudinger ligation. *Nature Protocols* **2**, 2930-2944 (2007).
189. Lam, Y.Y., Tan, A., Kempe, K. & Boyd, B.J. Metabolic glycan labelling with bio-orthogonal targeting and its potential in drug delivery. *Journal of Controlled Release* **378**, 880-898 (2025).
190. Zaia, J. The 2022 Nobel Prize in Chemistry for the development of click chemistry and bioorthogonal chemistry. *Analytical and Bioanalytical Chemistry* **415**, 527-532 (2023).
191. Warren, L. The thiobarbituric acid assay of sialic acids. *Journal of Biolological Chemistry* **234**, 1971-1975 (1959).
192. Hunter, C.D. & Cairo, C.W. Detection Strategies for Sialic Acid and Sialoglycoconjugates. *Chembiochem* **25**, e202400402 (2024).
193. Waters, P.J., Lewry, E. & Pennock, C.A. Measurement of sialic acid in serum and urine: clinical applications and limitations. *Annals of Clinical Biochemistry: International Journal of Laboratory Medicine* **29 (Pt 6)**, 625-637 (1992).
194. Gottschalk, A. The Influenza Virus Neuraminidase. *Nature* **181**, 377-378 (1958).
195. McAuley, J.L., Gilbertson, B.P., Trifkovic, S., Brown, L.E. & McKimm-Breschkin, J.L. Influenza Virus Neuraminidase Structure and Functions. *Frontiers in Microbiology* **10**(2019).
196. Adler, L., Yehuda, S., Varki, A. & Padler-Karavani, V. Discovery and characterization of vertebrate sialoglycan-binding proteins. *Seminars in Immunology* **79**, 101978 (2025).
197. Nydegger, U.E., Fearon, D.T. & Austen, K.F. Autosomal locus regulates inverse relationship between sialic acid content and capacity of mouse erythrocytes to activate human alternative complement pathway. *Proceedings of the National Academy of Sciences* **75**, 6078-6082 (1978).
198. Zhou, Q.*, et al.* The selectin GMP-140 binds to sialylated, fucosylated lactosaminoglycans on both myeloid and nonmyeloid cells. *Journal of Cell Biology* **115**, 557-564 (1991).
199. Edgar, L.J.*, et al.* Sialic Acid Ligands of CD28 Suppress Costimulation of T Cells. *ACS Central Science* **7**, 1508-1515 (2021).
200. Nair, R.R.*, et al.* Advances in phenylboronic acid and phenylboronic ester-based responsive systems for precision medicine. *Biomaterials Science* **14**, 661-683 (2026).
201. Jangid, A.K. & Kim, K. Phenylboronic acid-functionalized biomaterials for improved cancer immunotherapy via sialic acid targeting. *Adv Colloid Interface Sci* **333**, 103301 (2024).
202. Eltaib, L. Polymeric Nanoparticles in Targeted Drug Delivery: Unveiling the Impact of Polymer Characterization and Fabrication. *Polymers (Basel)* **17**(2025).
203. Gruber, S. & Nickel, A. Toxic or not toxic? The specifications of the standard ISO 10993-5 are not explicit enough to yield comparable results in the cytotoxicity assessment of an identical medical device. *Frontiers in Medical Technology* **5**(2023).

204. Petiti, J., Revel, L. & Divieto, C. Standard Operating Procedure to Optimize Resazurin-Based Viability Assays. *Biosensors* **14**, 156 (2024).
205. Bopp, S.K. & Lettieri, T. Comparison of four different colorimetric and fluorometric cytotoxicity assays in a zebrafish liver cell line. *BMC Pharmacology* **8**, 8 (2008).
206. Svensson, E., von Mentzer, U. & Stubelius, A. Achieving Precision Healthcare through Nanomedicine and Enhanced Model Systems. *ACS Materials Au* **4**, 162-173 (2024).
207. Kim, H. & Xue, X. Detection of Total Reactive Oxygen Species in Adherent Cells by 2',7'-Dichlorodihydrofluorescein Diacetate Staining. *Journal of Visualized Experiments* (2020).
208. Cossarizza, A.*, et al.* Guidelines for the use of flow cytometry and cell sorting in immunological studies (second edition). *European Journal of Immunology* **49**, 1457-1973 (2019).
209. Houser, B. Bio-Rad's Bio-Plex® suspension array system, xMAP technology overview. *Archives of Physiology and Biochemistry* **118**, 192-196 (2012).
210. Elliott, A.D. Confocal Microscopy: Principles and Modern Practices. *Current Protocols in Cytometry* **92**, e68 (2020).
211. Schaapherder, J.S.H.*, et al.* Exploring Siglecs: Potential Modulators of Immune Cells in Food Allergy and Therapeutic Applications. *Clinical & Experimental Allergy* **55**, 889-900 (2025).
212. Lozano-Rodríguez, R.*, et al.* The prognostic impact of SIGLEC5-induced impairment of CD8+ T cell activation in sepsis. *eBioMedicine* **97**, 104841 (2023).